Simple Harmonic Motion

in

Classical and Quantum Phase Space

-

Fundamental Rest Mass Quanta as
Simple Harmonic Oscillations of
the Spacetime Continuum,
Driven by Cosmic Expansion

By Martin Gibson

August 1, 2013

Martin Gibson
P.O. Box 2358
Southern Pines, NC 28388
910-695-9274
martin@uniservent.com

Simple Harmonic Motion in Classical and Quantum Phase Space

Abstract

In classical mechanics, natural, including man-made, repetitive motion sustained over extended time frames can be studied using the model of Simple Harmonic Motion (SHM) in which an oscillator and its support framework is deemed to be a closed system in that energy, momentum and related properties of the motion are conserved. In fact no system is completely closed and the energy of such motion is in some measure damped or otherwise lost to the background of the system. Still SHM can be closely approximated by driving the oscillation with controlled energy input. The oscillation of displacement and momentum in SHM can be accounted for succinctly with the use of planar phase space (PS_2) modeling in which the correspondence of the dynamics of linear oscillation and Uniform Circular Motion (UCM) is utilized. Accounting for energy, force, action, and power oscillation is better handled by graphic modeling of sine and cosine wave functions.

In the first section, these models are briefly recapitulated. In the second section they are applied to an analysis of the energy of the oscillation, through the Hamiltonian and Lagrangian approach, with the graphic development of the action, via both Lagrange and Maupertuis, and the power of the oscillation, and their semi-periodic maximum moments. The two models are synthesized in a three-dimensional phase space that we are calling PS_3. In the process of this synthesis it is shown that there is necessarily a component of the dynamics that is present even in the absence of oscillation, an inertial invariant that is both a scalar and vector potential. Finally, the point oscillator of the initial development is replaced by torsion oscillation as a disk, which can be represented by PS_2. The synthesis also suggests a quantum application of the modeling. Section three shows the development of rotation of the action and power moments with attendant torques which sustain the oscillation and result in the property of angular momentum, with an invariant Lagrangian as well as Hamiltonian. A review of the nature of body forces and stress or surface forces models PS_3 as a system of rotating stress force and corresponding strain, and the model is fully developed as an emergent quantum phenomena driven by an expanding spacetime fabric (STF) coupled with necessary geometric constraints. The neutron is shown to be the resonant state of PS_3. Spin and charge as elaborations of the angular momentum is developed, along with beta-decay for both ordinary and anti matter.

The Verification section derives a gravitational quantum, Newton's gravitational constant and law, ties beta-decay to cosmic expansion and thereby predicts the Hubble rate, which is shown to be an exponential rate. In the process the reason for the neutron-electron mass ratio is developed along with the nature of the missing mass of beta decay. Finally, the value of elementary charge is derived, with some interesting observations about the structure of the fine structure constant.

The Conclusion section waxes philosophical, concludes the PS_3 model deserves a proper vetting, and the Asides offer supporting information.

Table of Contents

Figures and Photos

Figures and Photos (continued)

Introduction

Nature is repetitive. Sure, she always offers something new and is in constant change; yes she changes, but in recurring patterns. Day follows night follows day. Summer follows winter follows summer. Heat follows cold follows heat. Given sufficient breadth of vision most, if not all, linear processes of change prove to be phases of a bigger cycle, where the extents of the cyclic pattern are found to be the extremes of some linear dimension. Birth to youth to maturity to old age to death is linear enough for the individual living creature, but from the perspective of her species, the line resonates in each and every birth.

A realist would say there is small wonder that those stuck upon the terminating line of life should look for comfort in the endless circle. Rather, as one who has had sufficient experience of finding an uncharted route prove to be a roundabout, I would say there is little reason to be satisfied with the boundaries of one dimension if one has yet to reach the vista and added breadth of higher ground.

From the smallest of atoms to the largest of galaxies, nature displays herself in circles and cycles and all manner of recursiveness magnificent to behold. What is more wondrous yet is that all of this can be understood in an ideal, simplified manner, in a fundamental form by the concept of simple harmonic motion (SHM) or simple harmonic oscillation, the changes in position and momentum accounted for by comparing motion about a circle with motion of the same periodic frequency along a simple line segment, its diameter. Some examples of physical processes that clearly embody the concept are pendulums of relatively small arcs of motion, massive objects attached to springs that extend and compress, and stretched strings that vibrate in sinusoidal fashion, each in response to some extraneous impulse that sets them in motion. In reality each of these systems involves inherent components and external connections that drain away the energy of oscillation over time, but in the ideal world of the mind, free from such external and inherent interaction, once set in motion these systems oscillate indefinitely. So we can learn much from an ideal description.

This discourse is intended for a general readership with some level of technical education or experience or the ability to gain the same through self-directed effort. (The Internet is the obvious source of information in this regard. Wikipedia in particular has excellent graphics, including animations, to help explicate the ideas.) It is for those with curiosity and will hopefully have something new for novice and expert alike; therefore, it will take pains to explain some basic concepts in some detail, while not avoiding the use and some assumed knowledge of special language.

In our description of oscillation, we define the above referenced line segment as $2r_0$ long, the diameter of a circle with a radius of r_0. The naught subscript in this discussion indicates a unit value, or in some cases characteristic value of the corresponding property that the letter represents, in this case, a change in position, i.e. a displacement or length along some linear dimension, such as x or y or q. As

such, r_0 equals x_0 equals y_0 equals q_0 equals 1 unit of length of some undefined system of measurement, without regard to the direction it is headed.

To the expert, if I depart from a rigorous notation in this piece with respect to vector notation, I apologize. I assume that the reader knows the difference between a length as a *scalar*, i.e. the magnitude of the difference between two positions in space (or time) as measured by an appropriate scale, and length as a *vector*, which adds to this magnitude the direction of the linear difference starting at one end of a standard or the other. Virtually any scalar can be made a vector by taking its gradient, the direction it is likely to change in space or time.

I will mention one refinement in the concept of direction, that of *sense*, which we generally think of as the sign, as $+x$ or $-x$, of a direction otherwise understood. Thus x_0 and y_0 can be understood as explicit vectors of either sense with respect to the x and y co-ordinates of some rectilinear system, q_0 as a generalized vector that may correspond to any x_0 or y_0 or even z_0 depending upon the defined context, and r_0 as a vector of inherently indeterminate or changeable direction and sense.

Simple Harmonic Motion and Two Dimensional Phase Space (PS_2)

Accounting for Displacement and Momentum

Let us consider a simple pendulum, a plumb bob at rest, hanging from a string about a meter long just above a central point, free to move in any angle, θ, of 360 degrees or 2π radians. We place a piece of paper under the bob with a circle of radius $r_0 = x_0$ its diameter clearly marked. For future reference we draw a second diameter 90 degrees or ½ π radians from the first, and we extend both diameters through to the edge of the paper and label one of the diameters $+x$ and the other one $+y$ as in Figure 1. We place the paper so that the center cross hairs of the circle are directly beneath the point of the plumb bob. The one I am using weighs about a pound and if you unscrew the collar that retains the line from its top, it reveals a miniature bob weighing about an ounce, nested away like a Russian doll.

It doesn't matter which way we orient the paper, as indicated by the dotted line axes x'–y' or what we call them. In fact, we can wait until we set the pendulum in motion, swaying back and forth along a gentle arc, before we turn the paper so that the x diameter and axis aligns with the arc of the oscillating plumb bob, designated in Figure 1 as O_l. An ideal pendulum, once set in motion, will swing back and forth forever. "Ideal" means the system which includes the table and the paper and the pendulum and the tripod from which the pendulum is suspended, along with the gravity that makes it all work, is isolated from any other activity which might effect it. The energy in such system is defined as being conserved, i.e. no energy is lost or gained from the system. In reality, the oscillation will cover a smaller and smaller arc over time due to *damping* and other causes, that is to say, it loses energy to the air around it and to the tripod through friction and other forces at the strings attachment. If we are to keep it going, we must *drive* the oscillation by adding a small amount of energy, ideally the amount that is damped away, as we might push a child in a swing to keep her going. In an ideal situation with no damping or driving, or in a controlled setting with driving offsetting the damping, the oscillation operates at its resonant angular frequency, which we designate as ω_0. The angular frequency measured in radians, θ, is related to a cycle or single period of the oscillation, T_0, and the periodic frequency, f_0, by

$$\omega_0 = \frac{2\pi}{T_0} = 2\pi f_0 = \frac{d\theta}{dt}. \qquad (1.1)$$

For reasons both practical and arcane, we will use angular frequency in our discussion unless noted otherwise.

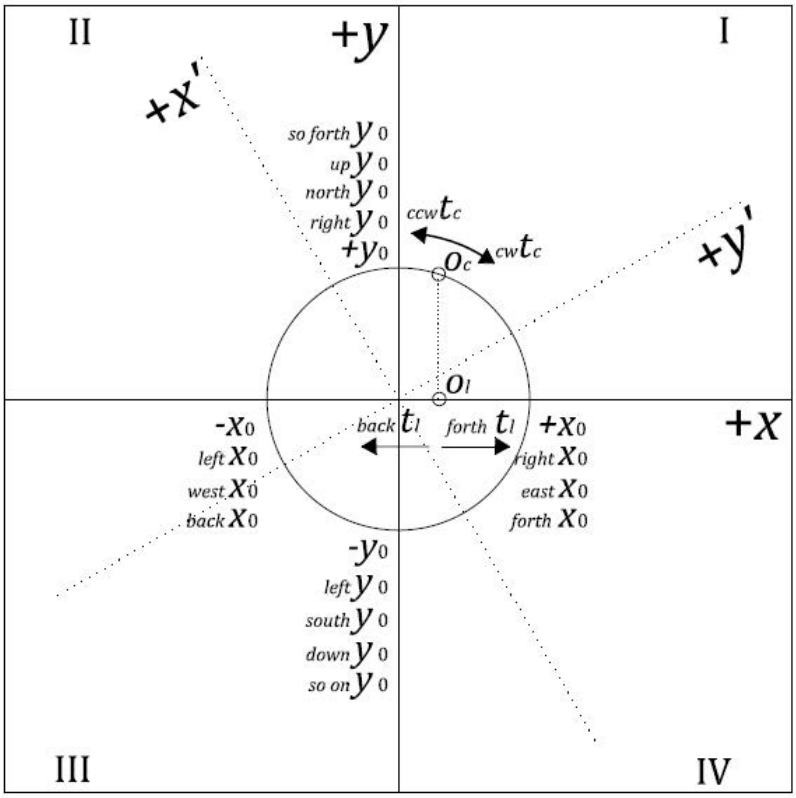

Linear and Circular Oscillation

Figure 1

We watch as the plumb bob swings back and forth along the *x*-axis and across the center point. At some point, since it is not ideal, the extent of its arc will lessen until it extends from the $+x_0$ to the $-x_0$ points where the axis crosses the circle. Notice that the terms *plus* x and *minus* x are simply reference designations to help us make *sense* of what is occurring. We just as correctly could have called these points *right* x and *left* x or *east* x and *west* x or *forth* x and *back* x or any of other terms as shown. Nor is it necessary, at this stage, that the *y*-axis have the same sense designations as the *x*-axis, though that will change. If we were surveyors, we might prefer east and west for *x* and north and south for *y*.

An interesting thing we note as the pendulum swings back and forth is that for small arcs, the frequency does not depend on the *amplitude* or extent of the oscillation along the *x*-axis. If we count the number of cycles that occur over a set period of time when we first set the bob in motion and count again after it has decreased to well within the circle, the frequency will be closely the same. We might think that if we change the size of the plumb bob it would affect the frequency, as in my case by removing the larger outer bob to leave the much less massive hidden bobby. In fact we find that it is unchanged.

The frequency, therefore, is not a function of the mass or, generally, the force that set it in motion in the first place. If we shorten the line that is suspending the bobs however, we find that the frequency increases. If we lengthen the line and hold it off of the table, the frequency decreases. We find that the resonant frequency of the oscillation is an inverse function of the length of the line suspending the plumb bob. It is inversely related to the *square root* of the length of the line, l_{pen}, and directly related to the square root of gravitational acceleration at the location of the pendulum, g_{pen}, as

$$\omega_0 = \sqrt{\frac{g_{pen}}{l_{pen}}}. \tag{1.2}$$

Squaring this statement and rearranging gives a statement for that acceleration,

$$g_{pen} = l_{pen}\omega_0^2. \tag{1.3}$$

It is worthy of note that for the pendulum system, the acceleration of g_{pen} is generally parallel to l_{pen}, or toward the earth, and perpendicular to the angular acceleration represented by ω_0^2, which oscillates about the center of the bob's travel, the point of rest or equilibrium represented by the center of our circle. In the case of O_l, the acceleration vector dips downward near each end of the bob's travel and points upward as it passes its point of equilibrium beneath its pivot. Wikipedia http://en.wikipedia.org/wiki/Pendulum demonstrates this oscillation.

We notice another feature of the system. The plumb bob over time begins to deviate from its arc along the *x*-axis and begin to follow an elliptical path, clockwise (cw) or counterclockwise (ccw). With a little help, we can nudge it into a circular path in a uniform circular motion (UCM), and we find that for a given length of pendant line, the frequency in the circular path is the same as the frequency along the diametric path. Since the circular path is longer than that of the diameter, this means that the average speed along the circle must be greater than the average along the diameter. We might suppose that the speed is constant along the circle, while obviously the bob stops at each end of its diametric travel. It must accelerate back toward the other end after it stops, and we wonder about its top speed on the way back.

When we study the system carefully, we find that if we had two bobs with equal pendulum length, one traveling the circular path at O_c and one traveling the diameter at O_l, so as magically not to interfere with each other, synchronized so that they both cross the *y*-axis at the same time, at any point in time the velocity of O_c in the *x* direction, i.e. projected on to the *x*-axis, equals the velocity of O_l on that axis. As shown in Figure 2, their speed, sense and direction along *x* are the same, and the maximum velocity of O_l, when it crosses the *y*-axis and is instantaneously parallel to the path of O_c, is the same velocity as O_c.

This coincidence means that the *momentum*, p_l, of O_l, which is equal to the *mass* of the bob times its velocity, equals the projected momentum of O_c along the *x*-axis, provided O_c has the equivalent mass as O_l. Since O_c has a constant angular velocity

and tangential speed and the same mass as O_I, it means that the projected momentum of O_c onto <u>any</u> diameter, including the one on the *y*-axis, is equal to the momentum of O_I along *x* at some point in time. The momentum of O_c along *y* is $\pi/2$ out of phase with its momentum along *x*, so that the magnitude of the momentum of O_c projected onto one axis can be read by its position with respect to the <u>other</u> axis. Thus, when O_I is at the origin or center of the circle and its displacement is 0, O_c is crossing the *y*-axis and the momentum of O_I at the origin position can be correctly read by the position of O_c on the *y*-axis.

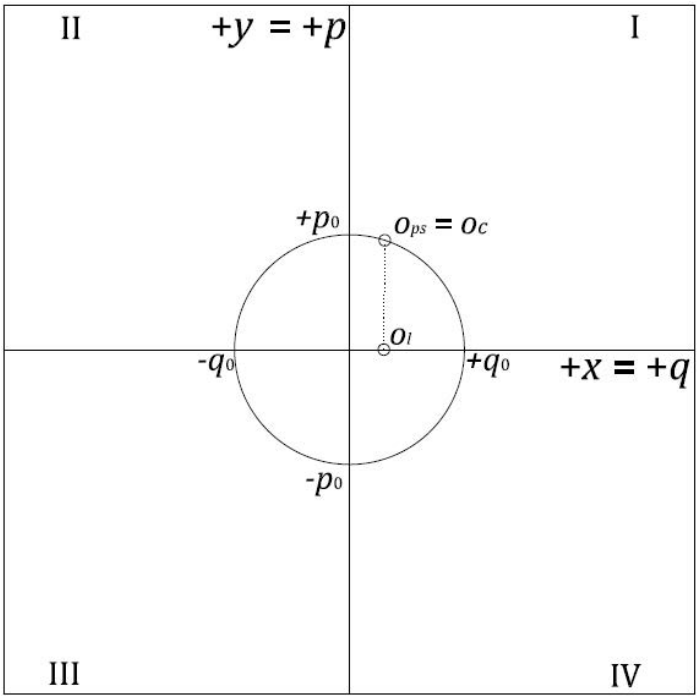

Transition to Phase Space

Figure 2

This provides us with a convenient analytical tool for investigating SHM known as phase space. Since the motion of a body or particle in UCM can be projected onto any arbitrary diameter, we can assign an axis associated with that diameter the designation *q* as a generalized co-ordinate, and the axis normal or perpendicular to it the designation *p* for the related or conjugate momentum. Conversely, we can project the linear motion of a one-dimensional oscillator onto an associated circle of UCM with the same effect, substituting O_{ps} for the circulating plumb bob, O_c. In the above diagram, *x* has become *q* and *y* has become *p*, though we could have done the same thing to any set of orthonormal axes.

There is an important caveat to this statement. I have said the "magnitude of the momentum of O_c . . . can be read" and not simply "the momentum of O_c", because momentum is a vector quantity. It has a direction, which is determined by the velocity, the speed and direction of travel of the oscillator. If O_c is traveling either cw

or ccw or overhead/underneath for that matter and its projected velocity on x or q is synchronized with O_l, it will make no difference to O_l which way O_c is circling. That is to say, in this case at O_l we cannot tell whether O_c is moving cw or ccw. All we know is that it is moving in the same direction relative to the x-axis as O_l. It does make a difference, however, if we are to use the y-axis to record p_l, the conjugate momentum of O_l. The sense of the momentum p_l indicates the direction O_l is traveling, while the sense of the position of O_l, q_l, indicates whether O_l, is to the left (negative) or right (positive) of the y-axis. As a result, half of the time p and q will be of different sense. They will be $\pi/2$ out of synch or out of phase.

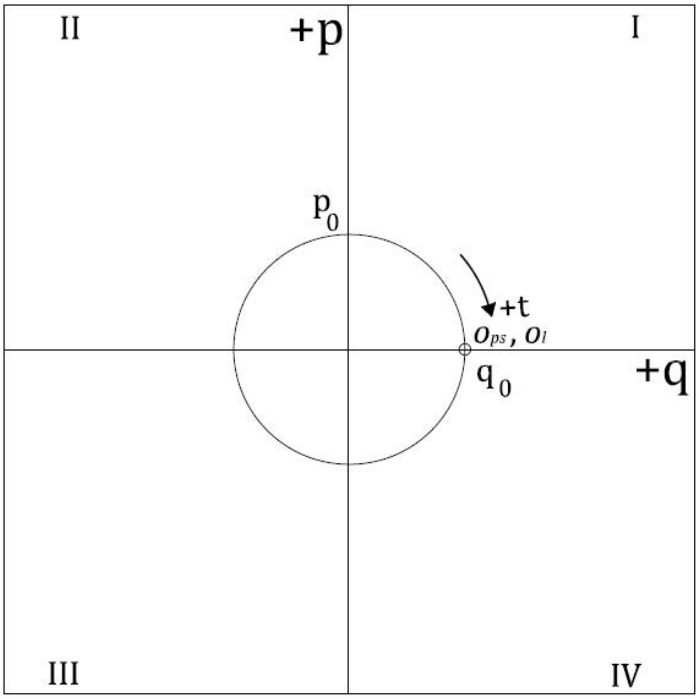

Phase Space with Simple Harmonic Motion

Figure 3

As seen in Figure 3, this dictates that for SHM in phase space using the standard configuration for the positive ordinate (y-axis) and abscissa (x-axis), unlike the paper plane onto which we have projected the traveling point of our plumb bob, O_{ps} can only move in one circular direction, cw, if we are to read the correct sense of the conjugate momentum of O_l from the p-axis component of the position of O_{ps}. Clearly, the rotational sense of O_l, conventionally given as + for ccw and – for cw in the Cartesian system or $+i$ and $-i$ using complex notation, is a subjective value determined by the point of reference of the observer. The same physical oscillation, viewed from the back side of phase space, as in Figure 4 in which the positive and negative sense of the q-axis are transposed, would be seen moving ccw, with the correct relative sense designations for both q and p in all four phases of the oscillation as seen below.

(It is serendipitous that the font images for generalized displacement, q, and its conjugate momentum, p, in non-italicized form of some font styles as here, are the mirror image of each other. If we took this at face value in the following figure, we would be forced to conclude that ccw rotation is not possible in this view either, since q appears to be leading p. In conclusion, the sense, direction and extent of momentum must lead the displacement values by one phase or $\pi/2$ in any representation, since that is what it does physically in SHM.)

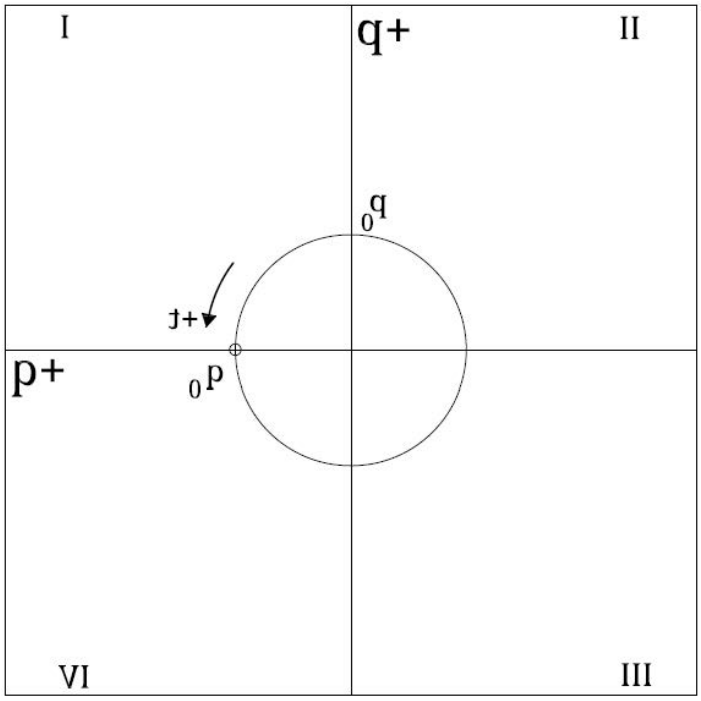

Phase Space Viewed from Below

Time is reversed

Figure 4

While the use of phase space in depicting the position and momentum flow of a simple harmonic oscillator is interesting, a greater interest might be the flow of energy in the system. Such energy is of two types that are transformable one to the other. In general, they are constantly in flux while their total in a closed system remains invariant. With respect to the present discussion of SHM, potential energy, $\mathcal{V}$, is a function of the position of the oscillator, O_l, and kinetic energy, $\mathcal{K}$, is a function of its velocity and its conjugate momentum. Therefore in Figure 3, $\mathcal{V}$is at a maximum, $\mathcal{V}_0$, when O_{ps} is at +/-q_0 where $\mathcal{K}$momentarily vanishes, while $\mathcal{K}$is at a maximum, $\mathcal{K}_0$, when O_{ps} is at +/-p_0 where $\mathcal{V}$momentarily vanishes. Clearly, the total energy of the system oscillates as does the oscillator, O_l, and it would be convenient and elucidating if we could map it onto phase space, so we will start with a few equations.

As stated, the potential energy of the system is a function of the displacement of O_l, so in derivative form the function, $\mathcal{V}'(q)$, can be written as the change in $\mathcal{V}$with

respect to a change in q which is equal to the resultant force, τ, which displaces it and which the gravitational field exerts on O_l in returning it toward its equilibrium position, where the force vanishes at $q = 0$, as

$$\mathcal{V}'(q) = \frac{d\mathcal{V}}{dq} = \tau = m_{O_l}\ddot{q} = m_{O_l} q\omega_0^2 \tag{1.4}$$

Here we have used the dotted mechanical notation for time derivatives, where

$$\begin{aligned} \dot{q} &= \frac{dq}{dt} = v, \text{ velocity} \\ \ddot{q} &= \frac{d^2q}{dt^2} = a, \text{ acceleration} \\ \dddot{q} &= \frac{d^3q}{dt^3} = j, \text{ jerk} \end{aligned} \tag{1.5}$$

The kinetic energy of the system is a function of the momentum of O_l, so in derivative form the function, $\mathcal{K}'(p)$, can be written as the change in $\mathcal{K}$ with respect to a change in p which is equal to the velocity of O_l, where ω_0 momentarily slows to 0 at $\pm q_0$, or

$$\mathcal{K}'(p) = \frac{d\mathcal{K}}{dp} = \dot{q} = q\omega_0 \tag{1.6}$$

The force of (1.4) is related to the gravitational field force responsible for the acceleration found in (1.3), as

$$\tau = m_{O_l}\ddot{q} = \sin\phi\left(m_{O_l} g_{pen}\right) = \sin\phi\left(m_{O_l} l_{pen}\omega_0^2\right) \tag{1.7}$$

where the mass, m, is the mass of O_l and ϕ is the instant angle between the plumb line and its vertical direction at rest. Note that according to (1.2), the two bracketed terms are invariant conditions of the pendulum setup and therefore of the system being examined, but that transverse force, τ, varies sinusoidally with the oscillation, as determined by ϕ, so that

$$q = \sin\phi l_{pen}\,. \tag{1.8}$$

With respect to $\mathcal{V}$, if we assume SHM and no damping or loss of energy, then q_0 is an initial condition determined by the force used to displace the plumb bob and set the oscillation in motion which establishes the angle ϕ, which in the context of phase space is the invariant angle for O_{ps}, or

$$\tau = \tau_0 \sin\phi_{Ops} = m_{O_l} q_0 \omega_0{}^2 = \left(m_{O_l}\omega_0{}^2\right)\sin\phi_{Ops} l_{pen} \tag{1.9}$$

A similar statement can be made for $\mathcal{K}$, as

$$c = c_0 \sin\phi_{Ops} = q_0\omega_0 = \sin\phi_{Ops} l_{pen}\omega_0\,. \tag{1.10}$$

We should note that the conditioning properties and parameters, g_{pen}, l_{pen}, ω_0, as well as the initial condition that establishes ϕ, are not a part of phase space, and in fact are orthogonal to, i.e. outside it, just as the tripod, table, string and earth are outside our Figure 1-4 paper planes. Those familiar with such things will recognize that the term in brackets in (1.9) has the form of the spring constant, k_s, of Hooke's Law for

elastic bodies in compression as in a spring-mass mechanism exhibiting SHM. I have not included any graphics of this mechanism, which are easily found on Wikipedia and elsewhere on the Internet.

In the case of such mechanism for which k_s is a measure of the stiffness of the spring material, the restorative force of the spring, τ_0, after compression or extension is equal to k_s times the strain or change in length of the spring, which would be q_0 in phase space. The spring constant then is

$$k_s = m_{O_l}\omega_0{}^2 \tag{1.11}$$

Unlike the pendulum, for which the restorative force of gravity is operating normal to the plane of phase space and the line of the initiating force, it first appears that the initiating and restorative force are anti-parallel in the case of the spring-mass mechanism; that is, parallel but of opposite sense. Careful analysis shows, however, that in the case of the spring, the equivalent of the gravitational force is actually distributed throughout the spring, normal to its travel, so the mechanisms are analogous. The spring at the points of maximum extension and compression stores the maximum potential energy, $\mathcal{V}_0$, and the oscillating mass, at the point of initial rest, exhibits the maximum kinetic energy, $\mathcal{K}_0$, which are expressed here as characteristic, unit values.

One other mechanism of SHM that exhibits some of the features of both spring-mass and pendulum oscillation is that of a transverse wave on an ideal stretched string. We do not include any harmonics of such wave action in this analysis and assume only a fundamental characteristic frequency in keeping with SHM. Such a mechanism has two primary conditioning properties, tension stress, f_t, or force per unit area, and inertial density, ρ, mass per volume of the oscillating medium. In the case of a string, which is modeled along one dimension, the cross-sectional component of the stress and the planar parallel component of the volume in the density cancel in the following equation and we are left with the tension force parallel to the string, τ_t, and linear inertial density, λ, in their determination of the square of the transverse wave speed as

$$c^2 = \frac{f_t}{\rho} = \frac{\tau_t / \mathrm{A}_0}{m / r_0 \mathrm{A}_0} = \frac{\tau_t}{\lambda} \tag{1.12}$$

From (1.10) we can see that for a given instance of SHM of frequency, ω_0, we have the following

$$c_0^2 = q_0^2\omega_0{}^2 = \frac{\tau_t}{m_{O_l} / q_0} \tag{1.13}$$

$$k_s = m_{O_l}\omega_0^2 = \frac{\tau_t}{q_0} \tag{1.14}$$

showing that the spring constant can be understood as the linear force density of the oscillation medium, be it gravitational field, elastic continuum/body or stretched

string, where the linear unit is expressed in terms of the characteristic displacement, q_0. There is a difference, however, between the oscillating string and the other two examples of SHM in that the mass, m, in the first two examples is that of a separate body, the plumb bob and the oscillating weight, both of which generate a body force, F_b, due to their initial acceleration, a, from rest according to Newton's second law of motion

$$F_b = ma \,. \tag{1.15}$$

The oscillation media or fields, i.e. the gravitational field/pendulum line and the spring, respond in equal and opposite direction to F_b, according to Newton's third law of motion but as instances of stress force τ_t. In both cases the body force of the massive object moves transverse or normal to the stress force, which is a tension stress force. In the case of the pendulum, this transverse motion is apparent. In the case of the spring, it may be less obvious, but the tension in the coils of the spring or the molecular bonds of an analogous solid elastic body that provides the restorative force is oriented normal to the travel of the massive body.

The relationship between the tension force in the oscillation field, τ_t, and the transverse force of the oscillating body, τ_s, can be described as the operation of a stress field, a type of tensor field. A tensor is a mathematical description of the way forces or velocities or other properties distribute in space and time, as when you swing a mallet down on a tomato and watch it explode out on all sides. Try this. It's fun in a juvenile sort of way.

A tensor is essentially a description of redirection of some conserved property often involving rotations and is therefore an elaboration of trigonometry. A stress field has two essential components with their corresponding forces, tension/compression, directed normal to the surface of a small unit volume of space, and shear, directed along the edges and in the plane of each surface of that unit. Since stresses describe the relationship of a force to some surface area, those stress forces are also called surface forces. A good example of the interaction between a body force and a stress force is a person jumping on a trampoline.

In the case of SHM on an ideal stretched string, the mass is the mass of the string itself, of the oscillation field, and the force it exhibits is a stress force. Whatever type of force may displace the string and initiate the oscillation, its ongoing SHM is an oscillation of stress forces in which a portion of the longitudinal tension stress transforms to transverse tension stress before recoiling in alternating direction to either side of its position of rest. It is like the trampoline bouncing back and forth sans person, like a drumhead. In this case the transverse force of the oscillation is

$$\tau_s = -\cos\theta\tau_0 = \pm i\sin\phi\tau_t \tag{1.16}$$

There are two generally recognized types of waves on a string, traveling and standing or stationary. Traveling waves are customarily modeled on an indefinitely

long string, so that their shape is that of a graph of the sine (or cosine) function of an angle, θ, as it increases from 0 through one cycle of 360 degrees or 2π radian, with the function of q mapped with respect to the ordinate and the angle mapped to the abscissa. If the angle represents an event rotating or cyclically occurring at a uniform rate, i.e. UCM, the abscissa can represent time and time can be measured in radians of either *cyclic or linear* change. A snapshot of a transverse wave *in* time and *over* an interval of space looks like such a graph and a video *over* time exhibits SHM at each point along its length. The result is the familiar sinusoidal wave of Figure 5.

A wave traveling on a string of finite length will eventually reach the string ends, which we assume to be rigidly fastened to immovable objects, so that the oscillation is not damped. The wave is reflected at these ends and begins to travel back down the string toward the other end. Waves traveling in opposite direction reinforce and cancel each other as they interfere, according to the wave half-length, πq_0. The points of cancelation form nodes where the string exhibits no transverse motion, every πq_0, and antinodes or points of maximum displacement at the half points between each node. If we have some very precise grips, we can clamp the nodes in the following graph at $-\pi/2$ and $\pi/2$ along the θ axis and the point at q_0 will continue to oscillate in SHM. If we view this graph as a physical half wave in motion with respect to axis θ, the graph of p between 0 and 2π maps out the conjugate momentum for q, starting from its position at q_0 for $\theta(0)$.

We should not loose sight of the fact that within the context of a one-dimensional oscillator, momentum is always in the same direction as the displacement over time, as seen here, though their magnitudes, p and q, are still out of phase by $\pi/2$. The following phase graph Figure 5 shows both p and q map to the ordinate and the phase propagation, θ, over time maps to the abscissa. The phase space diagram above then rotates the q and θ dimensions from the phase graph clockwise $\pi/2$, or using complex notation, by a factor of $-i$; q mapping to the abscissa and θ mapping to the circle contour at a distance of $|r_0| = |p_0| = |q_0| = +1$ from the Phase Space origin.

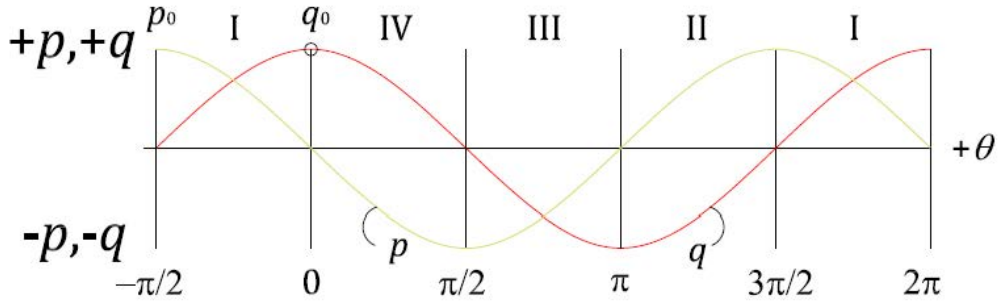

Phase Graph of Momentum, p, and Displacement, q

$p = \sin\theta\, p_0$, $q = \cos\theta\, q_0$

with counter-clockwise phasing and sense of function determined by standard Cartesian co-ordinate system

Figure 5

From this it is straightforward to define a two dimensional phase space, $PS_2 = \theta$, where $\theta = 0$ lies on the positive abscissa and the senses of the trigonometric functions are taken from projection onto the appropriate co-ordinate axis of a complex plane, where $p_0 = +iq_0$

$$r\left(\theta\right) = r_0 e^{i\theta} = q_0 \cos\theta + iq_0 \sin\theta \tag{1.17}$$

It is important to the following development to emphasize that θ is essentially a clock and at time $\theta = \pi$, the direction of time in phase space with respect to the conjugate momentum has reversed itself from its initial direction at time $\theta = 0$. In other words, in such a phase space, time oscillates.

Finally, as those musicians who play string instruments will know, a string doesn't simply oscillate in one dimension normal to the string, as in the plane of the phase graph. It is free to move transversely all about the string, and we can imagine an ideal condition under which it moves in UCM about the position of the string at rest. Under these circumstances the point q_0 circulates in the manner of O_c and O_{ps} in the above diagrams, clockwise and counterclockwise depending on the end of the θ axis from which it is viewed.

Simple Harmonic Motion and Three Dimensional Phase Space (PS_3)

Accounting for Potential, Energy and Time

Let's next consider a simple harmonic motion or oscillation (SHM) in PS_2, where,

$$p^2 + q^2 = r_0^2 = 1, \tag{2.1}$$

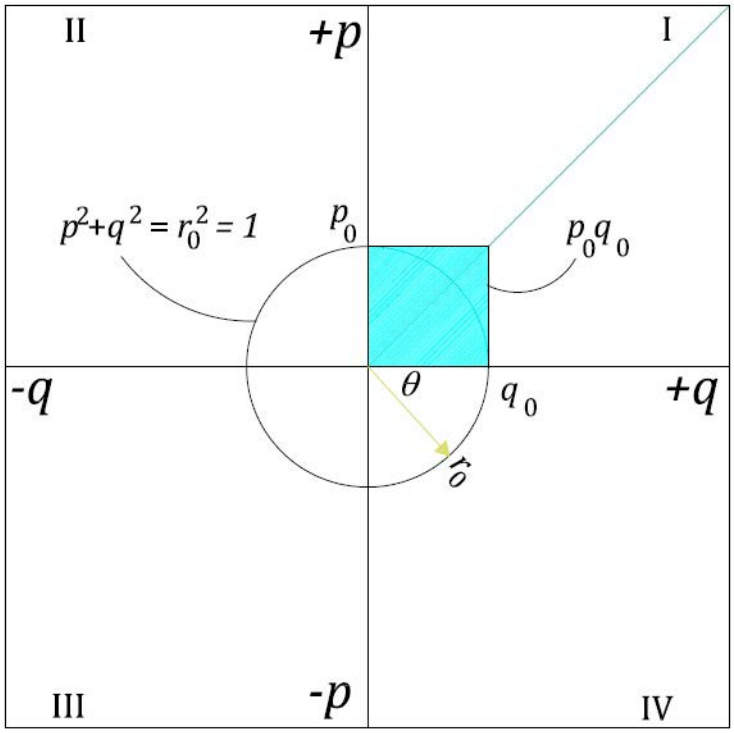

Figure 6

In Figure 6, the square designated as the product p_0q_0 represents the total energy or Hamiltonian, $\mathcal{H}$, of the system that cycles about phase space at the cyclical frequency $\omega_0/2\pi$, for an invariant energy of

$$\mathcal{H} = p_0 q_0 \omega_0 = 1. \tag{2.2}$$

Since the total energy of the system is conserved, this means that the Hamiltonian is equal to the total, at any point in time, of $\mathcal{K}$ and $\mathcal{V}$ which oscillate sinusoidally, as

$$\mathcal{H} = \mathcal{K} + |\mathcal{V}| \tag{2.3}$$

The absolute value for $\mathcal{V}$ indicates that the potential energy is always negative due to the fact that its components τ and q are always of opposite sense, while $\mathcal{K}$ is always of positive sense, since its components p and c are always of the same sense, as seen in Figure 9. In these graphs p and c are represented by the same line. For both $\mathcal{K}$ and $\mathcal{V}$ the two components are always of the same relative magnitude.

The Hamiltonian is related to another relationship between $\mathcal{K}$ and $\mathcal{V}$, the Lagrangian, $\mathcal{L}$, referring to (1.4) and (1.6), though in this case $\mathcal{K}$ is defined as a function of the rate of change in q over time instead of the momentum, as

$$\mathcal{L} = \mathcal{L}(q,\dot{q}) = \mathcal{K} - |\mathcal{V}| \tag{2.4}$$

and since $\mathcal{K}$ and $\mathcal{V}$ oscillate in magnitude between 0 and 1 out of phase with each other, it is clear that the Lagrangian is not invariant, except in a case of UCM in which $\mathcal{V}$ is the scalar invariant product of $\tau_0 r_0$ and $\mathcal{K}$ is the scalar invariant product of $p_{0\tan} c_{0\tan}$, tangential momentum and velocity. The product $p_0 q_0$ has the units of action, $\mathcal{S}$, which is generally defined as the time integral of the Lagrangian, $\mathcal{L}$,

$$\mathcal{S}_t = \int_{t_i}^{t_f} \mathcal{L}(q,\dot{q})\, dt \tag{2.5}$$

but is also defined as by Maupertuis as the displacement integral of an impulse, $\mathcal{J}$,

$$S_q = \int_{q_i}^{q_f} \mathcal{J}(q) \cdot dq \tag{2.6}$$

the impulse being the time integral of a force which is equal to a change in momentum, Δp,

$$\mathcal{J} = \int_{t_i}^{t_f} \mathcal{F}(t)\, dt = \Delta p \tag{2.7}$$

Thus, in the context of SHM in phase space, the integral of the change in momentum over the displacement path of the oscillation is equal to the time integral of the Lagrangian over the same path. Let's see how this graphs out using the sine/cosine functions with respect to Maupertuis.

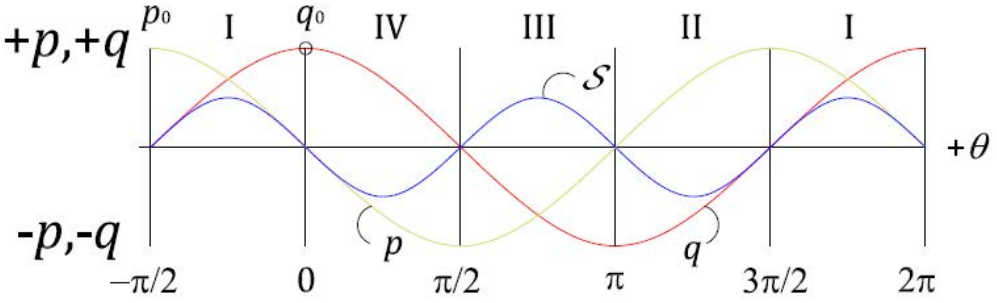

Phase Graph of Action

$\mathcal{S} = pq$

Figure 7

In Figure 7 we see that the action varies sinusoidally at twice the frequency and half the amplitude of the phase cycle, peaking at mid phase in each direction. We can add the force graph to this in Figure 8, which is the inverse of the q graph, and plot the power of the oscillation, $\mathcal{P}$, which is the product of the force and velocity, the latter being the same as the momentum graph or

$$\mathcal{P} = \tau \dot{q} = \tau c \tag{2.8}$$

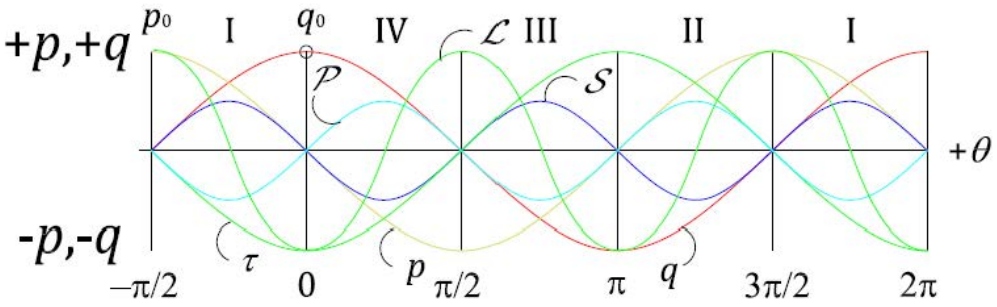

Phase Graph of Force, τ, and Power, $\mathcal{P}$

$\tau = -\cos\theta\, q_0\, m\omega^2 = -m\omega^2 q$

$\mathcal{P} = \tau c$, where $c = p/m = q\omega$

Figure 8

It is clear that the power graph is the inverse of the action graph. We can next plot the kinetic and potential energy curves, which will also give us the Lagrangian, the green curve in the first graph, and the invariant Hamiltonian shown in the second.

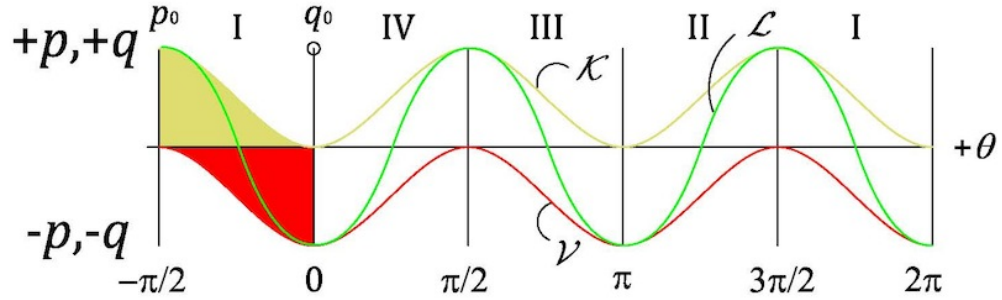

Lagrangian: $\mathcal{L} = \mathcal{K} - |\mathcal{V}| = \mathcal{K} + \mathcal{V}$ (Green curve)

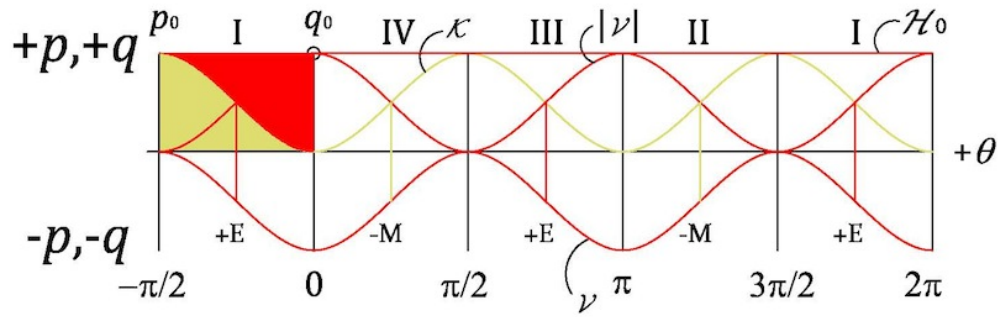

Hamiltonian: $\mathcal{H}_0 = \mathcal{K} + |\mathcal{V}|$ (Invariant red curve)

Phase Graph of Kinetic, $\mathcal{K}$, and Potential, $\mathcal{V}$, Energy

$\mathcal{K} = pc = \sin^2\theta\, p_0 c_0$, $\mathcal{V} = \tau q = -\cos^2\theta\, \tau_0 q_0$

Shaded areas are phase integrals of Kinetic (gold) and Potential (red) Energy.

Figure 9

The next few graphs show some integrals and areas under the curves for reference.

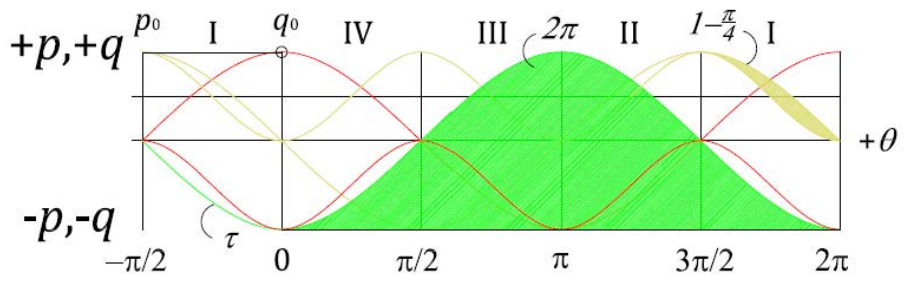

Fundamental Single Cycle Curves
Momentum, Displacement, Force (shown), & Velocity

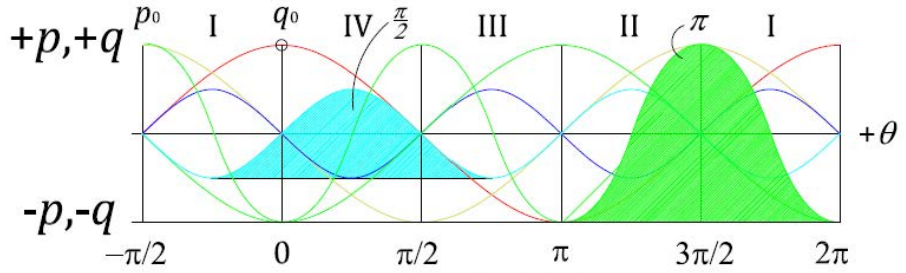

Derivative Double Cycle Curves
Action, Power (shown), & the Lagrangian (shown, full amplitude)

Various Integrals/Areas under the Whole Curves

Figure 10

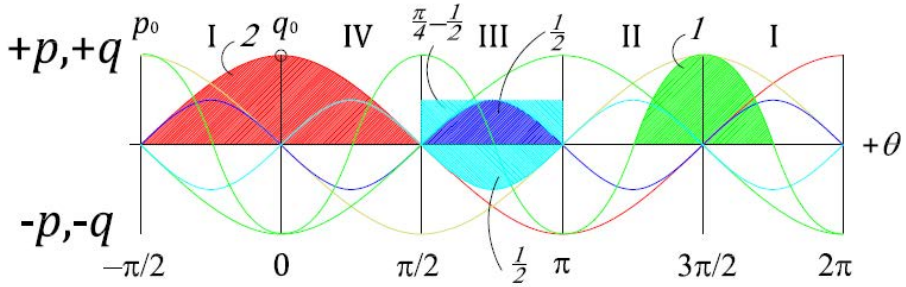

Single and Double Half Cycle Curves
Displacement, Action , Power, & the Lagrangian shown

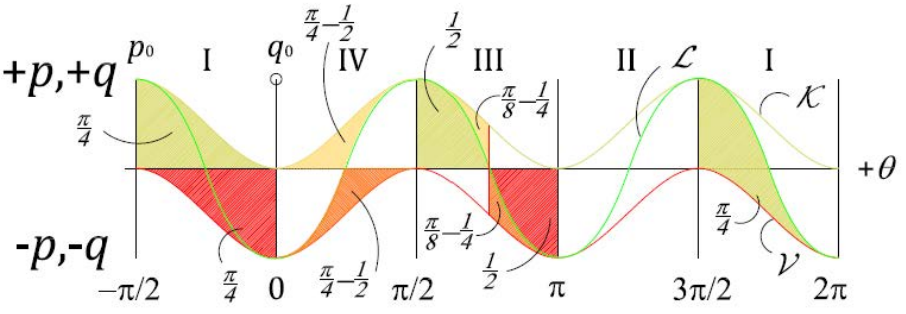

Lagrangian, Kinetic and Potential Energy Half Cycle Curves and Components

Various Integrals/Areas under the Half Curves

Figure 11

Obviously, the action varies over the range of each quadrant, as seen in the

following graph, though its total is invariant from quadrant to quadrant, as

$$\mathcal{S} = p\int_{-\pi/2}^{0} dq = p\dot{q}\int_{-\pi/2}^{0} dt - \dot{p}q\int_{-\pi/2}^{0} dt = pq = \tfrac{1}{2}p_0q_0 \qquad (2.9)$$

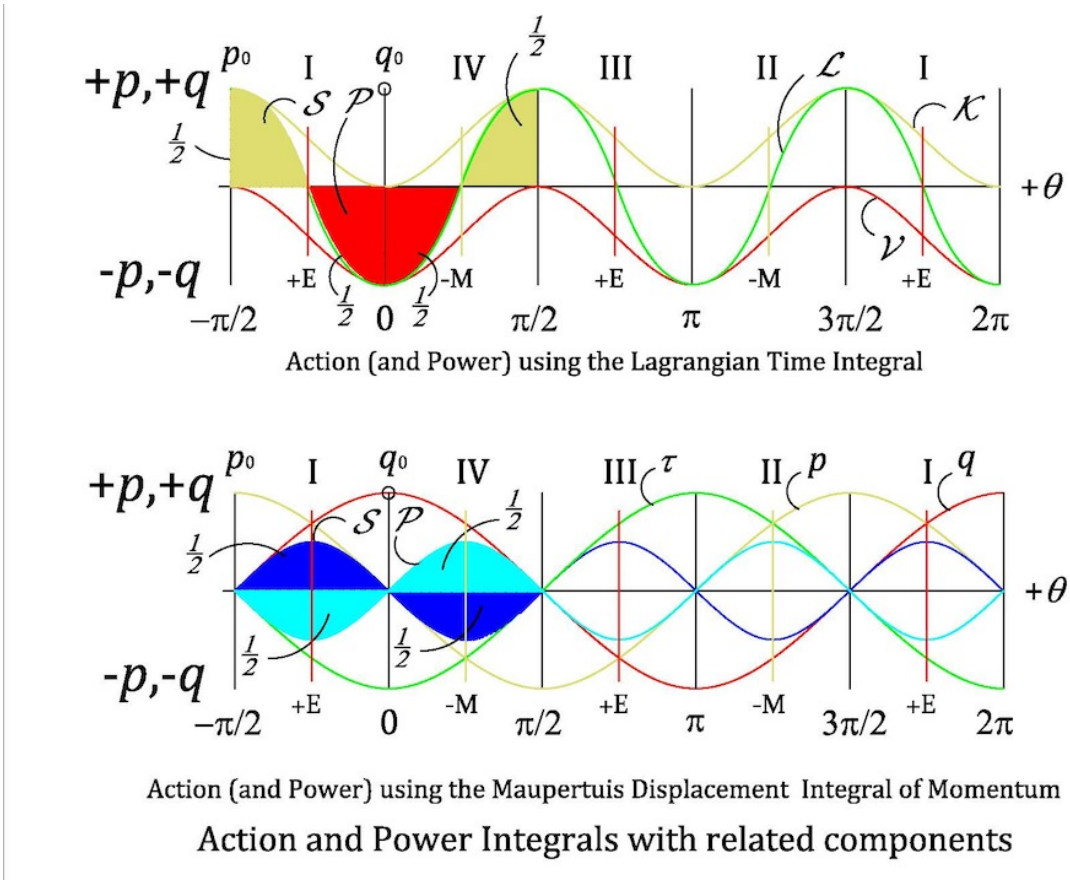

Figure 12

The action due to Maupertuis and that due to Lagrange offer different pictures of the energy transformation of the oscillation. While Maupertuis is an integral over the displacement path, the filled areas of the curve show that the action and its inverse, the power of the oscillation are in operation throughout the cycle, i.e. over time, peaking with their rate of transformation greatest, at the half point of each of the four phases. While Lagrange is an integral over time, the filled areas show that the action is concentrated in space at the center point of the oscillator's path as an expression of kinetic energy, with the power concentrated at the extremes of displacement as an expression of potential energy. This will be important later in our discussion.

Next is a direct comparison of the graphs of Maupertuis and Lagrange for one phase of the cycle as

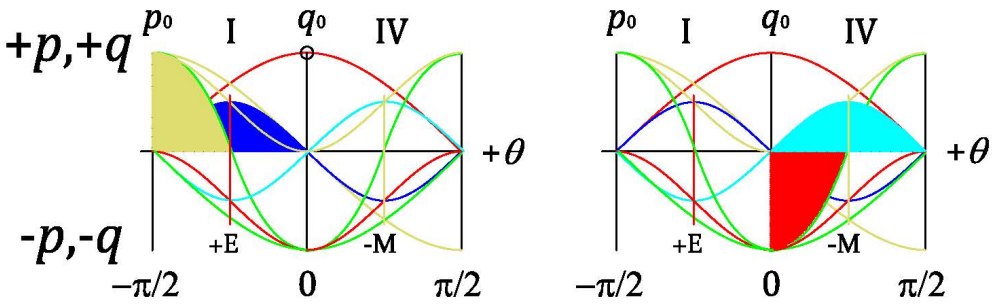

Figure 13

We would next like to apply this to phase space to see what it tells us. All images in Figure 14 show the condition in phase I at the moment of maximum action (and power charging) at the point +E, where the designation indicates that it is a potential energy/mechanical analog for electrical charging or capacitance. In Figure 13 above, the –M indicates a moment of maximum power (and negative action) in the kinetic energy/mechanical analog for electrical discharge and magnetic inductance. The moment senses indicate the direction of travel of the oscillator.

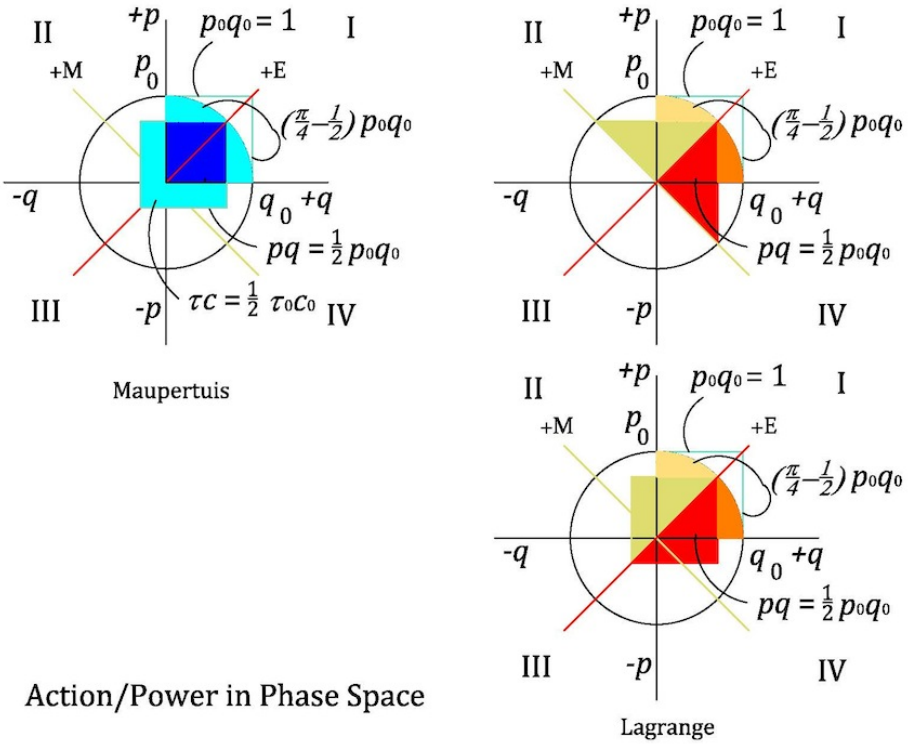

Figure 14

There are two configurations shown for the Lagrange method. The unit squares representing the energy of the system are positioned so that the square area in quadrant I is equal to ½ of the total as are the diagonal-halved red and gold sections of each. For Maupertuis this is equivalent to the area under the curve above. In this scenario, the unit square pivots around the center of the circle clockwise.

The fact that we are dealing with an invariant quantity, p_0q_0, suggests that we might want to plot the product as a hyperbolic curve to phase space in each of the four quadrants. The following Figure 15 shows that beyond the colored range of the kinetic (gold) and potential (red) energies, here along the positive axes, the values for p and q exceed the system constraints as the curves approach each axis asymptotically. The solution is to collapse the hyperbolic curves toward the circle center with a bit of origami, by folding forward along the axes and backward at the lines that cross the curves parallel to the axes. Make a copy and do this, which represents the elements of the oscillatory field that are orthogonal to the phase space. The peach sections are duplications of the adjacent kinetic and potential components, which fold up against them as the four quadrants are brought together.

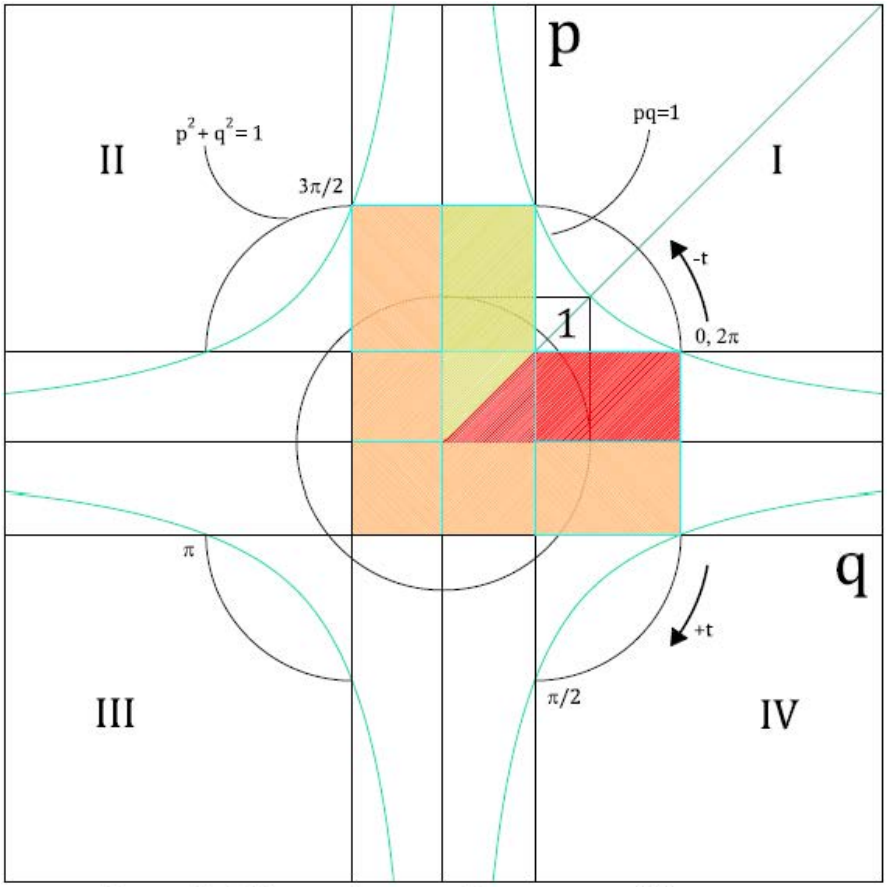

Inertial Invariance Superposition
orthogonal to Phase Space

Figure 15

When folded, the center square inside the circle and composed of four smaller squares folds in eight triangles upon itself, and represents the inertial potential of the system. The geometry of this arrangement, which arises naturally in this scenario, is such that when the hyperbolic curves intersect the phase space circle as shown in Figure 16, with the unit square offset as shown, the area of the rectangle when the kinetic is at a maximum is unitary and remains so as the distal vertex moves along the hyperbolic curve between the *p* and *q* axes to the position of maximum potential energy. This energy flow is shown in Figure 16.

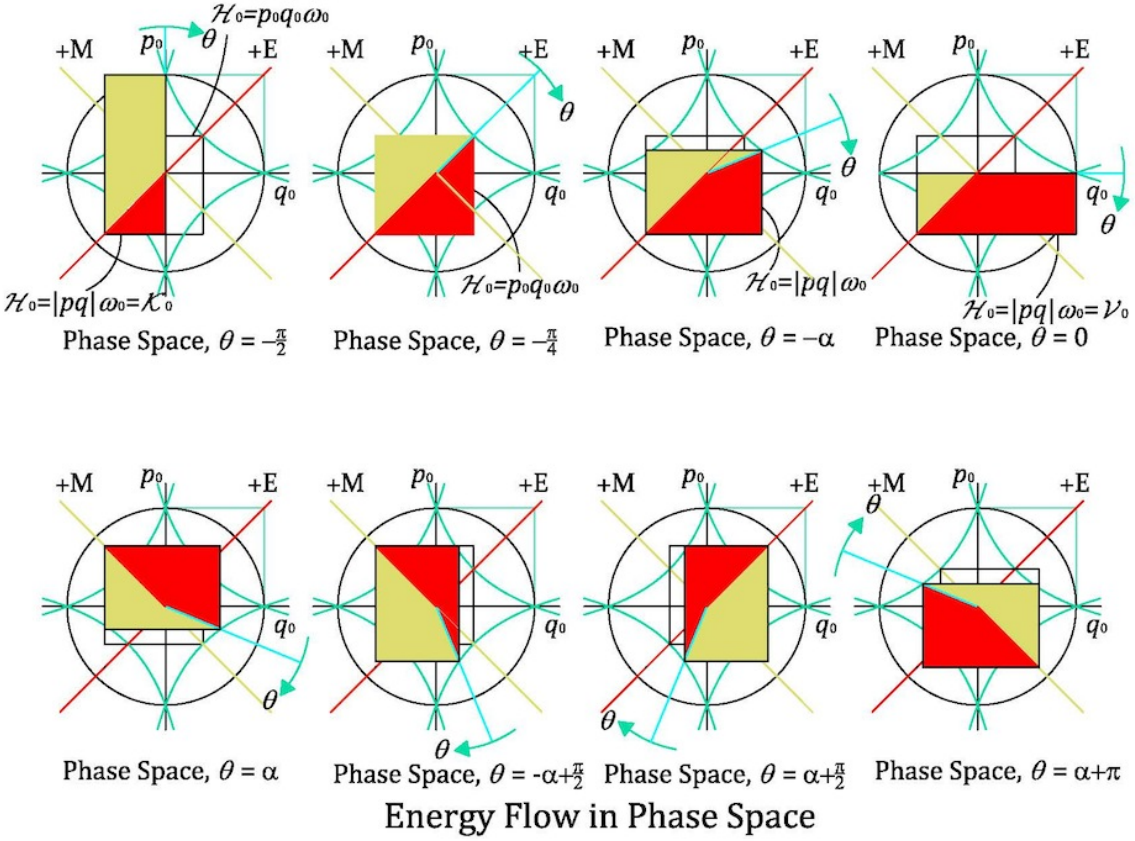

Figure 16

Here the off-manifold or extra-dimensional components of the energy are shown as θ rotates about the phase space with the motive end of the rectangle moving along the hyperbolic curve in the extant phase. This is indicative of the three dimensional nature of the energy. The importance of this contrivance can be seen in the next chart, Figure 17.

In the first figure at the upper left we have a superposition of the kinetic and potential energies of the oscillation, with the defining physical property dimension components of the energy and phase space shown on the dimension lines. In the upper right we have the condition if the oscillator was stopped at its point of maximum displacement with a retention of potential energy. Manually returning the

oscillator or oscillating medium to its point of equilibrium, stops the oscillation, thereby removing all kinetic and potential energy from the system. However we are still left with an invariant inertial potential component of units mass-displacement.

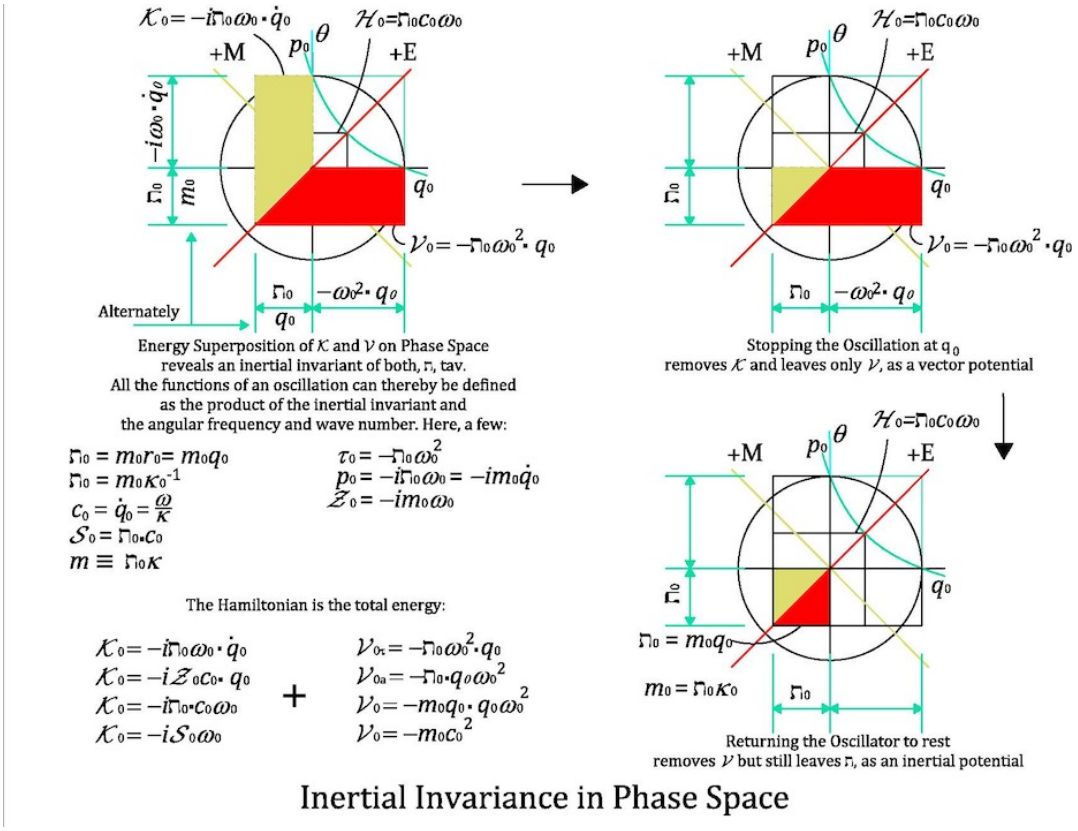

Figure 17

This inertial invariant, which I am calling ⊓, (tav), can also be understood as the invariant ratio of the mass of the oscillator and its angular wave number, κ_0, which is conjugate to the frequency as

$$\kappa_0 = \frac{\omega_0}{c} \tag{2.10}$$

$$\therefore m_O = \sqcap \kappa_0 \tag{2.11}$$

shows that with SHM mass is essentially the wave number of the oscillation. In addition, the invariants $\mathcal{S}_0$ and c_0 are related to the inertial invariant as

$$\sqcap = \frac{\mathcal{S}_0}{c_0} \tag{2.12}$$

In a quantum application, this is

$$\sqcap = \frac{\hbar}{c}. \tag{2.13}$$

Here $\hbar$ (h-bar) is the invariant quantum of action of quantum theory. The value in this development is that the various functions of the oscillation we have discussed, in addition to several others, can be stated in terms of the inertial constant and the various orders of derivatives and integrals of the frequency and wave number using the Euler identity, without recourse to extraneous properties. Figure 18 gives such

frequency derivatives, followed by a second chart combining frequency and wave number derivatives and integrals.

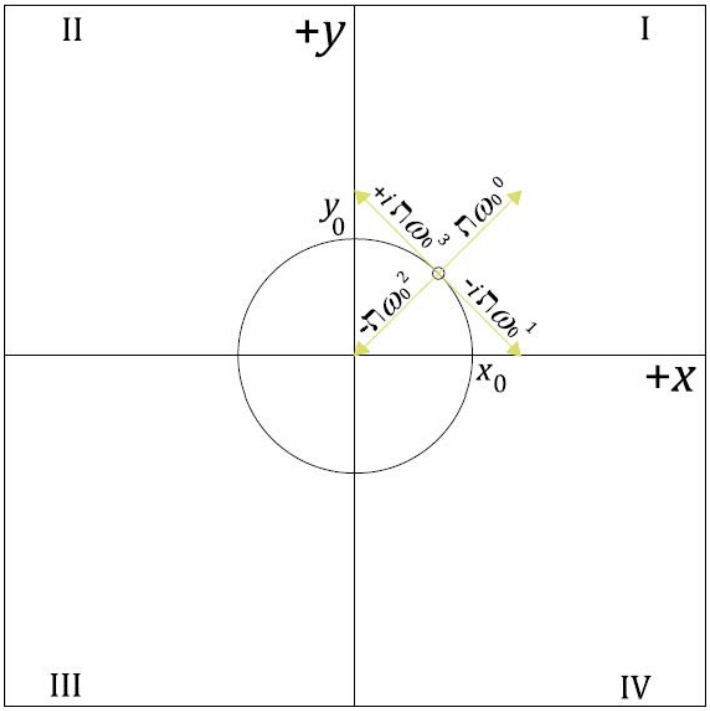

Phase Time Differentials - Uniform Circular Motion

Figure 18

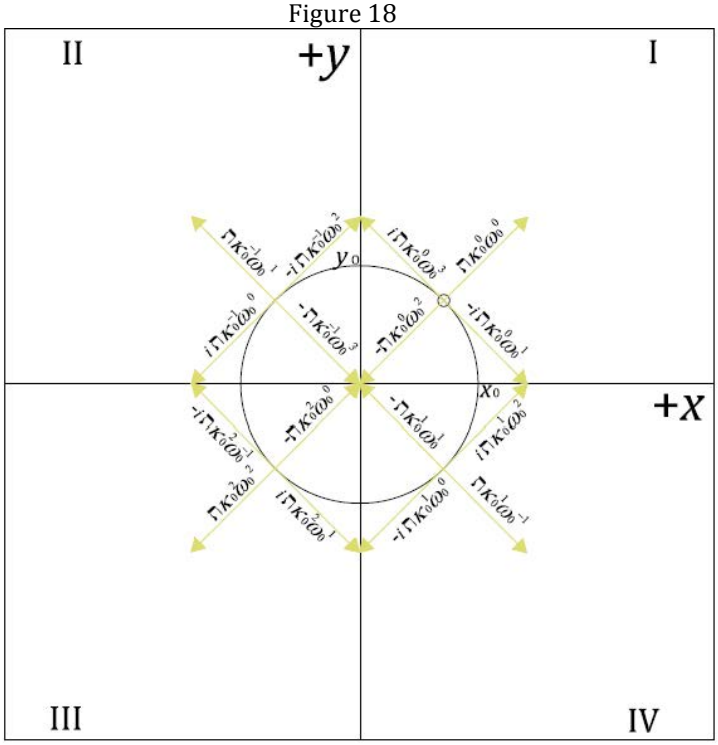

Phase Space & Time Differentials - Uniform Circular Motion

Figure 19

This next chart gives the equivalent properties of the functions. See the Matrix of PS_3 Functions and Invariants chart after the Conclusion section for another representation.

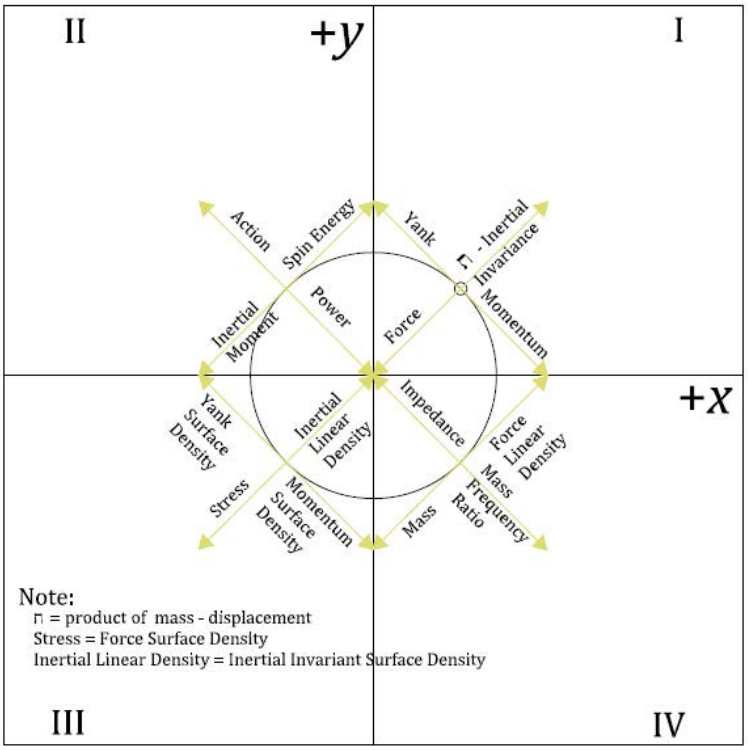

Phase Space & Time Functions - Uniform Circular Motion

Figure 20

Figure 21 maps the energy of the previous graphs in *phase time* to 2-dimensional *phase space*. The arrows for the kinetic phases (gold) and the potential phases (red) in the upper left graph are a mapping of the motion of the oscillator up and down with respect to the space ordinate as at 0, and to the right over linear time, thus completing the sine curve path. The second figure on the upper right reverses the direction of the flow at each of the E and M moments to collapse the first into a cyclical time arrangement designated by the phase/quadrant for superimposing onto a cyclical phase space. The reason for this is found in the fact that the direction of increasing potential energy is always counter to the direction of increasing kinetic energy as in a gravitational field. Following the red arrow from either of the E points in this figure to the adjacent M moment and then by the gold arrows to the next E moment is the equivalent of lifting an object in the terrestrial gravitational field and releasing it to fall back to earth. The work of lifting is done by the action of the wave, twice per cycle. The reversal of polarity here is a unique and necessary feature of SHM, which indicates that within such a closed system, time is cyclical. In the final figure the collapsed graph is superimposed onto phase space, which has transposed *q* and *p* axes so that the senses of the two depictions are synchronized with the displacement and the momentum.

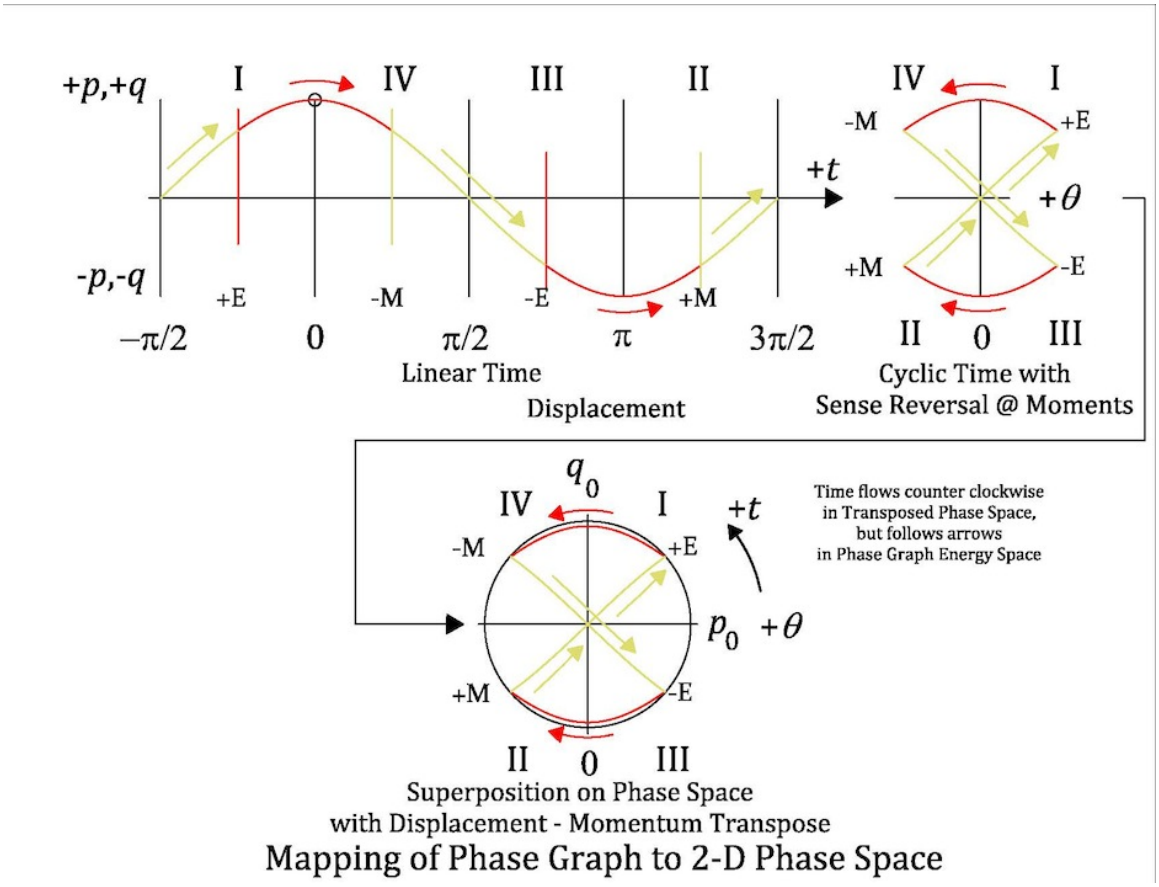

Figure 21

Thus the potential energy that is a function of displacement is graphically superimposed on the regions of greatest displacement in phase space and the kinetic energy that is a function of velocity is graphically superimposed on the regions of greatest momentum and oriented in the general direction of positive momentum. Note that the rotation over time is now ccw, but this is only for phase I and IV, at which point it reverses from III to II.

We can now begin to clear up some features that may have been apparent to the reader earlier. Figure 6 shows the total energy of the system as equal to the unit square, which overlaps the boundary of the phase space and the single phase or quadrant area of $\pi/4$. In Figure 9 the same total energy is depicted as the straight, therefore invariant line $\mathcal{H}$ equal to one, while its $\mathcal{K}$ and $\mathcal{V}$ components are shown as integrals, as areas under the Lagrangian curve, each equal to $\pi/4$. Obviously some interpretation is in order.

$\mathcal{H}$ is correctly shown as an area in Figure 6 as it is extra-dimensional to the linear dimensions of p and q and in fact is dimensionally the product of these for its two components as

$$\mathcal{H} = \mathcal{K} + \mathcal{V} = \tfrac{1}{2} p\dot{q} + \left|\tfrac{1}{2} \dot{p} q\right| = p_0 q_0 \omega_0 \qquad (2.14)$$

In phase I, $\mathcal{K}$ goes from 1 at p_0 to 0 at q_0 and $\mathcal{V}$ goes from 0 at p_0 to -1 at q_0. At the mid-point between the two, +E, each are equal to ½ $p_0 q_0 \omega_0$.

As shown in Figure 9, the line $\mathcal{H}_0 = p_0 = q_0 = 1$, is the absolute difference between the $\mathcal{K}$ and $\mathcal{V}$ curves at any point in time and any point in the phase graph. The Lagrangian, $\mathcal{L}$, on the other hand is the relative difference between the $\mathcal{K}$ and $\mathcal{V}$ curves, relative to the ground state represented by the θ, time axis. Thus $\mathcal{L}$ is zero when the distance from θ is the same for both components. Though the (straight) curve in this figure for H equals 1, the integral for $\mathcal{K}$ and $\mathcal{V}$ shown by the gold and red areas under the curves are $\pi/4$ each and $\pi/2$ for the area under the Hamiltonian, which is obviously greater than 1. This is because the line represents the value of $\mathcal{H}$ over time, i.e. at any point in time, which happens not to change, and the area under the curve for each of $\mathcal{K}$ and $\mathcal{V}$ represents the magnitude of the phase space over which the energy ranges, $\pi/4$ for each. Looking at the top graph in this Figure of the Lagrangian, it is evident that the areas of red and gold that are not between the Lagrangian curve and the θ axis and which equal $\pi/4$ minus ½ each, as seen in Figure 11, cancel leaving the ½ values each for the action and power, which is net kinetic and potential energy for a total of 1 or the Hamiltonian. We can see the symmetry in the following in which the action is differentiated and the power integrated with respect to time.

$$\mathcal{H} = i\mathcal{S}\omega_0 - i\mathcal{P}\omega_0^{-1} \tag{2.15}$$

Morphing the colored integrals in the lower graph of Figure 9 by pulling the base of the vertical line for q_0 where it crosses at $\theta(0)$ to the base of p_0 at $\theta(-\pi/2)$, and repeating for the next three phases, then rotating as in Figure 21 gives us the following:

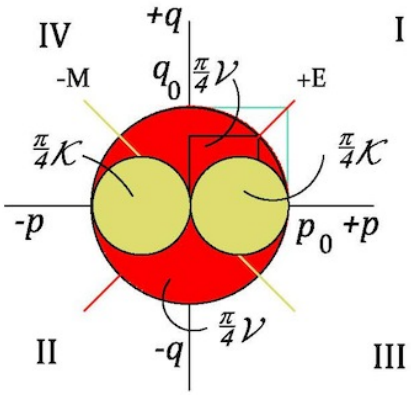

Collapse of $\mathcal{K}$ & $\mathcal{V}$ Integrals to Phase Space

π/8 of each in each phase

Figure 22

Note that the area of the region in each phase represented by $\mathcal{K}$ and $\mathcal{V}$ are each one half of what they are in the phase graph of Figure 9. We are getting close to a breakthrough. While our phase space representation, PS_2, so far has been two dimensional, the superposition of the energy component of an oscillation suggests

we look for a three dimensional representation, PS_3, or at least a two dimensional representation in spherical space, i.e. on a topological 2-sphere. In fact, the surface area of a sphere is twice the surface area of a circle if you count both faces of the circle's disk. This means that an octant, which is the equivalent of one quadrant of a one sided phase space, has an area of $\pi/2$, which is the area under the curve of $\mathcal{H}_0$ in Figure 9. In the phase sphere we are creating, the line for the Hamiltonian becomes a geodesic or great circle for the sphere and the area under the Hamiltonian curve for four quadrants or an area of 2π, is one half the spherical area and represents the energy/action/power integrals over one cycle of time and one hemisphere.

To construct PS_3 from the Figure 21 bottom figure, we pick up the left and right sides of the energy path from the intersection of the circle and p-axis, folding along the q-axis, and pinch them together at the apex of the hemisphere, like a phase space taco. We also rotate the $+p$-axis and the phase space circle around the q-axis as shown in Figure 23. Note that the point at which the taco is pinched together is r_0 from the

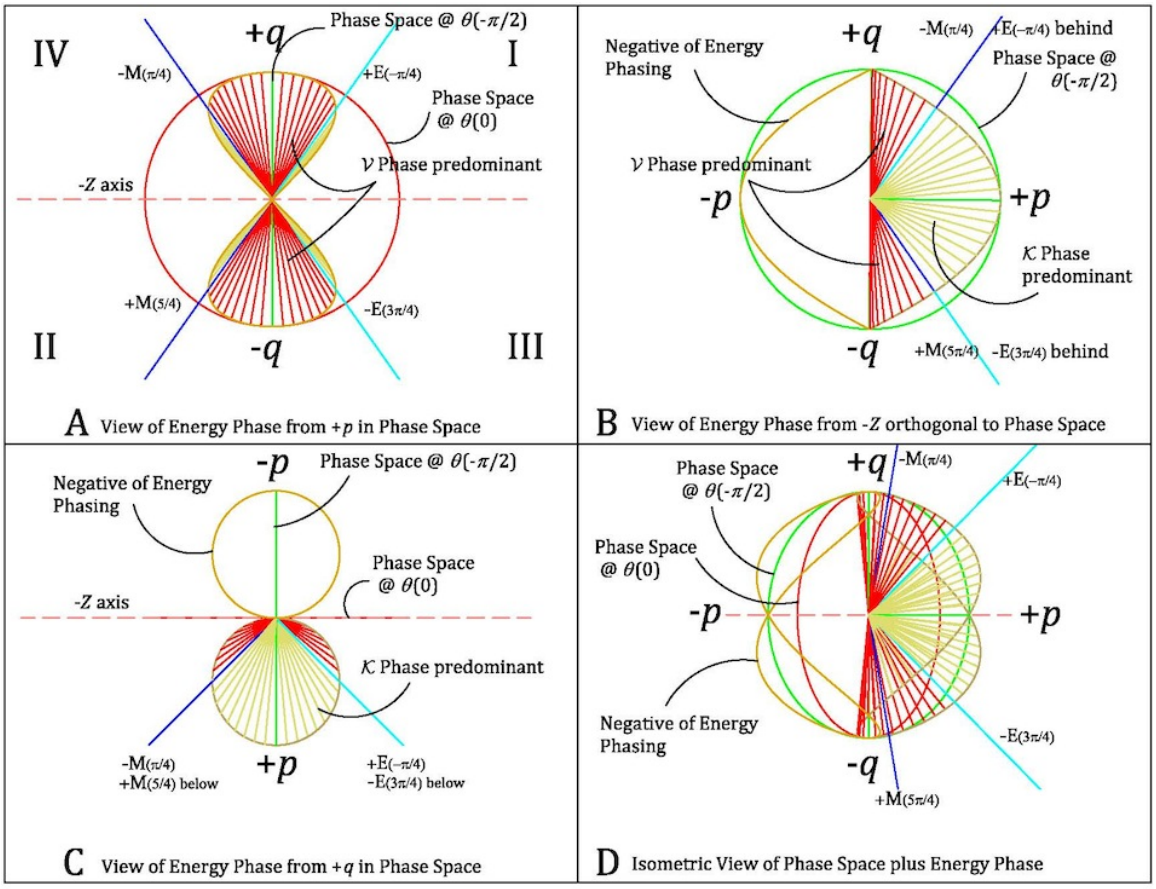

Superposition of Energy Phase Space and conventional Phase Space for Reciprocal Path Oscillation

Figure 23

center of the rotated phase space and the phase sphere and that it is at the point in phase space where q is zero, that is the oscillator, O_{ps}, is at zero displacement. Note

also that the point at $+p$ where the taco is pinched and along the radial behind it, the left and right halves of the phase space are sealed together, creating and separating the upper and lower sections, so that as O_{ps} cycles around the taco edge, it crosses its own path at each half cycle as one might draw a figure 8 with one stroke instead of drawing two circles.

Figure 23-A shows the view from the $+p$-axis on the surface of the hemisphere. Each of the spokes has length r_0, originating at the center of the space and terminating in the oscillator path for O_{ps}, and is separated from the one on either side by a 5 degree segment of the space. There is no significance to the 5 degree magnitude of separation other than as a convenient way of dividing and depicting the cycle in the creation of the graphic. There is significance, of course, at the transition between the red and gold radii, colored blue and cyan, at $\pi/2$ separation midway along the path in each quadrant, as they represent the E and M moments of energy transitions. The oscillation moves through each of the segments in the same interval of time. The colors are as in the previous graphs, red for potential and gold for kinetic, corresponding to the energy phase being transited by the oscillator O_{ps}.

Figure 23-B is a view from the great circle boundary of the hemisphere, parallel to a newly defined z axis. Figure 23-C is the view from the $+q$-axis. Finally Figure 23-D is an angled view from the qz plane. O_{ps} follows the same general path on the upper left figure as the arrows shown in the bottom figure of Figure 21. The geometry as shown is accurate and not simply suggestive as with Figure 21. The path starts at $+p_0$ at $\theta(-\pi/2)$, arcs through +E to $+q_0$ at $\theta(0)$, returns through –M to cross itself and the original phase space circle at $+p_0$, $\theta(\pi/2)$, before arcing through –E to $-q_0$ at $\theta(\pi)$,through +M to complete the cycle at $+p_0$, $\theta(3\pi/2)$.

Note that at each pass through $+p_0$, O_{ps} is traveling in the $+z$ direction so that the total path generates an angular momentum vector parallel to the $+q$-axis through the center of the lower circle in 23-C above the point, $+p$. As O_{ps} moves, it rotates PS_2 with it along the path, pivoting it around the q-axis, so that with each two octant path, PS_2 completes a π or one half rotation and flips its surface orientation, here from left to right. O_{ps} travels at a constant angular velocity in PS_2, and PS_2 rotates on edge at the same constant angular velocity in PS_3.

Aside #1
A reading of Aside #1 at this point is recommended, but optional.
End of Aside #1

Figure 23 is a depiction in PS_3 of a linear oscillator, O_l, in PS_2. The energy relationships remain the same from our earlier discussion, in which the Hamiltonian is invariant, the Lagrangian oscillates between +1 and -1, and the oscillator passes through four maximum action/power moments, two mechanical capacitive and two mechanical inductive, over each cycle.

It would be interesting to see if there is a corollary in PS_3 to the UCM of O_c in PS_2. Remember that in that instance we had a uniform angular velocity and a constant displacement magnitude of r_0, therefore a constant potential energy with respect to the center of motion of, $\mathcal{V}_0$, and a constant rotational kinetic energy of $\mathcal{K}_0$, therefore an invariant Lagrangian of zero. Every possible point, O_{ci}, on the circle of motion in PS_2 is a $+q_{0i}$, $-q_{0i}$, $+p_{0i}$, and $-p_{0i}$ along with every point in between with respect to some set of axes, q_i-p_i,.

We might imagine, therefore, that each of the radii shown in the 4 figures of Figure 23 represents a radius of intersection with respect to different paths along the surface of PS_3, each with its own phase space, PS_{2i}, and its own point of maximum conjugate momentum, p_{0i} at the location $+p_i$, forming a circle, C_{+p} in the zp plane. All share the same radius of maximum potential at $+q_{0i}$ and $-q_{0i}$ and each and every PS_{2i} intersects at and rotates in unison with, i.e. at the same frequency as, the q-axis or rotation θ. We will call this rotation, ϕ, a rotation not of a point in PS_2, but rather of a disk PS_2 normal to θ. At any point in time, four paths of oscillation, whose points of zero displacement on C_{+p} are $\pi/2$ apart, are at one of the four action/power moments, +E, -M, -E, and +M, so that these moments rotate in unison with θ, which rotates to the right hand rule as an axial vector parallel to the $+q$-axis. Each of the paths has an anti-path or polar opposite, defined as the path with an equilibrium point π apart on C_{+p}, so that they share the front and back sides of a common PS_2, though the O_{ps} for each are π apart in their cycle. Thus the two back-to-back PS_2's incorporate the instant +/- E's, and +/- M's, which creates an effective armature, a disk formed by the instant PS_2's that rotates on end with θ, and in turn rotates about an axial vector, ϕ, orthogonal to θ, its ends intersecting the circle, C_{+p}, creating two torques of opposite chirality along the circle as it rotates.

It is important to point out that the pair of PS_2's just described, which we will call disk ϕ, are the only "real" PS_2's in the system, as each of the others is simply a 2π circuit with respect to a reference point on the circumference of disk θ designated $+p_i = O_{psi}$, indicating where θ crosses C_{+p} on its path. Each such crossing is unique to the circumference of θ, and there is a 1 to 1 correspondence between their circumferences. Thus the path of each O_{psi} traces a path as seen in Figure 23 on the surface of the sphere PS_3, as disk ϕ rotates on its rim with θ and about its axial vector in PS_3. Thus the θ of our original PS_2 in the zp plane becomes ϕ after rotation into PS_3.

Figure 24 shows the superposition over one cycle of the paths of two such PS_2's separated in ϕ by $\pi/2$. In this representation, the induction moments, +/- M, of the original path of $PS_2(-\pi/2)$ are coterminous in PS_3 with -/+ E, the capacitive moments of $PS_2(\pi)$, which leads it in space and lags it in time by $\pi/2$. The co-incidence of these moments is therefore separated in time by one half cycle. The inverse or negative paths of these two PS_2's can be seen in 24-C, completing the cloverleaf pattern. Each PS_2 and its inverse are co-extensive in phase time, but of alternate sense, i.e. they have an angular separation of π in phase space.

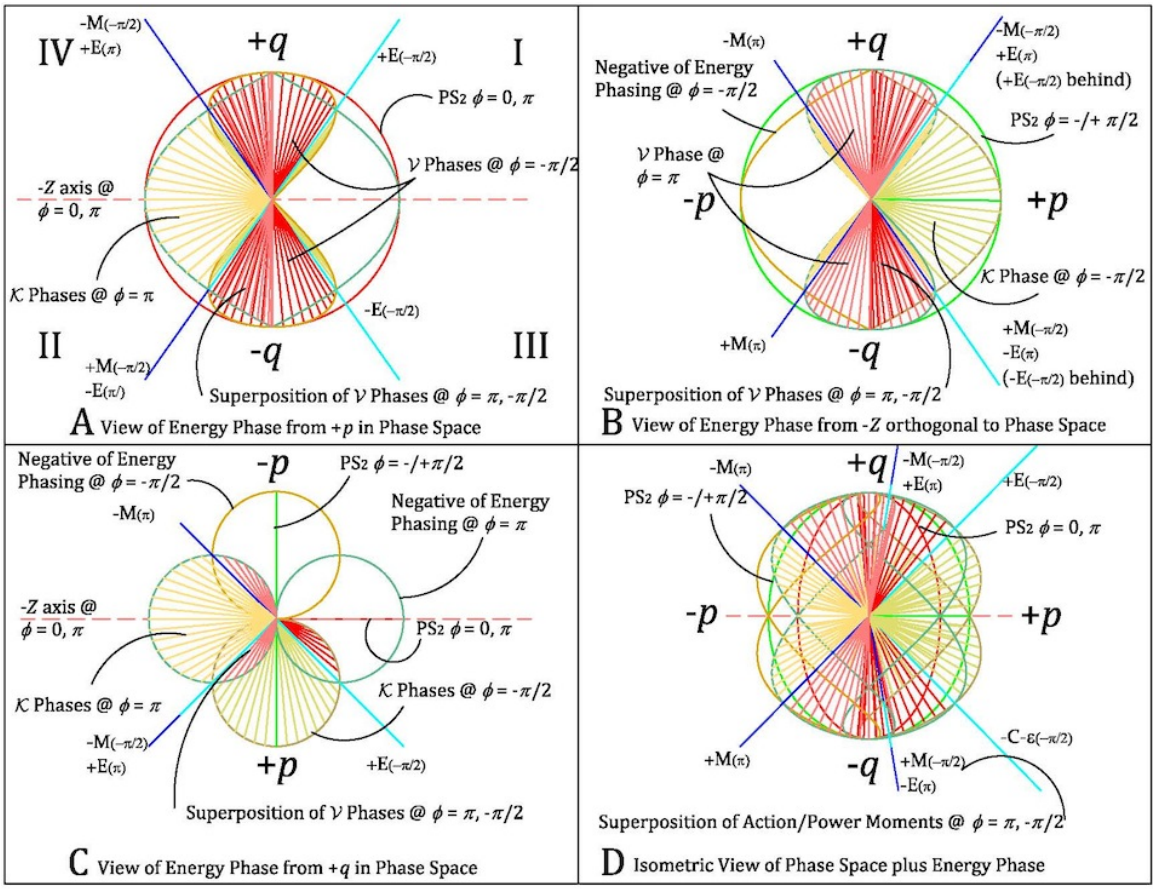

Superposition of Energy Phase Space and conventional Phase Space for Cyclical Path Oscillation (Phase Space Rotates as ϕ about $+q/-q$ Axis)

Figure 24

It bears emphasis that the action/power moments are contiguous with, in the plane of, disk ϕ, but remain fixed over time at an angular displacement of $\pi/4$ from both the θ / q-axis and the plane of circle C_{+p}. While they rotate with θ, it is the rotation of ϕ about its axis in the zp plane that actually advances the moments and thereby the rotation of θ and not the other way around. This advance constitutes a tangential, in terms of our phase graphs, longitudinal momentum component of the otherwise transverse oscillation of the O_{psi} between $+q$ and $-q$, which generates the angular momentum of θ.

Simple Harmonic Motion and Rotational Oscillation or Spin Space

Accounting for the Generation of Spin and Charge

If we were to sum up all the paths over one cycle of PS_3, by summing up the paths around the *q*-axis, it would look something like the views in Figure 25. The similarity of 25-A with Figure 22 is clear. The concentration of the potential energy components about the +/- *q* poles and the *q*-axis and of the kinetic energy around the +*p* circle is instructive. The persistence of the action/power moments is also clear. This indicates the invariant, maximum value of the action and power of the oscillation over time and the energy fields indicate the invariance of both $\mathcal{V}$ and $\mathcal{K}$ and hence the existence of an invariant Lagrangian of 0, as

$$\mathcal{L} = \mathcal{K} - |\mathcal{V}| = |p_0 \dot{q}_0| - |\dot{p}_0 q_0| = 0 \tag{3.1}$$

The Hamiltonian is obviously invariant. In the earlier case of (2.14) we had determined a Hamiltonian of 1 and therefore an average $\mathcal{V}$ and $\mathcal{K}$ each of ½. In the case of PS_3, the energies are doubled due to the presence of the inverse components of the phase space paths as seen in 23-C, thus $\mathcal{V}$ and $\mathcal{K}$ each equal 1.

$$\mathcal{H} = \mathcal{K} + |\mathcal{V}| = |p_0 \dot{q}_0| + |\dot{p}_0 q_0| = 2 p_0 q_0 \omega_0 \tag{3.2}$$

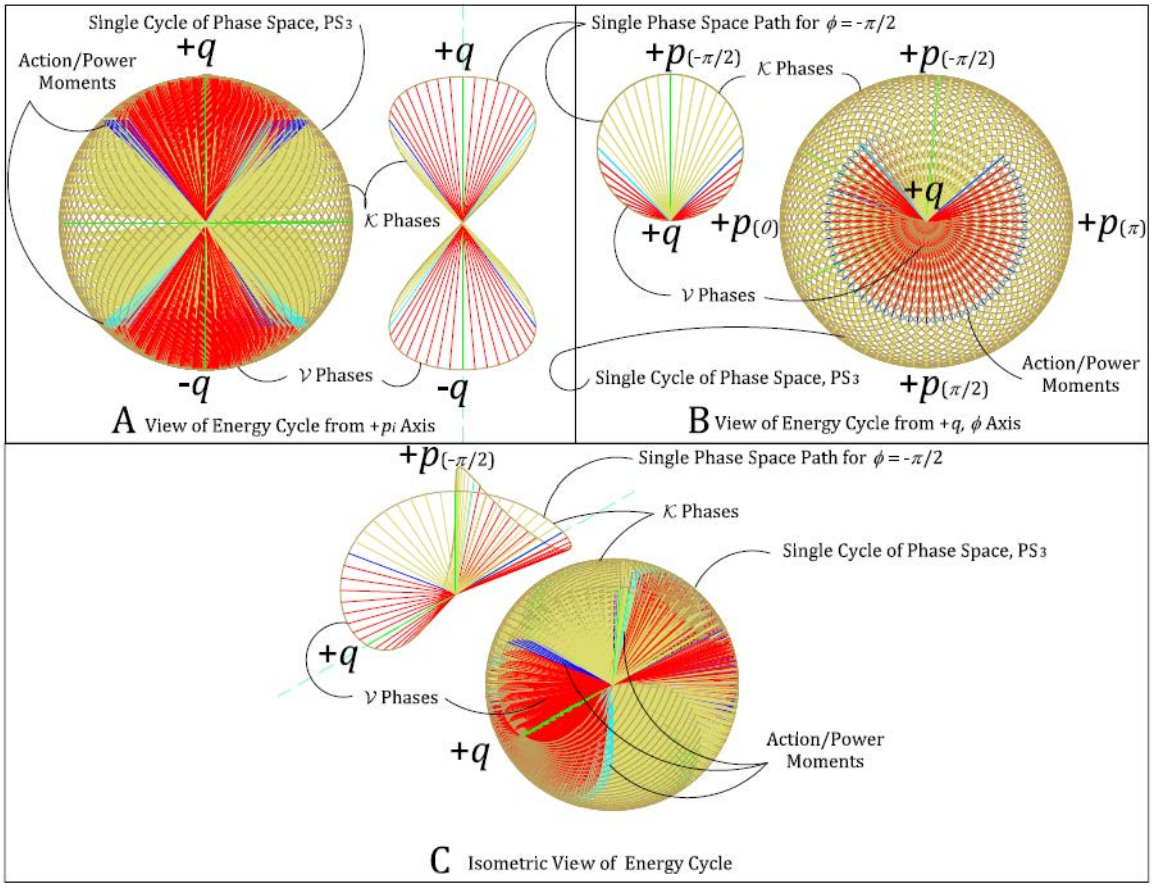

Superposition of Phase Spaces over Whole Energy Cycle
for Cyclical Path Oscillation (Phase Space Rotates as ϕ about +*q*/-*q* Axis)

Figure 25

The action/power moments as shown in Figure 24-C have an orthogonal projection along any +p co-radial in the zp plane of $1/\sqrt{2}$ and as in 24-A, along the +/-q-axis of $1/\sqrt{2}$. With respect to its initial position in C_{+p}, each moment, +/-M_i and +/-E, has an orthogonal distance to its $+p_i(-\pi/4)$ radial of $\sqrt{3}/2$ and a distance from the PS_3 center to the projection along the radial of $1/2$. Thus, the sine of the angles $\boldsymbol{\varepsilon}$ and $\boldsymbol{\mu}$ between each moment and the equilibrium radial at $+p_i(-\pi/4)$ of +/-K is $\sqrt{3}/2$ and the cosine is $1/2$. This is depicted in the following Spin Diagram 1 of Figure 26.

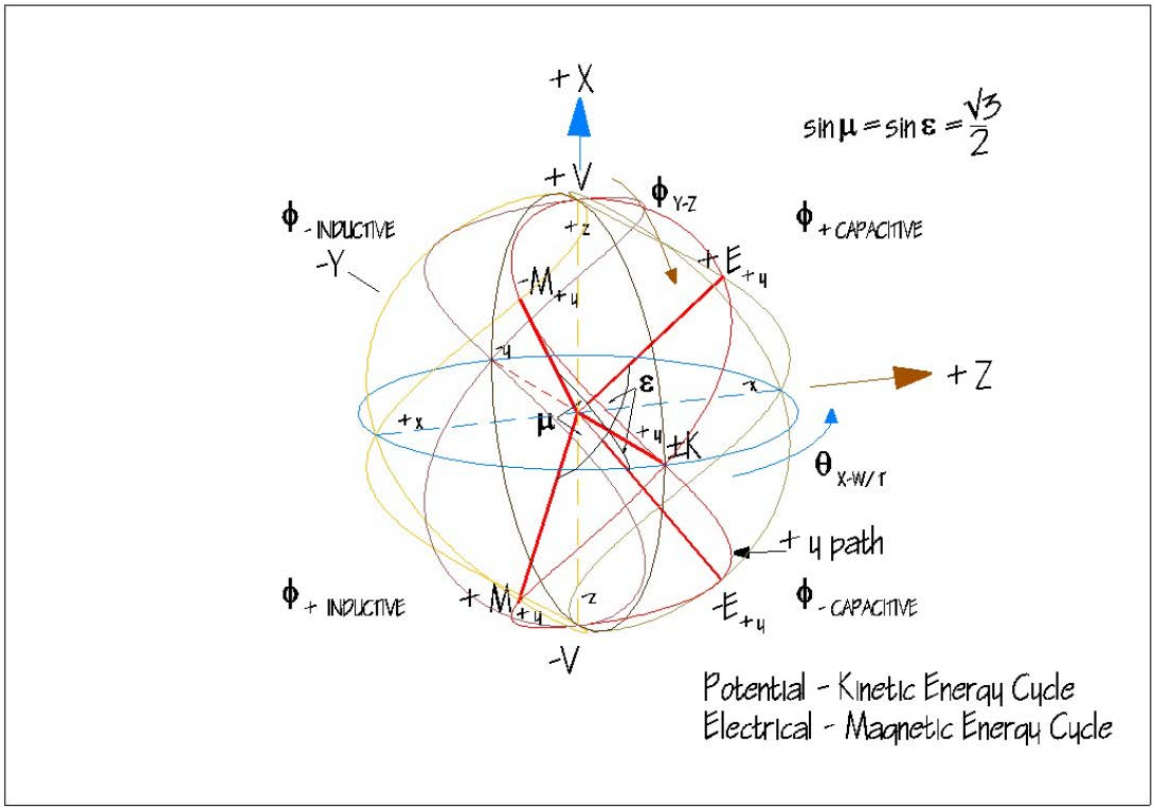

Figure 26 – Spin Diagram 1

Those with a more technical background will see in this last paragraph a suggestion of a quantum interpretation of this model and they would be correct. The action in the quantum case is Planck's reduced quantum of action or $\hbar$ (h-bar) as previewed in (2.13). We must ask then, just what is it that oscillates to produce a quantum PS_3. The reader might be tempted to suggest a lepton or perhaps a quark field, but we will pursue a more classical approach, and to do so we will need to take another aside, this time into an analysis of stress.

In the description of the creation of the PS_3 model for a linear oscillation, O_l, we referred to Figure 21 as a jumping off point from our discussion of phase space and the phase graphs in the interests of continuity by showing that PS_3 was a natural extension of that discussion. We will now look at another way of developing that model for a cyclical oscillation, O_c, from a discussion of stress.

Aside #2
A reading or review of Aside #2 is recommended at this point.
End of Aside #2

Based on the aside comments concerning stress, strain and elasticity, we can state that the theory of general relativity models space as an elastic medium, albeit coupled with time so that the stress tensor has an additional dimension, that of time. In that theory, particles of matter and energy couple with spacetime in a manner that warps or distorts, i.e. strains that spacetime, resulting in its curvature. Such curvature in turn directs the motion or travel of these particles along geodesics or energy conserving paths through spacetime that we recognize as gravity. A gravitational field therefore consists of the curvilinear strain of spacetime, stress-induced by large aggregates of mass and energy, upon which individual particles of mass and energy are constrained to follow. Such spacetime is elastic in the sense that it becomes distorted from rectilinearity by a transiting celestial body as the body moves through it, but returns to its general undistorted configuration after the body moves on.

Some authors would say that it is not space that distorts due to the presence of mass/energy, but time. In fact, in general relativity space and time are not considered as separate properties, but rather interchangeable components of a 4-dimensional spacetime. This is a topic that we could spend volumes on, but it suffices to point out that time is a means of accounting for changes in the configuration of particles or bodies of mass and energy observed to be *in space*. It is my opinion that time is simply a measure of distortions, changes or motion in or of space. If there were no motion or other change in space, there would be no time. If time is therefore a comparison of two different rates of change in space, the most fundamental of such changes in terms of its scope is the expansion rate of the universe. This appears to be exponential, due to the perceived acceleration of universal expansion. By comparison the speed of light as a calibrator of time is important but of secondary primacy, since it is a measure of the rate of change of position of electromagnetic waves occurring *in an expanding universe* of apparently finite age, and therefore would appear to be conditioned by any changing stress and density of that expansion, perhaps invariant over time, perhaps not. If time itself expands linearly along with each of three spatial dimensions due to cosmic expansion, then the speed of light, *c*, will be invariant by definition. However, this does not speak to whether all the processes that occur now in one second, would have occurred 13 billion years ago in one second. Perhaps some would, perhaps some wouldn't.

Our interest here is not primarily with time, however, but stress within the context of Simple Harmonic Motion and Uniform Circular Motion. We can envision an instance of static stress, such as a loaded beam, in which the stress is not a function of time, but discussions of SHM necessarily involve time or at least frequency. We want to return to our discussion of PS_3, 3 dimensional phase space and the phase sphere, and examine how it might relate to an oscillation of stress and surface force

without the need of a body force, either as an initiating factor or an ongoing component of SHM.

We will start by imaging a single point in an inertially dense spacetime. The time component I am referring to in this "spacetime" is not some "unseen" dimension, but rather the same 3 dimensional space that we saw a moment ago, *all of it*, however changed by whatever has transpired within it, including by an ongoing expansion. What I mean by an "inertially dense" spacetime is a three dimensional modeling space, a virtual 3-D blackboard so to speak, that is everywhere inert, that is it will not change unless we, or other things within it, including expansion, do something to make it change. Such change, once engendered, can be represented by an additional, fourth dimension where we keep track of the changes. We can call that dimension a record or a history of change or we can call it time, but it does not exist "out there" in some other realm of multitudinous, corresponding 3-D spaces. That fourth dimension is all in our head, but that's alright, since so is the 3-D blackboard. Once we put a point in spacetime, it stays there unless and until we erase it. Oh, and this spacetime is the same thing as the one all around us that we call the universe.

This single point is so far out in extra galactic space that there is no other body, no point of light visible to us since we have no Hubble space telescope with us. Even our bodies are invisible. Just our minds and the single point that we can see. We want so see what happens to this point if we allow a condition of isotropic expansion of the space around it. The entire region around the point is moving away from it, which is another instance of inertia. There are after all two types of inertia, position inertia, q, in which a body at rest at some position stays at that position vis-à-vis our position, and momentum inertia, p, in which a body in motion along some trajectory stays in motion along that trajectory vis-à-vis our trajectory or position. Simple harmonic motion is a process that relates the ordered interplay of these two types of inertia so that we have the emergence of a concept of frequency, ω, and its inverted notion, time, t, as in how many <u>times</u> does the SHM occur while something else is occurring.

To my knowledge, inertia is not generally characterized as being of two types such as this, though this is consistent with Newton's first law. We can always find a trajectory and velocity parallel to a moving body that will put us in its rest frame, a rest frame that would otherwise be a moving frame to us. Rest inertia in this sense is always relative to a co-moving frame of reference of other bodies, but this does not preclude a rest frame defined by isotropic red-shift in an expanding cosmos.

It should be remembered that the rate of expansion, as given by the Hubble rate, H_0, at approximately 73 kilometers per megaparsec per second, is actually quite small. This indicates the universe is expanding, straining, at approximately 2.37… x 10^{-18} meters per meter per second, which is approximately 88.6 times smaller than the reduce Compton wavelength of a neutron, $\lambda\!\!\!^{-}_{C,n}$, a virtually undetectable length on the human scale. The meter of course does not represent a natural length scale. If

this strain, which as a ratio of relative length change per time is not length scale dependent, is figured with respect to $\lambda\!\!\!^{-}_{C,n}$, the length augmentation per second from expansion relative to that scale is 4.97… x 10^{-34} meter per $\lambda\!\!\!^{-}_{C,n}$ per second. This is approximately 30.78 times the generally accepted, theoretical smallest length scale of 1.61… x 10^{-35} meters, the Planck length. But the second does not represent a natural time scale either. Assuming the speed of light in a vacuum to be invariant, the time taken for light to transit a distance equivalent to $\lambda\!\!\!^{-}_{C,n}$ is the inverse of the angular frequency, obtained as

$$t_{C,n} = \frac{\lambda\!\!\!^{-}_{C,n}}{c} = \omega_{C,n}^{-1} = 7.00...x10^{-25} \text{ seconds} . \quad (3.3)$$

This indicates that the expansion strain rate with respect to a neutron scale of length and time, $t_{C,n}$, is the dimensionless strain number per time using a theoretical neutron radian, θ_n, as the time scale,

$$H_0\omega_0^{-1} = 1.65...x10^{-42} / t_{C,n} \quad (3.4)$$

The strain distortion length per meter at this time scale is

$$\lambda\!\!\!^{-}_{C,n} H_0\omega_0^{-1} = 3.48...x10^{-58} \text{ meter}/\theta_n \quad (3.5)$$

(3.4) is, once again, 30.78 times the theoretical smallest time scale, the Planck time at 5.39… x10^{-44} seconds. This ratio of times and lengths will be examined in the Verification section. However, (3.5) is 2.15… x 10^{-23} smaller than the Planck length. No experimental device currently available or to this writer's knowledge, even conceivable can penetrate to the Planck scale, let alone this much smaller scale.

Nuclear and other subatomic particle interactions, presumably occurring at or near the speed of light, operate on a scale that dwarfs this expansion rate. The length of time it would take light, whose velocity is supposed to be scale invariant, to transit the strain distance per meter is 7.90… x 10^{-27} seconds, during which time the expansion strain would be a mere 1.87… x 10^{-44} meters per meter, nine orders of magnitude less than the Planck length. The length of time it would take light to transit *this* distance is approximately 6.24… x10-^{53} seconds, again nine orders of magnitude less than the Planck time. Thus any random variation in position or conjugate momentum in the phase space of a nucleon dwarfs in scale any achievable determination of an absolute position in space and time.

Still, we would like to find a way to gauge the expansion locally, if indirectly. We have our position-inertia as discussed at the location of our point, and we can assume, instead of a second point, a translucent, momentum-inertial sphere around the central initial point at a scalable distance that we call r_0, moving out at a yet to be determined expansion rate. It is important that while we think of the way this and additional spheres will respond to changes in themselves and their positions, between each other and in their environment, we must understand that essentially they are not "things" at all. They simply represent loci of dynamic stress equilibrium, strain movements and their relationships in a small section of a single spacetime continuum in response to its overall expansion.

Our position-inertia is what we normally call mass, m, while our momentum-inertia is our old friend from phase space, conjugate momentum, p, which at r_0 is p_0. In terms of a position in spacetime, the mass is a measure of the inertial constant, ת, times the square root of the Gaussian curvature of the phase sphere PS_3 which we will designate as K, which happens to also be the angular wave number, κ, represented by the sphere or

$$\kappa = \sqrt{\mathrm{K}} = \sqrt{\frac{1}{r_0^2}} = \frac{1}{r_0} \tag{3.6}$$

Thus the unit mass, m_0, is

$$m_0 = ת\kappa_0 \tag{3.7}$$

the linear inertial density over the distance r_0 is

$$\lambda_0 = \frac{ת\kappa_0}{r_0} = ת\kappa_0^2 \tag{3.8}$$

The time rate of change in the unit momentum at the spherical shell per unit of surface area, is

$$\frac{\dot{p}_0}{\mathrm{A}_0} = \frac{\tau_0}{\mathrm{A}_0} = f_{t0} \tag{3.9}$$

As shown, this is equal to the stress at the surface of the sphere. It is important that we understand what this means. If we are standing at a point in space at which every point around us is moving away from us at some finite speed, with the understanding that the same is happening for every other point, we have to ask ourselves what determines this speed. If the whole of the space around us were to be infinitely inert, it would mean that it could not move at all and there would be no expansion. If the whole of that space had zero inertia, it would mean that whatever and whenever some agency put it into motion, the expansion would be instantaneous. The fact that it has a finite speed that appears to be increasing over time, indicates that such space has an inertial component. Like a massive flywheel that requires decreasing energy input per radian of motion over time in order to accelerate, such a space, due to its inertial property would be expected to accelerate its expansion over time. With expanding spacetime such inertial acceleration constitutes a stress force field.

For an isotropic force field moving out from a central point which has no dimensional component, that is a radius of zero and a vanishing surface area, the stress at the point is infinite. This is physically untenable, so instead of a point we are compelled to assume that some geometric domain intervenes between the isotropic outward expansion force and the center point of the sphere. With expansion we should expect the generation of a spherical loci at radius, r_0, at which the expansion tension stress equals the reactive stress, establishing the elastic potential energy density of the interior of the sphere.

Once equalized, given only a tension component of the stress, we would expect a dilatation or increase in r_0 related to the expansion rate. As discussed in the Aside #2 on stress and strain analysis, however, there are other components of stress

including lateral compression, shear and torsion to consider. The net effect of this would be the production of torsional, i.e. limited rotational oscillation and the creation of a central angular acceleration of the sphere that works counter to any dilatation at its surface. Since the spherical discreteness we are examining is a locus of stress equilibrium in an otherwise continuous manifold, and not a discrete body in isolation in a true vacuum, we would not expect full rotation of the sphere, which would create unsustainable axial strain and stress at the poles of the rotation. Rather we would expect axial oscillation in keeping with our model of PS_3. Once initiated, with increasing expansion stress, the increasing rotational strains are anticipated to accelerate tangentially and therefore centrally, resulting in a net differential central force radiating isotropically and responsible ultimately for coupling with a gravitational field.

If we let the sphere expand, we will once again have no way to gauge the expansion around it, and if we keep it fixed, we are in the same pickle. (At this point we have no measuring rods and no clocks.) We think about it for a few minutes and realize isotropic expansion implies expansion about all points, so that if we put some additional, similar spheres around the single one and keep them all sized at r_0, allowing them all to touch, we might eventually be able to notice some variation in their motion with expansion. We can get twelve such spheres around the initial sphere, as in Photo 1, and find it interesting that the only way we can get them all in place is to create a lattice of four axes about the first sphere. We notice that each axis is normal to an arrangement of the central sphere with six spheres forming a hexagonal disk around it, and that each such arrangement has three sets of two opposing spheres in common with three other disks, making a system of 4 intersecting disks around a central sphere of equal size.

Cuboctahedral Lattice
Photo 1

Tetrahedral Aperture
Photo 2

Octahedral Aperture
Photo 3

We find that each and every sphere on the periphery of this arrangement has two other spheres in direct contact with it in the form of an equilateral triangle and in fact each sphere belongs to two such groups on opposite sides. We can transpose any three by rolling them simultaneously about the six in which they are nested, by a turn of $1/3\ \pi$. This rearranges the axes, bending three of them at the center around the first and affects the symmetry, but in the end returns the thirteen spheres to the

same tight density they had originally. Turning them back restores the 4-axial symmetry.

Now, if we allow the space around them to expand isotropically, after a period of time they each end up a distance αr_0 apart from the central sphere and from each in the adjacent pair on either side on the periphery. If we draw lines connecting the centers of each sphere, we notice the emergence of some recognizable geometry. The lines joining the twelve, periphery spheres form a cuboctahedron, which is the polyhedron formed by drawing a line between the midpoints of the 4 edges of each face of a cube. This creates a diamond on the face of each of the 6 cubic faces and an equilateral triangle where each of the 8 cubic vertices had been. This means that the twelve spheres in their pre-expansion position form a similar rectilinear grid, a cube with a sphere centered at each of its edge midpoints, for which the previously mentioned 4 axes are the cubic diagonals. The 8 vertices of this cube are positioned in the regions outside the three spheres about each corner and the centers of each sphere coincide with one of the midpoints of the cubic edges. The cubic edge measures $2\sqrt{2}r_0$ in this initial configuration.

What we have is the superposition core of an interlaced 3-axis rectilinear or hexahedral lattice centered through the cubic faces and a 4-axis alternating double tetrahedral plus octahedral lattice centered along the diagonals. The first lattice actually embeds a 3-axis octahedral lattice through the center of each sphere and a second 3-axis stretched rectangular lattice with a $\pi/4$ twist between adjacent axes through the periphery spherical centers and around the central sphere. The second lattice embodies the obvious local tetrahedral lattice along the diagonals. I have called it local, because if this close packing of spheres is carried out indefinitely, each sphere will have tetrahedral packing in each direction at each of its diagonals, but the diagonal and therefore lattice axis will run through an octahedral cell before entering another tetrahedral cell and then another sphere.

Looking at Photos 2 and 3, we do some quick checks and find that the cosine of each angle of the equilateral triangles of $\pi/3$ is ½ and the sine is $\frac{\sqrt{3}}{2}$ for an area of $\sqrt{3}r_0^2$ spanned by the three spherical centers, while the spherical cross-sectional area is $\frac{\pi}{2}r_0^2$; a difference for the tetrahedral "free space" aperture of $0.16125\ldots r_0^2$. The computation for the diamond on the six cubic faces is a bit simpler since each side is $2r_0$ for an area of $4r_0^2$ minus the spherical cross section of πr_0^2 for a difference for the octahedral "free space" aperture of $0.85840\ldots r_0^2$. This means that the octahedral aperture is 5.32330 . . . times larger than that of the tetrahedral aperture. It also means that the inertial density of the spheres is less about the customary cubic surface axes than about the diagonal axes, where we include only the area within the corresponding cuboctahedral surface, by a factor of

$$\frac{\pi}{4}\Big/\frac{\pi/2}{\sqrt{3}} = \frac{\sqrt{3}}{2} = 0.86602\ldots \qquad (3.10)$$

If we define the density as the ratio of the cross-sectional areas of the adjacent spheres to the corresponding aperture we have

$$\frac{4\pi}{0.85840\ldots}\Big/\frac{3\pi}{0.16125\ldots}=0.25046\ldots \tag{3.11}$$

Cuboctahedral Lattice showing both hexahedral and octahedral components

Photo 4

Lattice extension along 3-axes surfaces develops octahedron with stability of vertices and density of surfaces

Photo 5

Cuboctahedral Lattice

Lattice extension along 4 axes diagonals develops cube with instability at vertices and porous surfaces

Photo 6

Photo 4 shows additional elements to the cuboctahedron suggestive of an extended lattice. These configurations are made with small magnetic spheres, which have magnetic dipoles analogous to a neutron or proton magnetic moment. Photo 5 shows the stability of extension along the hexahedral 3-axes and density of the octahedral, diagonal 4-axes. Photo 6 shows an extension along the 4-axes with instability evident at the cubic vertices and a much greater porosity of the cubic surfaces. The internal structure of both Photo 5 and Photo 6, as in an indefinitely extended lattice, is the same cuboctahedral lattice. It is only at the boundaries, principally of the hexahedral component and in particular of the vertices, that the instabilities and therefore the differences emerge.

It is worth noting in the context of this lattice geometry that a cuboctahedral edge length is equal to the diameter of the central sphere, so that it is also equal to the radius of a sphere, *R*, circumscribed through the vertices. The distance from the center of the central sphere to the midpoint of the cuboctahedral edges is $\sqrt{3}/2\,R$ and from that center to the cubic faces is $\sqrt{1/2}R$. The first of these coefficients is the sine of the angles $\boldsymbol{\varepsilon}$ and $\boldsymbol{\mu}$ mentioned earlier in connection with Figure 26 and is significant to quantum mechanics as the magnitude, *S*, of the spin angular momentum of all fermions, for which the quantum spin number is $s=\frac{1}{2}$ and *S* is

$$S=\sqrt{s(s+1)}\hbar=\sqrt{\tfrac{1}{2}\left(\tfrac{1}{2}+1\right)}\hbar=\sqrt{3}/2\,\hbar \tag{3.12}$$

where $\hbar$ has been previously discussed as an invariant action. In terms of our discussion of PS_3 and SHM then, if $R = q_0$,

$$S=\sqrt{3}/2\,\mathcal{S}_0=\sqrt{3}/2\,\pi c\ . \tag{3.13}$$

The value $\sqrt{\frac{1}{2}}$ is the coefficient of q_0, p_0, τ_0, and c_0, at the moments +/-E and +/-M, when the action and power each reach a maximum ½ in PS_2 and an invariant ½ each as they rotate in PS_3.

No other Platonic or Archimedean polyhedral lattice embodies these significant, fundamental geometric coefficients. The takeaway from this is that isotropic expansion performed globally results in the emergence of the above-described lattice without any exogenous constraints. Of interest is the fact that this analysis suggests that the principal axes affected by expansion are the 4 axes of the diagonals. Assuming an inertial spacetime, this means that the principal tension axes in the locale under investigation, and thus on the surface of the central sphere, are these four diagonals and not the three cubic face axes. Thus the shear and shearing rotational/torsion stresses that would be expected by elastic stress-strain analysis to accompany an expansion tension are then about these axes and in the plane of each of the eight triple spheres delineating the cubic vertices. The inertia is more concentrated about these axes in response to such stress. These are free to rotate about the diagonals with less inertial resistance from other spherical domains than are the four spheres defining each cubic face about the three cubic face axes.

It is of interest that there is a two-dimensional correspondence to this three dimensional emergent phenomena. Rayleigh-Benard convection is the designation for the formation of a hexagonal lattice pattern of cells in a shallow layer of fluid subjected to gravity and a temperature, i.e. energy, gradient from below, in conjunction with the viscosity and thermal properties of the fluid. In the case of our current thought experiment, gravity and the properties of the fluid are replaced by the inertial properties of spacetime and the energy gradient is due to its isotropic expansion. The resulting planar convection cells are replaced by the stress/strain oscillations of spacetime. The form each emergent phenomenon takes is due to geometric constraint.

An essential aspect of this inertial spacetime is the concept of continuity, that is that the points *right next to* any given point cannot be transposed. While we can see that a lattice can emerge from stretching such continuity, it does not follow that such continuity can emerge from a collection of points not inherently so constrained, i.e. points free to move in the manner of a random walk vis-à-vis other points. Assuming an inertial, and within certain limits, elastic continuum, we would expect that with continued expansion and the geometric constraints of PS_3 and the above emergent lattice, that on some scale determined by the inertial density of the continuum, instances of torsion would occur.

In Figure 27, we have an example of such torsion operating in two orthogonal directions. There are two sets of co-ordinates shown with capital letters for reference purposes in keeping with the prior development of PS_3, one for the diagonal and one for the surface axes. The lower case co-ordinates indicate points in the field that are moved by the stress/strain relationship. In graphic #1, we have

defined a square with edges of $\sqrt{2}$ in keeping with the cuboctahedral description and our prior development of the moments E and M in PS_2 and PS_3. The torsional stress potential of #1 results with expansion in the defined strain of #2 shown by the co-ordinate pairs, followed by a second torsion strain in #3, which sets up a recoil stress potential indicated by the axial vector ϕ in #4. Upon recoil, the potential ϕ becomes the active axial vector $\boldsymbol{\phi}$, and initiates the angular momentum vector $\boldsymbol{\theta}$ in #5. This last step gives the Spin Diagram seen in Figure 26, which is advanced about $\boldsymbol{\theta}$ by half a rotation from #5.

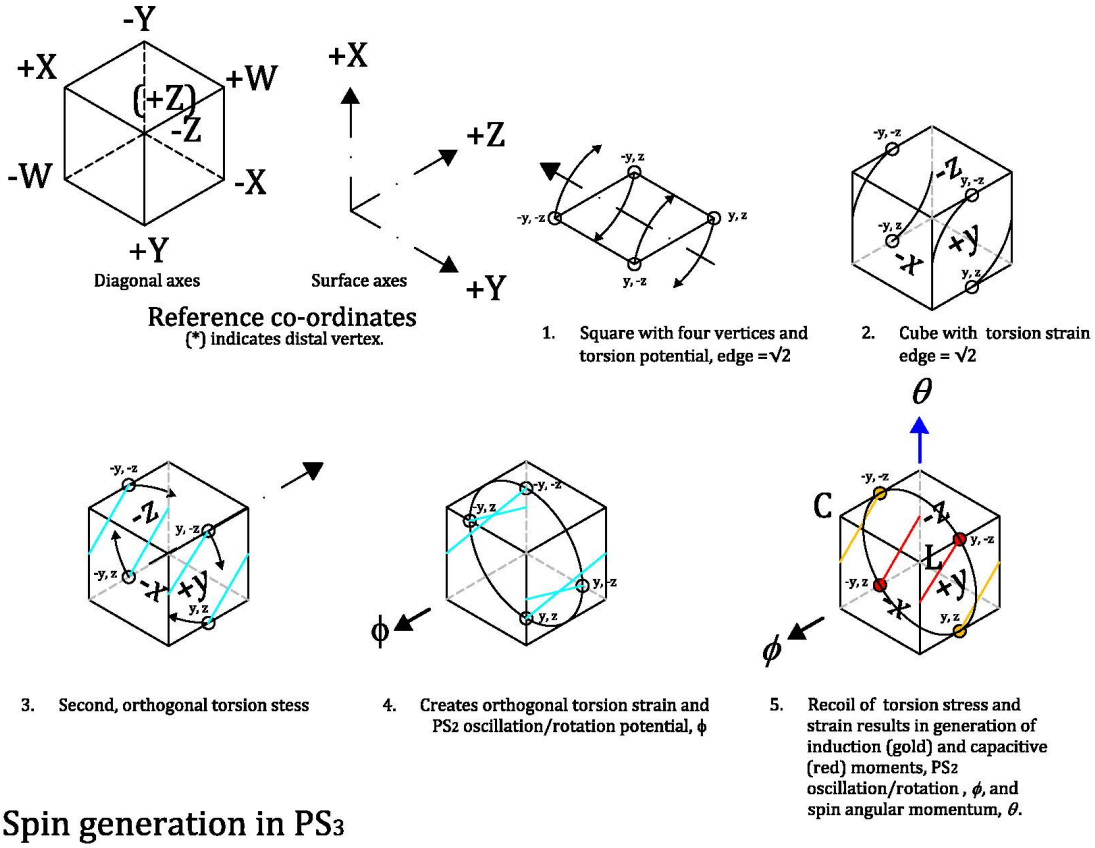

Figure 27 – Initial Strain State

In #5, the various *y,z* strains are colored to reflect their functional states at the point in time at which they constitute the +/- E and +/- M moments as shown. Figure 28 shows a continuation of the rotation of $\boldsymbol{\theta}$ over one cycle at ½ π stages or phases. As we will see, this is the resonant state of PS_3 which is recognized as the neutron. Each of the four phases consists of a ½ π rotation about $\boldsymbol{\phi}$ followed by a ½ π rotation about $\boldsymbol{\theta}$ according to the axial vectors shown. Each of these rotational sequences is equivalent to a right hand twist at each of the upper diagonals as shown. Such a sequence of twists, as well as the corresponding sequence of double rotations, rotates the permanently displaced +/- *x* faces of the cube about the X axis, while the +/-*y* and the +/-*z* faces alternately oscillate about their initial positions along axes Z and Y.

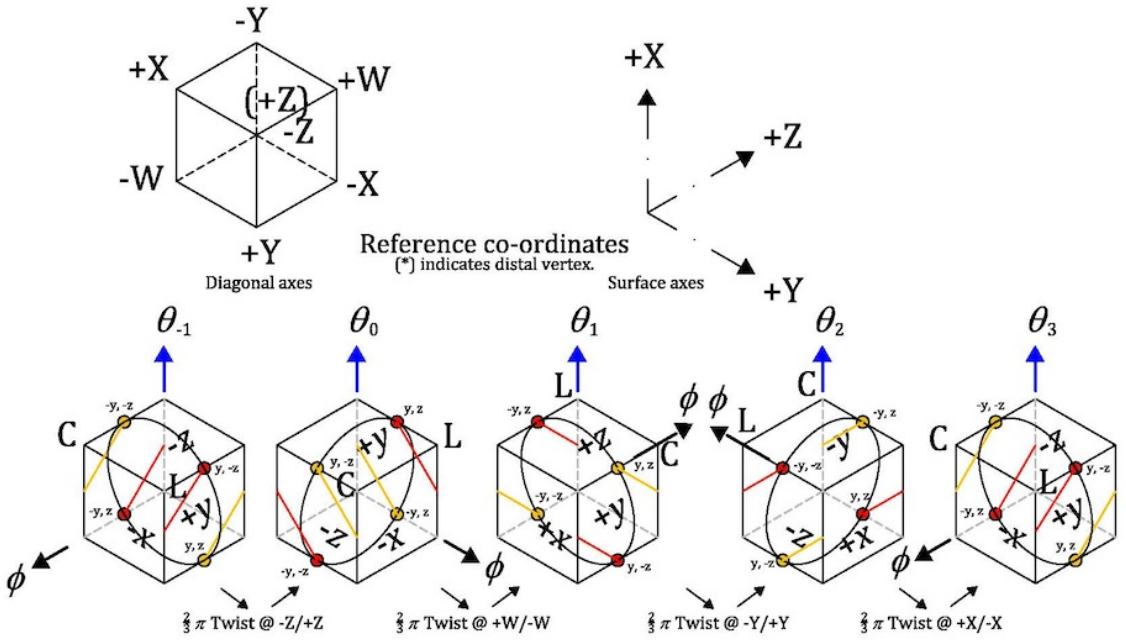

Combination of PS2 rotation, ϕ, and PS3 spin, θ, each over $\frac{1}{2}\pi$ is equivalent to a twist at diagonal axes of $\frac{2}{3}\pi$ as shown. The result is an oscillation of the torsion stress and strains, here shown with representations for each phase. The capacitive, C, and inductive, L, torques are found by crossing the two equilibrium or unstrained positions into the capacitive moments for the capacitive torque and the two inductive moments into their equilibrium or unstrained positions for the inductive torque. This particular sequence represents the resonant condition which is recognized in quantum phenomenology as the neutron. The quarks of the standard theory are the nodes/antinodes of the oscillation.

Resonant spin state, the neutron

Figure 28 – Resonant Strain State

The twisting motion of the triplets about the diagonals constitutes an oscillation of the tetra-octahedral lattice and the principle stress/strain relationship in the continuum responsible for generating the property of spin. Why it is this and not the hexahedral lattice that is primary can be found in the notion of the conservation of angular momentum. Such conservation directs the energy flow in a torsional stress into whatever structure incorporates the smallest moment of inertia. The moment of inertia, *I*, of the cuboctahedron of Photo 1 is less about the diagonal axis through the tetrahedral aperture (*TA*) as shown in Photo 2 than about the surface axis through the octahedral aperture (*OA*) in Photo 3. Assuming uniform density of the spheres, the sum of the distance from each spherical center to the associated axis gives a measure of *I* as

$$I_{TA} = 6(1) + 2\left(3\left(\tfrac{1}{\sqrt{3}}\right)\right) = 6\left(1 + \tfrac{1}{\sqrt{3}}\right) = 9.46410\ldots \qquad (3.14)$$

where 1 is the distance from the central sphere to each of the 6 adjacent spheres in the central plane and $\frac{1}{\sqrt{3}}$ is the distance from each of the triple spheres about the pair of *TA*s to the corresponding axis, and

$$I_{OA} = 4(1) + 2\left(4\left(\tfrac{1}{\sqrt{2}}\right)\right) = 4\left(1 + \sqrt{2}\right) = 9.65685\ldots \qquad (3.15)$$

where 1 is the distance from the central sphere to each of the 4 adjacent spheres in the central plane and $\frac{1}{\sqrt{2}}$ is the distance from each of the quadruple spheres about

the pair of *OA*s to the corresponding axis. This gives a slight advantage to torsional oscillation about the diagonals.

As a description of this oscillation, we can rotate diagonal -Z with its two pairs of triplets by a rotation of $2/3\ \pi$ ccw. This moves the cubic face +*y,* onto which we can draw an arrow pointing up, to the top with a rotation ccw of ½ π of the arrow to point left. We repeat the same rotation diagonal +W, which moves +*y* back to its original position, but now rotated ccw π from its original orientation with the arrow pointing down. At diagonal –Y we repeat the procedure, which rotates +*y* to the bottom of the cube, presumably in the same orientation as when it was on top. (You can peek if you want and make sure, but the arrow does point left.) Finally we focus on diagonal +X and rotate the axis as before. +*y* returns to its original position with the arrow pointing up. No co-ordinates have been harmed in the making of this movie. No entanglement of an arbitrary *x*, *y* and *z*, so that we have to untangle them every even number of rotations. The net effect is a sustained angular momentum of the system about the top face. An oscillation over 4 axes creates a rotation in three without an actual complete bodily rotation of the center sphere. In fact, when we analyze its motion, it very accurately embodies the motion of the PS_2 disk in the PS_3 sphere. In short, the expansion of an inertially dense spacetime overtime naturally and necessarily leads to the emergence of a discrete unit, i.e. a quantum, oscillation with angular momentum of ½ $\mathcal{S}_0$. It is such oscillation that is described by PS_3.

There is a more work needed to nail this down. If we cross the action/power moments of PS_3, with respect to their positions prior to displacement on the equilibrium circle C_{+p} into those positions for the +/-M and from those positions into the moments for +/-E, we obtain two axial vectors or torques, one for the two capacitive moments, $\mathbf{C}\varepsilon$, and one for the two inductive moments, $\mathbf{L}\mu$. The angles for this crossing, μ for the inductive and ε for the capacitive moments, are $\pi/3$.

These torques necessarily rotate synchronically with the moments in $\boldsymbol{\phi}$ with the inductive torque leading the capacitive torque by ½ π, both inclined away from the angular momentum vector. These apply a maximum torque to each of the θ axes of the rotating PS_2 disk, mitigating the recoil of θ to align with ϕ, and advancing the rotation of the restorative force of SHM. They also generate a magnetic moment antiparallel to the angular momentum or spin vector. Thus

$$\left[\left(-\mathrm{M}\times p_{-3\pi/4}\right)+\left(+\mathrm{M}\times p_{+\pi/4}\right)\right]=\mathbf{L}_{\mu} \tag{3.16}$$

$$\left[\left(-\tau_0\times -q_0\right)+\left(+\tau_0\times +q_0\right)\right]\sin\mu=2\left(i\tfrac{\sqrt{3}}{2}\tau_0 q_0\right) \tag{3.17}$$

$$\left[\left(p_{-\pi/4}\times +\mathrm{E}\right)+\left(p_{+3\pi/4}\times -\mathrm{E}\right)\right]=\mathbf{C}_{\varepsilon} \tag{3.18}$$

$$\left[\left(-q_0\times +\tau_0\right)+\left(+q_0\times -\tau_0\right)\right]\sin\varepsilon=2\left(-i\tfrac{\sqrt{3}}{2}\tau_0 q_0\right) \tag{3.19}$$

While the two components in each torque can be represented as one axial vector, in terms of the magnitude of the torque, they operate separately on each half of the rotations $\boldsymbol{\phi}$ and $\boldsymbol{\theta}$. These are shown in Figure 29 for the resonant state, the neutron.

The upper figure shows the four figure eight paths of points +/- y, +/-z on the PS_2 disk prior to the torsional strain. PS_2, which is centered on the axial vector $\boldsymbol{\phi}$, is positioned so that the physical point +z is displaced to the point +q of PS_3 in Figure 23, one of the two functional points, +/-V, of maximum potential energy for +z *and all other points on the circle of* PS_2 . This is designated as the time $\theta\left(\frac{\pi}{2}\right)$, where the time $\theta(0)$ is represented by the position of the axial vector $\boldsymbol{\phi}$ parallel to the +Y axis. The moments +/-E and +/-M, represented by the black "X", are located at time $\theta\left(\frac{\pi}{4}\right)$, and $-M_{+z}$ indicates the position of +z when it is at the moment of maximum power on the discharge or induction leg of its cycle traveling in the –X direction. The angles $\boldsymbol{\varepsilon}$ and $\boldsymbol{\mu}$ are shown. It is important to note that the selection of the points +/-z and +/-y are arbitrary and that the moments E and M exist for all points on the circle C_{+p} that includes these four points.

The lower figure shows the oscillation at time $\theta\left(\frac{\pi}{2}+\frac{\pi}{4}\right)$ when +z has reached -M and the other points +y, -z, and -y have reached the other moments shown. The two torques generated by these moments are shown at $\mathbf{L}_{\mu}$ and $\mathbf{C}_{\varepsilon}$. Most significantly, the effects of these torques on what we will call the nodes and antinodes of $\boldsymbol{\phi}$ and $\boldsymbol{\theta}$ are shown by the small red, ε, and gold, μ, vectors along the $\boldsymbol{\theta}$ rotational path. The inset on the lower left of the figure enlarges these and also shows the condition of $\boldsymbol{\phi}$ at maximum potential energy point +/- V. All are as viewing the sphere from the exterior toward its center. Note that at the positions of +/-V and +/-W, ε and μ are orthogonal and that their dot product therefore vanishes and their cross product is maximum. At K_0 and K_{π}, they are parallel, the cross product vanishes and the dot product is maximum. We will see the effect of this on spin and charge in a few minutes.

Overtime, as the continuum continues to expand, its mechanical impedance decreases and the inductive torque advances and drops generally antiparallel to the angular momentum vector, reversing the direction of the magnetic moment vector to align with the spin and transmitting a portion of its power and energy as the electron, decreasing its frequency slightly in the process. In the event of a retarding of the inductive torque, which generally will not occur in the context of expansion, the capacitive torque drops generally anti-parallel to the spin vector, creating the antiproton and transmitting the positron.

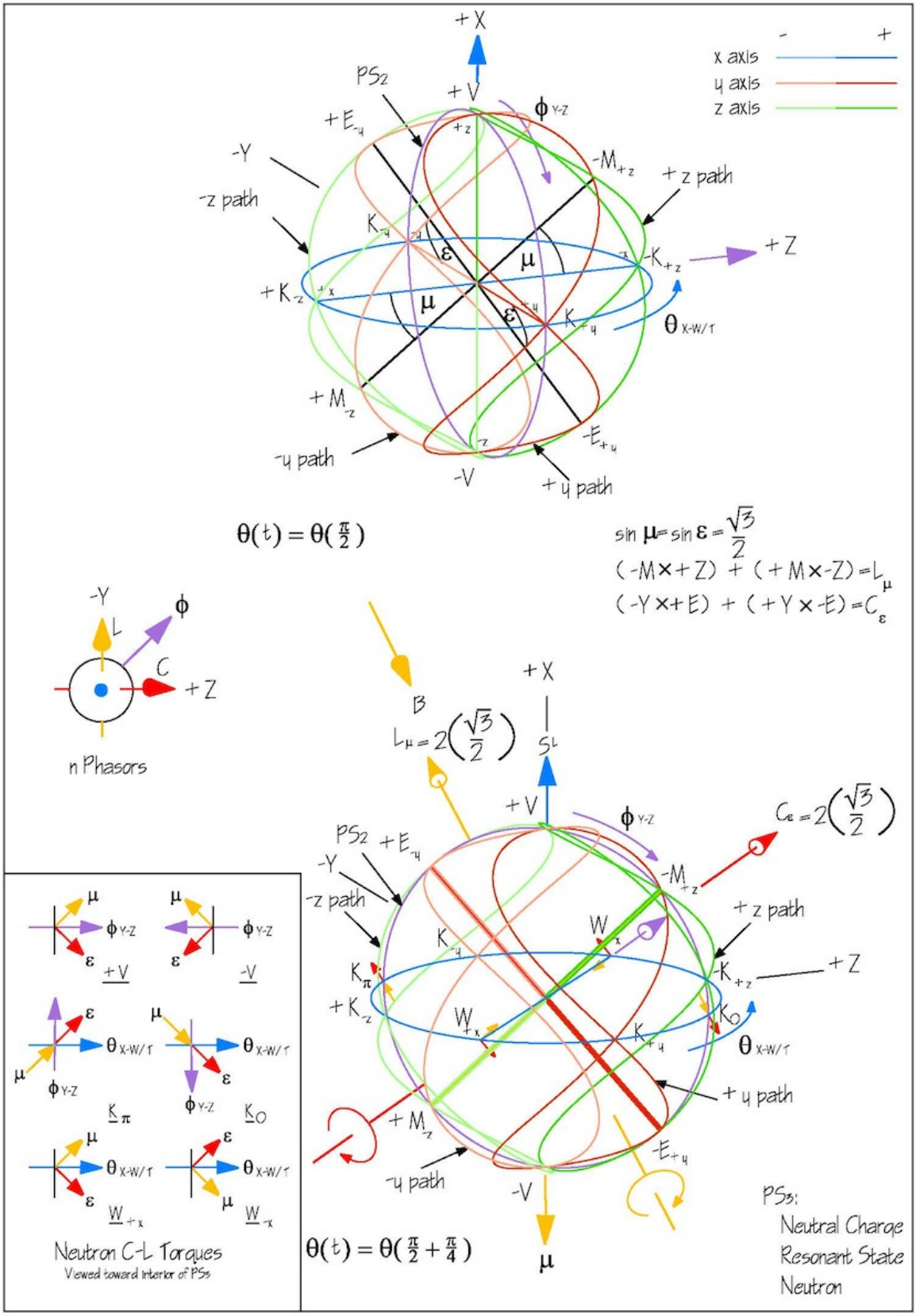

Figure 29 - Spin Diagram 2, Neutron

Figure 30 indicates the strain relationships associated with beta-decay and the emission of the electron. The drop in mechanical impedance and inertial density arising from spacetime expansion effectively pulls at the nodes of rotation $\boldsymbol{\phi}$, increasing the strain. These nodes are designated by the W points on the lower diagram of Figure 29. As we will see shortly, this is particularly significant at the W_{-x} node. Over time, this advances the $\boldsymbol{\phi}$ axial vector in $\boldsymbol{\theta}$ without a corresponding rotation of $\boldsymbol{\phi}$ itself. This is seen in Figure 30 as indicated at step 2. Recoil of the strain as indicated by the four point pairs results in a rotation reversal of $\boldsymbol{\phi}$ and a flip in the spin vector $\boldsymbol{\theta}$. A portion of the energy of PS_3 continues on as the emitted electron state.

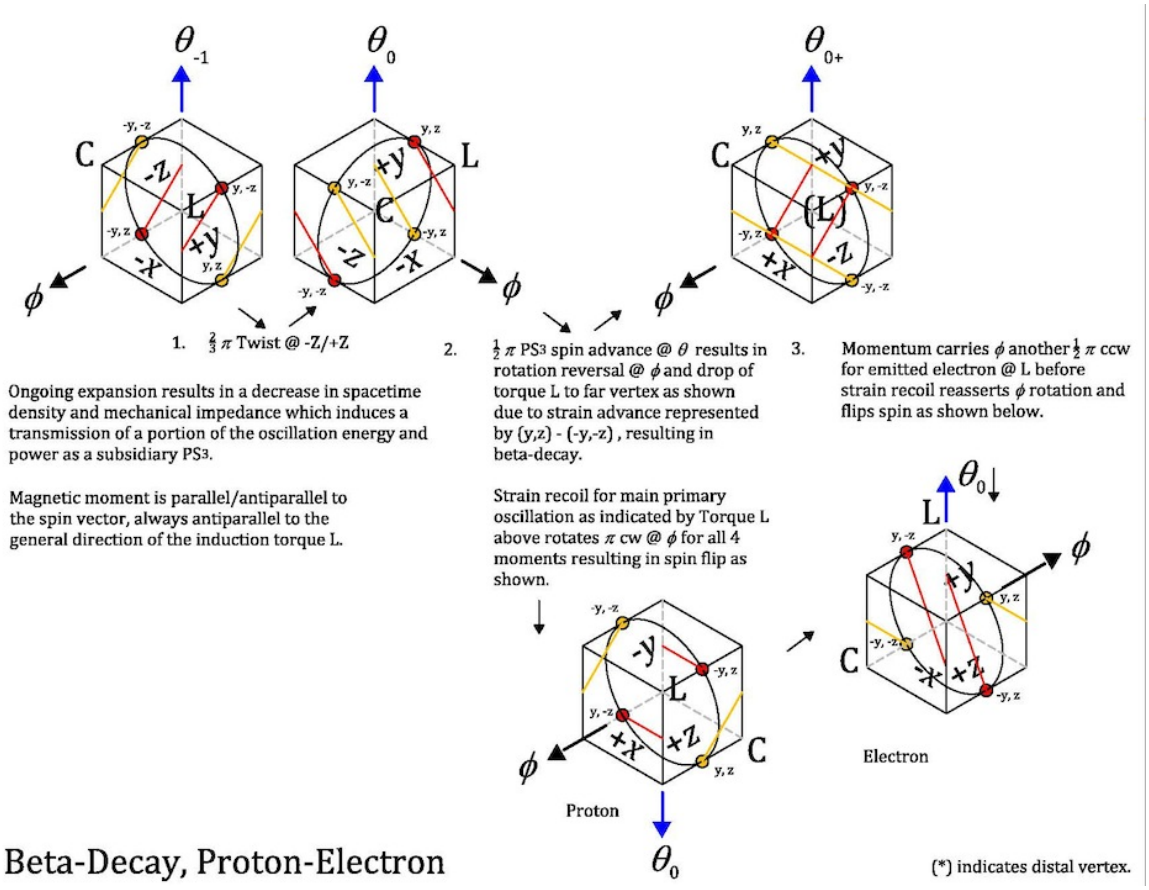

Figure 30 – Strain States of ordinary Matter at Beta-Decay

Let's do a quick review of what is occurring in this quantum oscillation. The energy of cosmic expansion results in an emergent oscillation of torsion stress and strain on a very small scale according to well-defined geometric constraints. The physical strain displacement and recoil paths incorporate well-defined functional points of maximum concentration of power and action, which act as torques rotating in synchronous manner with and conditioning the path nodes and antinodes, which we will refer to collectively as the nodes. The nature of that conditioning can be understood through analysis of the vector operations of ε and μ at the nodes. The results of this analysis can be read in the spin and charge tables, Figures 38-39.

We start in all cases by calculating the product of the torques $\mathbf{L}_{\mu}$ and $\mathbf{C}_{\varepsilon}$ and the PS_3 radials at the points shown to establish the magnitude of the vectors ε and μ at each of those points. As the torques lie along the diagonals of a cuboctahedron and the nodal points lie along its surface axes, the angle in all cases is 0.9553 . . . with a sine of $\sqrt{\frac{2}{3}}$. As a result, the magnitude of ε and μ in all cases is the magnitude of the torques for each half of the cycle, $\frac{\sqrt{3}}{2}$, times the sine or $\frac{1}{\sqrt{2}}$. The angle between ε and μ and the tangent vectors for each of the rotations $\boldsymbol{\theta}$ and $\boldsymbol{\phi}$ is in all cases $\frac{\pi}{4}$ with a sine and cosine of $\frac{1}{\sqrt{2}}$ while the angle between ε and μ at the points +/-V and +/-W is an invariant $\frac{\pi}{2}$ and at the points K_0 and K_{π} is either 0 or π. As stated, this means their dot product vanishes at V and W and the cross product vanishes at K.

The maximum angular momentum of PS_3 is determined by the points K where the kinetic energy is greatest. As seen in the charge table, the various dot products in all cases equal +/- ½ as a coefficient of the angular momentum. This is in keeping with the observed phenomena that all fermions have $\pm\frac{1}{2}$ spin angular momentum. In the case of the neutron, all the values of the dot products are positive, indicating a potential for the interacting torques and rotational dynamics to augment each other. It is thus an unstable condition, even though it represents a resonant state of PS_3. By analogy, a bridge that begins to oscillate at resonant frequency is inherently unstable.

With respect to the various cross products in the table, the radial sense designation used is a filled dot for a centripetally directed vector and a hollow dot for a counter-centripetal vector product. It bears mentioning that while ε and μ are equal at the given nodes, by their natures the differentials of the inductive or kinetic vector, μ, are always increasing and those of the capacitive or potential vector, ε, are always decreasing. For this reason, in the charge tables μ is always crossed into ε with the direction of the vector product given by the right hand rule.

Column 7 gives the charge at each node of the $\boldsymbol{\phi}$ rotation , W_{+x} and W_{-x}, (+/-W). Notice that while these two points are the nodes of $\boldsymbol{\phi}$, they are circulating on the $\boldsymbol{\theta}$ or C_{+p} circle, as indicated by the row headings. In the case of the neutron, the $\mu\times$ and the $\varepsilon\times$ are antiparallel and cancel, indicating a neutral charge for the neutron PS_3. Note also that the radial sense for $\mu\times\varepsilon$ at W_{-x} is centrifugal, indicating a potential for emission of energy from this node, while that at W_{+x} is centripetal, indicating a corresponding potential for retention of energy at this node.

Figure 30 gives a representation of the strain events at the point of beta decay for ordinary matter. Figure 31 gives the four phases of the rotational cycles of the electron and proton, with the relative positions of the C and L torques shown. Note that all the cubic representations of the strain states of PS_3 are out of phase from the

corresponding Spin Diagrams, by $\frac{\pi}{4}$ as each shows from Figure 27 #1, initial, undisplaced positions at the vertices of the square as the points strained to the (gold/red) power/action moments of the Strain States. The Spin Diagrams indicate positions from the normal vectors of an XYZ co-ordinate system displaced to those same moments.

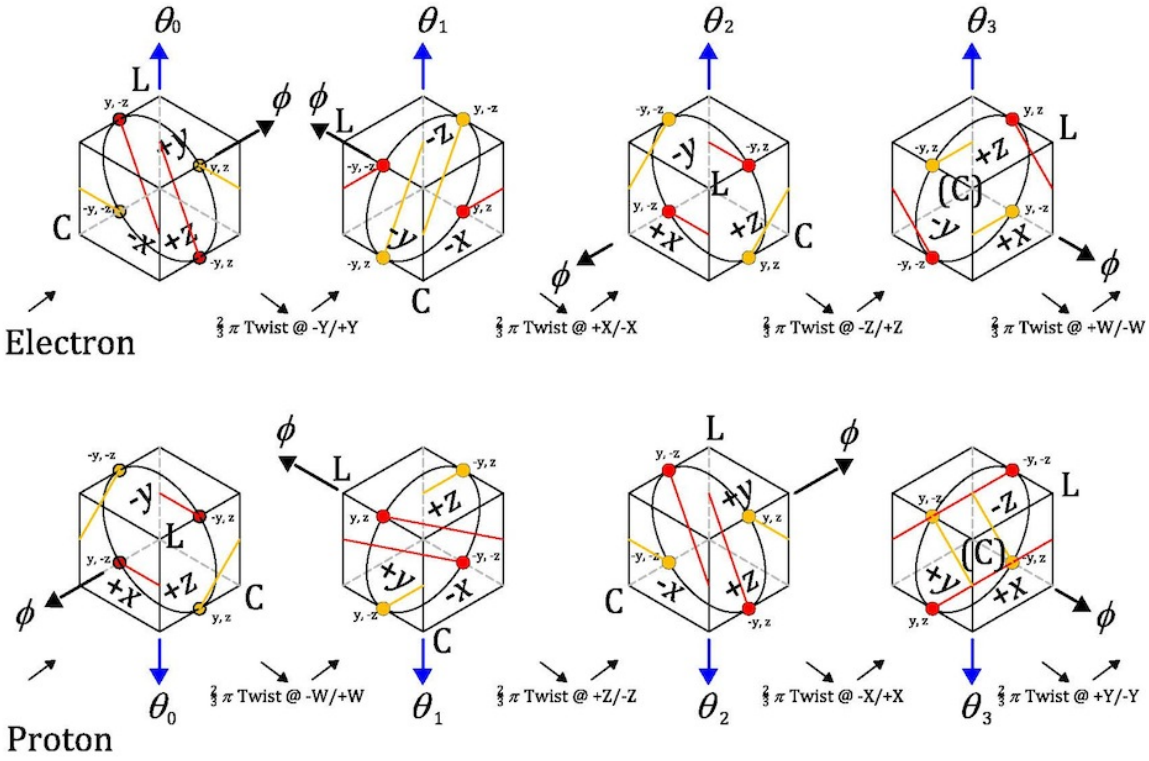

Proton & Electron Rotational Oscillation

Figure 31 – Inductive Strain States, Electron and Proton

The following Spin Diagrams for the proton and electron show the dynamics of Figure 31 in greater detail at a given moment in time, with the same nodal detail for the torques and their local vectors μ and ε as seen with the neutron in Figure 29. With respect to the charge table for ordinary matter, for the proton, the dot products of these vectors are of opposite sense at each of the nodal points with respect to $\boldsymbol{\phi}$ and $\boldsymbol{\theta}$, and are negative with respect to their common product, indicating the antiparallel nature of their effect. The spin magnitude remains ½ but the stability of the proton over the neutron is indicated by the opposite senses for μ and ε.

With respect to the cross products and charge, the condition at W_{-x} is centrifugal for both $\mu\times$ and $\varepsilon\times$ as it is for $\mu\times\varepsilon$ with the net result of a charge of +1. At W_{+x} the charge is similarly +1, but is is centripetally directed.

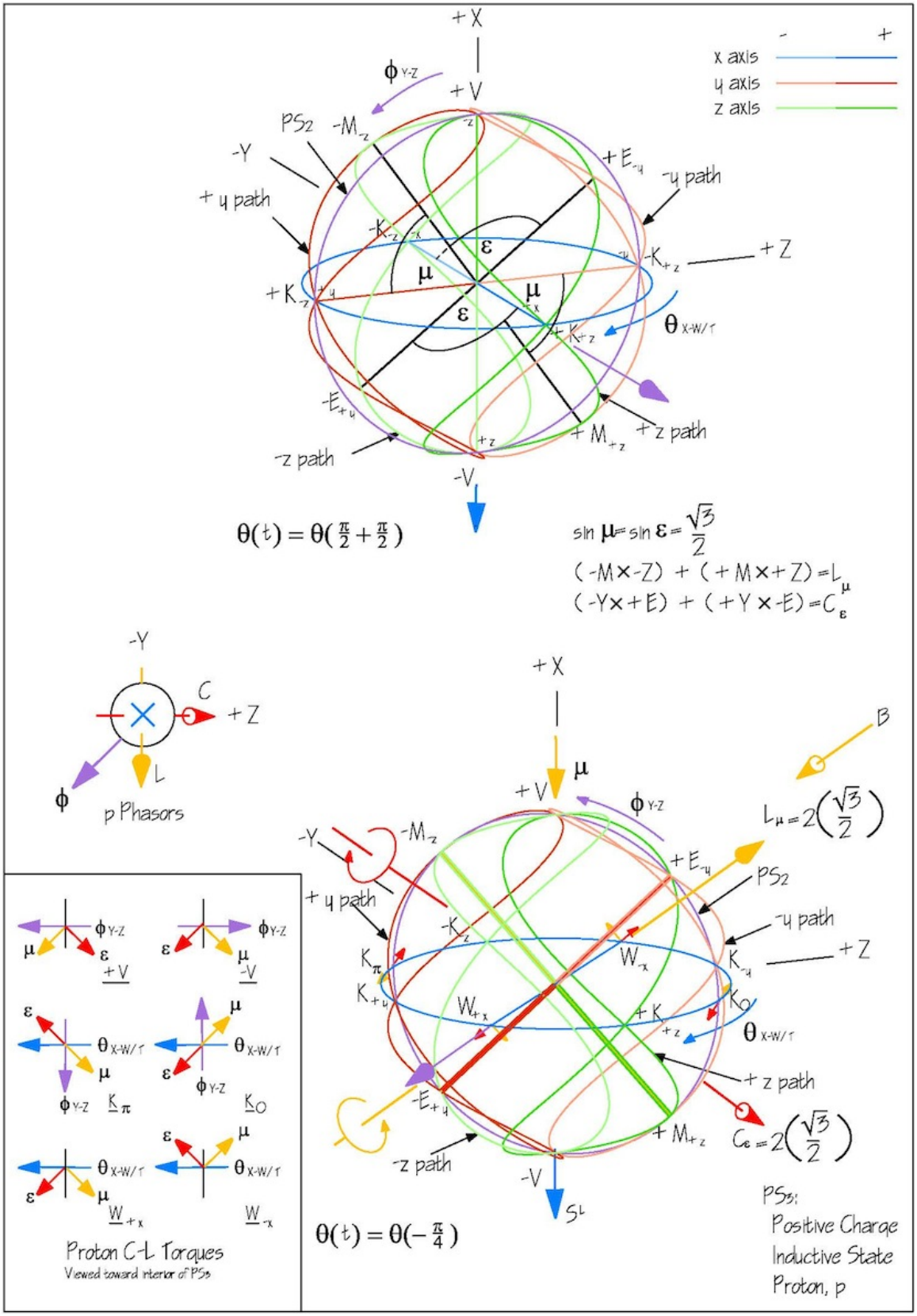

Figure 32 – Spin Diagram 3, Proton

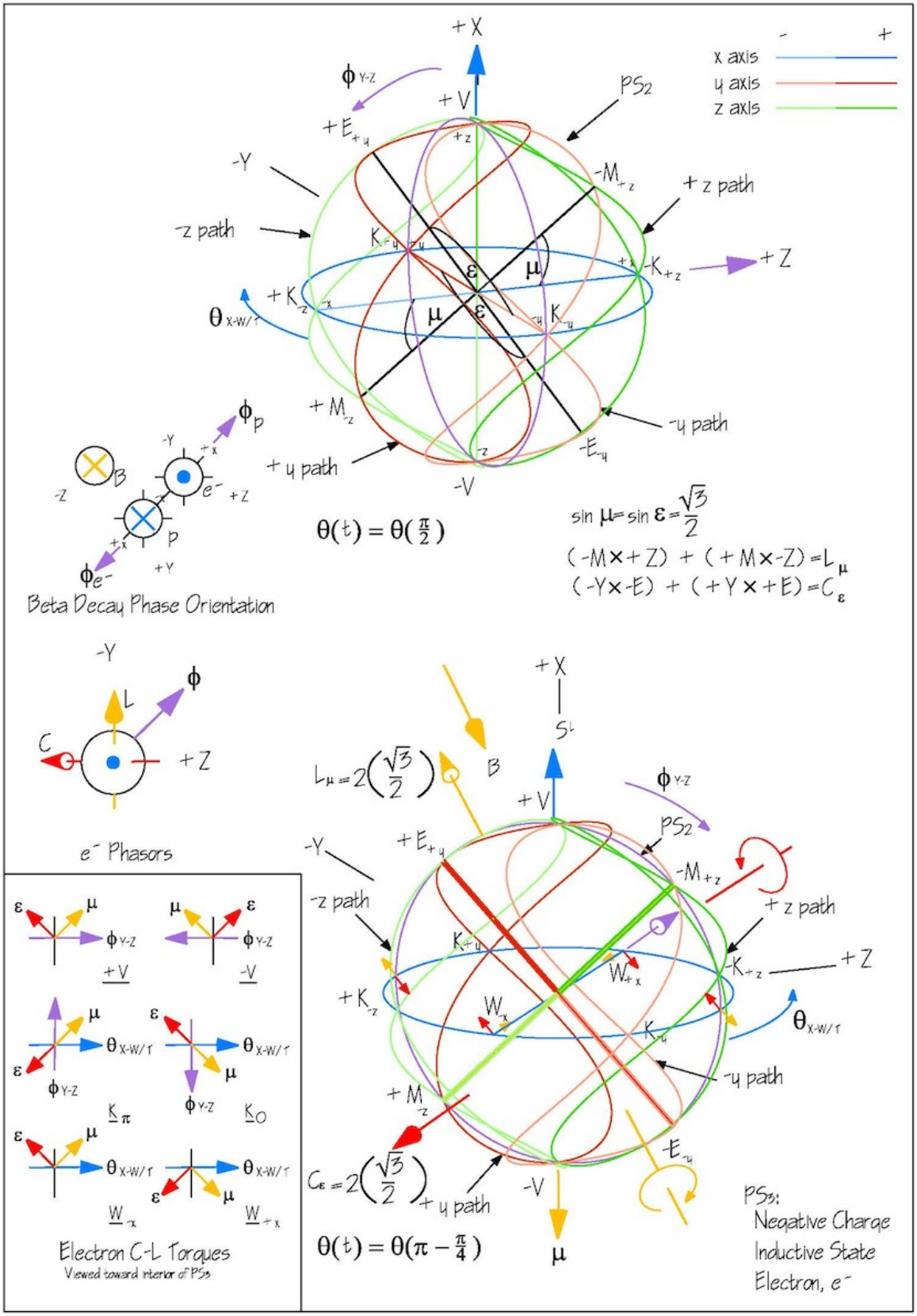

Figure 33 – Spin Diagram 4, Electron

In the case of Figure 33 for the electron, while the dot products of μ and ε remain negative due to the antiparallel nature of the vectors, the dot products of $\mu\cdot$ are all positive due to the inductive nature of the proton-electron strain states; the inductive torque is generally parallel to the direction of motion of all the nodal points of $\boldsymbol{\phi}$ and $\boldsymbol{\theta}$ in the electron. The $\varepsilon\cdot$ products are each antiparallel to that motion and therefore negative.

With respect to the cross products, as with the proton, at the K points $\mu\times\varepsilon$ vanishes and their individual products with $\boldsymbol{\phi}$ and $\boldsymbol{\theta}$ are antiparallel and therefore cancel. At W_{-x} the cross products are centripetal for both $\mu\times$ and $\varepsilon\times$ giving a net charge of 1, but antiparallel to $\mu\times\varepsilon$ for a negative charge as shown.

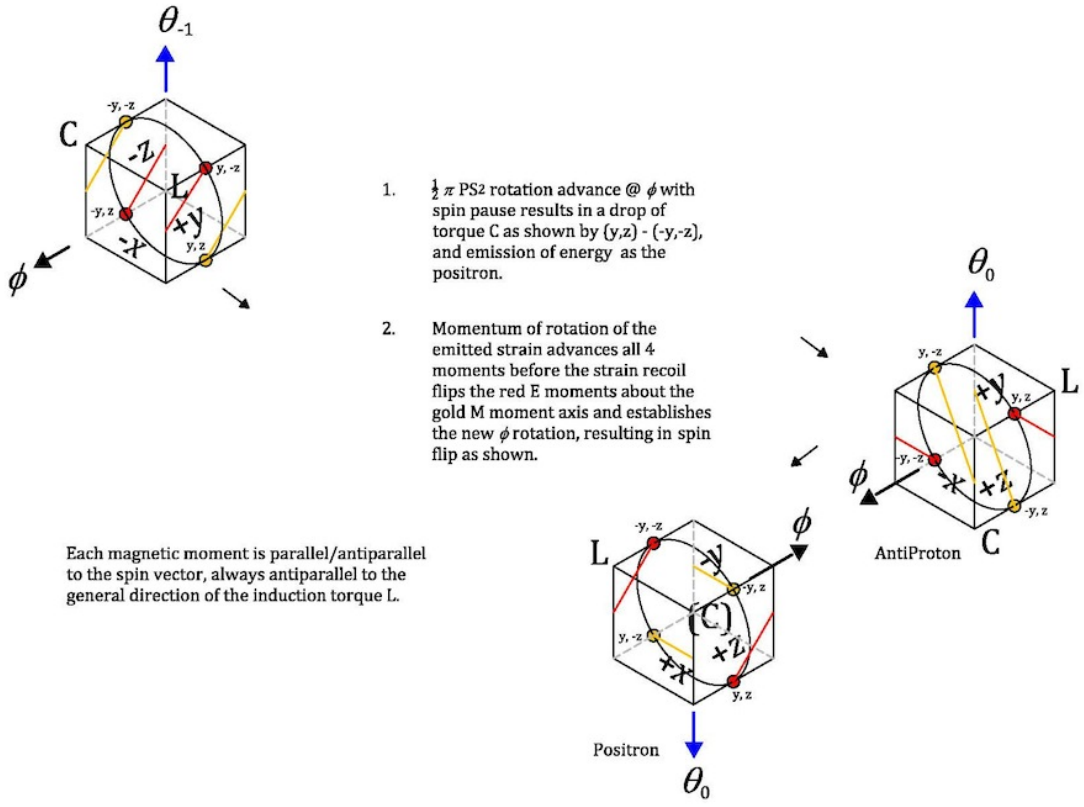

Figure 34 – Strain States of Anti Matter at Beta-Decay

Figure 34 is a representation of the strain states at the point of beta decay for anti matter. In this case, as can be seen there is an advance of the $\boldsymbol{\phi}$ rotational strain without a corresponding advance of $\boldsymbol{\theta}$, which emits the positron with a spin reversal. This is equivalent to a retardation in spin and indicates a general capacitive state, which is why it is rare in the context of an inductive, expansionary state of the

cosmos. Figure 35 represents the strain states for the antiproton and positron and shows the symmetry of the relationship with ordinary matter.

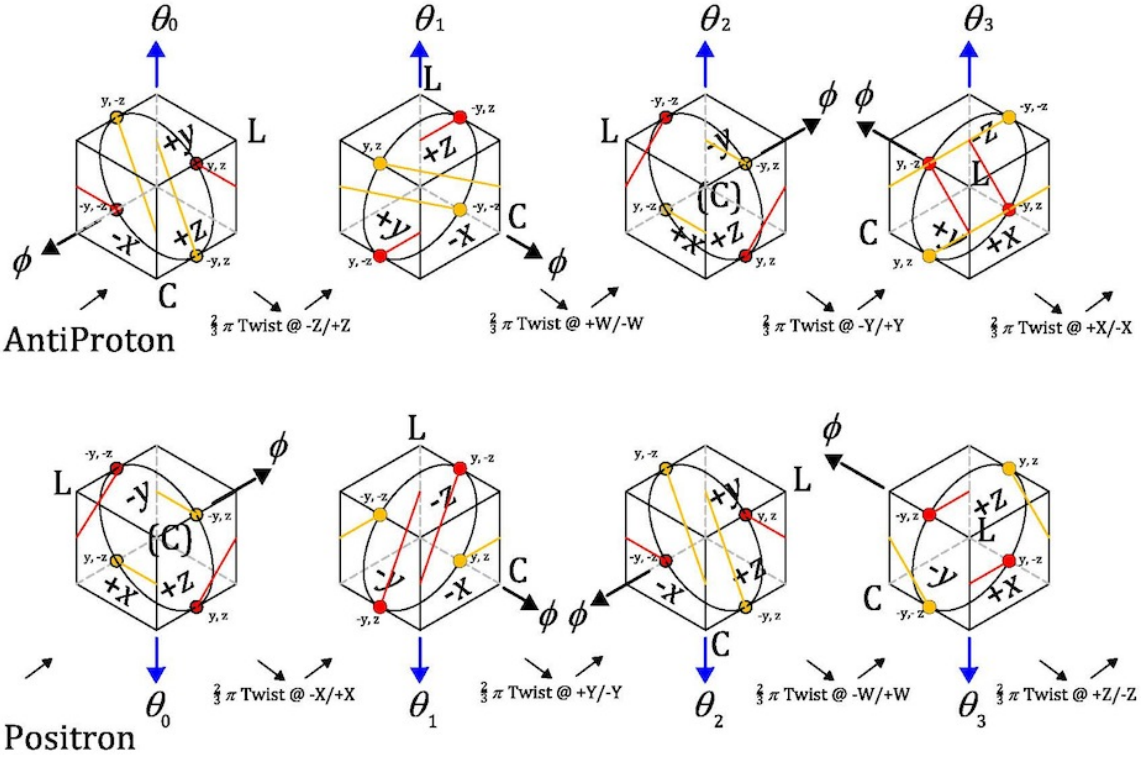

Figure 35 – Capacitive Strain States, Anti Proton and Positron

The corresponding Spin Diagrams for the antiproton and positron follow in Figure 36 and 37. With respect to the charge tables for antimatter, the neutron is said to be its own antiparticle, but it is simply the same resonant particle that undergoes a capacitive strain advance with the resulting different transformation of the torques C and L and opposite charge at the point of positron emission.

With respect to the dot products of μ and ε, the vectors remain antiparallel so the sense of their mutual products at K remains negative in both particles. For the dot products with $\boldsymbol{\phi}$ and $\boldsymbol{\theta}$, the senses are all opposite those of the proton and electron. This means for the positron that μ is antiparallel and ε is parallel to $\boldsymbol{\phi}$ and $\boldsymbol{\theta}$ at all nodal points, indicating a capacitive strain, phase state.

With respect to the cross products, the condition at W_{-x} is centrifugal for both $\mu\times$ and $\varepsilon\times$, indicating the point of transmission, but for $\mu\times\varepsilon$ is centripetal and antiparallel for a charge of -1. For the positron, at W_{-x} all are centripetal for a charge of +1.

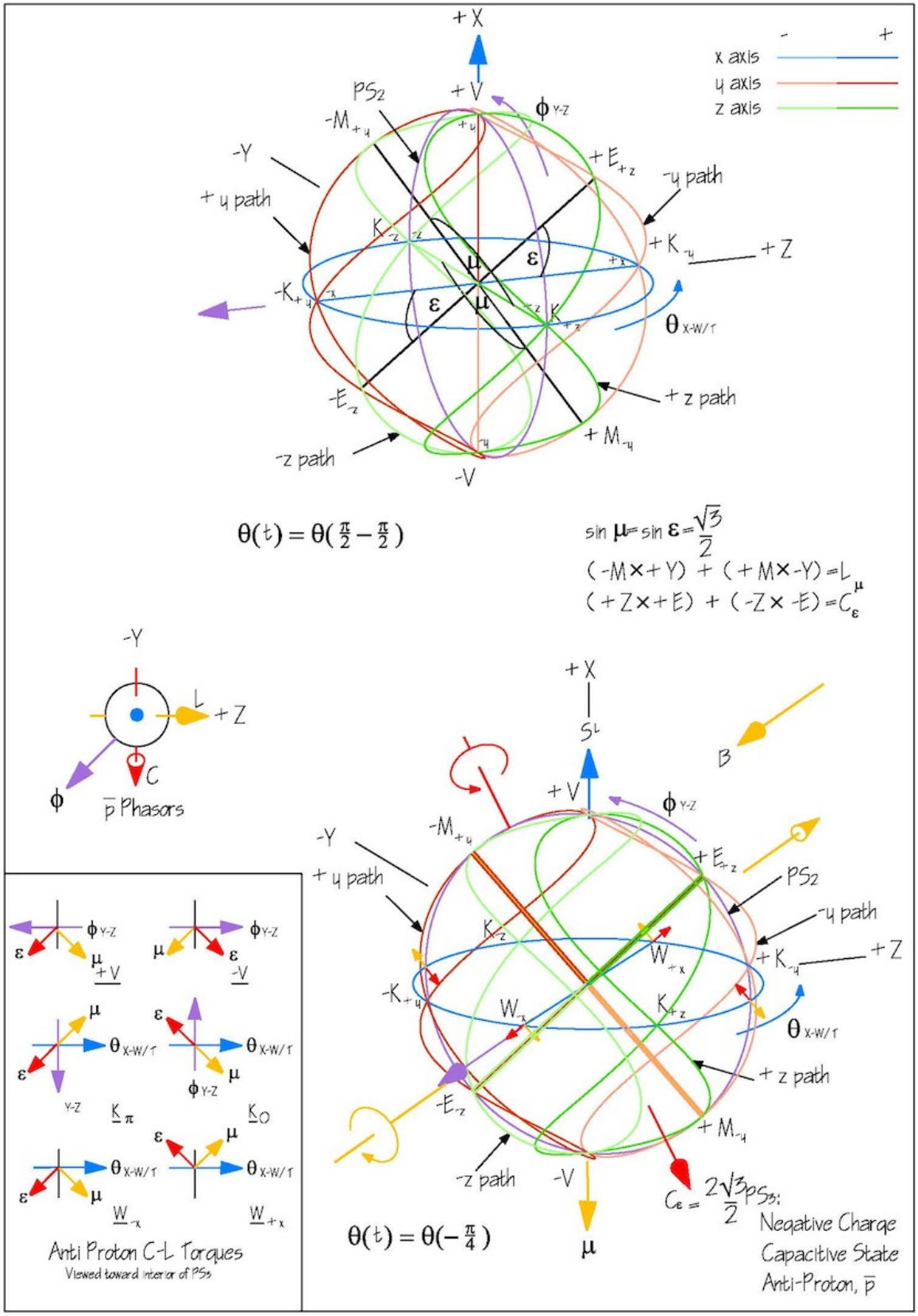

Figure 36 – Spin Diagram 5, the AntiProton

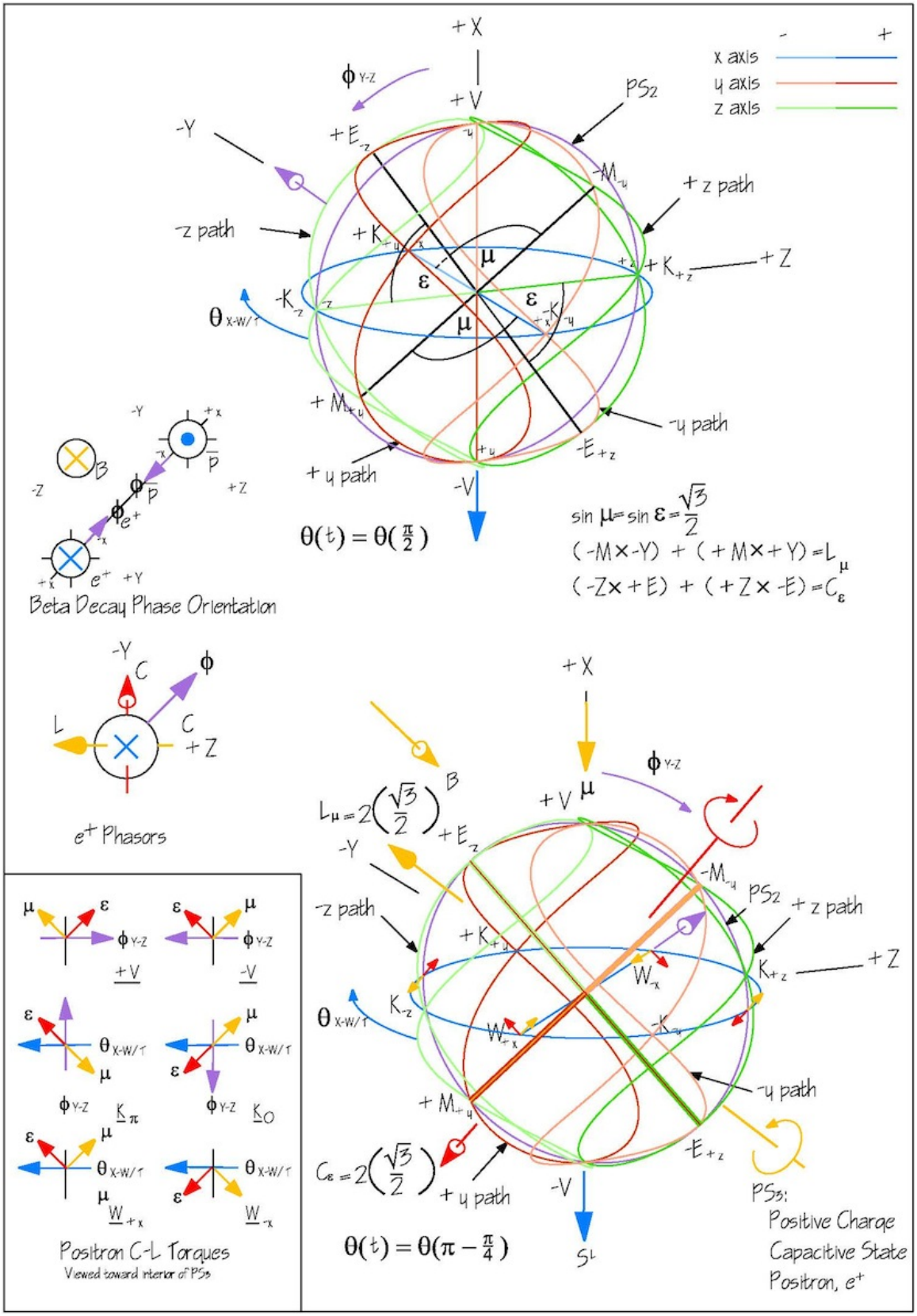

Figure 37 – Spin Diagram 6, the Positron

	1	2	3	4	5	6	7	8
Diagram, Node/Antinode, Rotation	$\mu\cdot\varepsilon$ $\varepsilon,\mu = \frac{1}{\sqrt{2}}$	$\mu\cdot$ Into θ,ϕ	$\varepsilon\cdot$ Into θ,ϕ	$S=\mu\times\varepsilon$ $\mu,\varepsilon=\frac{1}{\sqrt{2}}$	$\mu\times$ Into θ,ϕ	$\varepsilon\times$ Into θ,ϕ	$q=\frac{S}{\lvert S\rvert}\left(\mu\times+\varepsilon\times\right)$	Total Charge q_{W-}, q_{W+} $q_{V\pm}, q_{V\mp}$
Diagram 2 - Neutron								
W_{+x}-θ	0	$+\frac{1}{2}$	$+\frac{1}{2}$	$\bullet\frac{1}{2}$	$\bullet\frac{1}{2}$	$\circ\frac{1}{2}$	$\bullet 1\left(\bullet\frac{1}{2}+\circ\frac{1}{2}\right)=0$	
W_{-x}-θ	0	$+\frac{1}{2}$	$+\frac{1}{2}$	$\circ\frac{1}{2}$	$\circ\frac{1}{2}$	$\bullet\frac{1}{2}$	$\circ 1\left(\circ\frac{1}{2}+\bullet\frac{1}{2}\right)=0$	0
K_o-θ	$+\frac{1}{2}$	$+\frac{1}{2}$	$+\frac{1}{2}$	0	$\circ\frac{1}{2}$	$\circ\frac{1}{2}$	0	
K_π-θ	$+\frac{1}{2}$	$+\frac{1}{2}$	$+\frac{1}{2}$	0	$\bullet\frac{1}{2}$	$\bullet\frac{1}{2}$	0	
K_o-ϕ	$+\frac{1}{2}$	$+\frac{1}{2}$	$+\frac{1}{2}$	0	$\bullet\frac{1}{2}$	$\bullet\frac{1}{2}$	0	
K_π-ϕ	$+\frac{1}{2}$	$+\frac{1}{2}$	$+\frac{1}{2}$	0	$\circ\frac{1}{2}$	$\circ\frac{1}{2}$	0	
$+V$-ϕ	0	$+\frac{1}{2}$	$+\frac{1}{2}$	$\bullet\frac{1}{2}$	$\bullet\frac{1}{2}$	$\circ\frac{1}{2}$	$\bullet 1\left(\bullet\frac{1}{2}+\circ\frac{1}{2}\right)=0$	
$-V$-ϕ	0	$+\frac{1}{2}$	$+\frac{1}{2}$	$\circ\frac{1}{2}$	$\circ\frac{1}{2}$	$\bullet\frac{1}{2}$	$\circ 1\left(\circ\frac{1}{2}+\bullet\frac{1}{2}\right)=0$	[0]
Diagram 3 - Proton								
W_{+x}-θ	0	$-\frac{1}{2}$	$+\frac{1}{2}$	$\bullet\frac{1}{2}$	$\bullet\frac{1}{2}$	$\bullet\frac{1}{2}$	$\bullet 1\left(\bullet\frac{1}{2}+\bullet\frac{1}{2}\right)=+1$	
W_{-x}-θ	0	$-\frac{1}{2}$	$+\frac{1}{2}$	$\circ\frac{1}{2}$	$\circ\frac{1}{2}$	$\circ\frac{1}{2}$	$\circ 1\left(\circ\frac{1}{2}+\circ\frac{1}{2}\right)=+1$	+1
K_o-θ	$-\frac{1}{2}$	$-\frac{1}{2}$	$+\frac{1}{2}$	0	$\circ\frac{1}{2}$	$\bullet\frac{1}{2}$	0	
K_π-θ	$-\frac{1}{2}$	$-\frac{1}{2}$	$+\frac{1}{2}$	0	$\bullet\frac{1}{2}$	$\circ\frac{1}{2}$	0	
K_o-ϕ	$-\frac{1}{2}$	$+\frac{1}{2}$	$-\frac{1}{2}$	0	$\circ\frac{1}{2}$	$\bullet\frac{1}{2}$	0	
K_π-ϕ	$-\frac{1}{2}$	$+\frac{1}{2}$	$-\frac{1}{2}$	0	$\bullet\frac{1}{2}$	$\circ\frac{1}{2}$	0	
$+V$-ϕ	0	$+\frac{1}{2}$	$-\frac{1}{2}$	$\circ\frac{1}{2}$	$\bullet\frac{1}{2}$	$\bullet\frac{1}{2}$	$\circ 1\left(\bullet\frac{1}{2}+\bullet\frac{1}{2}\right)=-1$	
$-V$-ϕ	0	$+\frac{1}{2}$	$-\frac{1}{2}$	$\bullet\frac{1}{2}$	$\circ\frac{1}{2}$	$\circ\frac{1}{2}$	$\bullet 1\left(\circ\frac{1}{2}+\circ\frac{1}{2}\right)=-1$	$\left[-1\right]=-i1$
Diagram 4 - Electron								
W_{+x}-θ	0	$+\frac{1}{2}$	$-\frac{1}{2}$	$\bullet\frac{1}{2}$	$\circ\frac{1}{2}$	$\circ\frac{1}{2}$	$\bullet 1\left(\circ\frac{1}{2}+\circ\frac{1}{2}\right)=-1$	
W_{-x}-θ	0	$+\frac{1}{2}$	$-\frac{1}{2}$	$\circ\frac{1}{2}$	$\bullet\frac{1}{2}$	$\bullet\frac{1}{2}$	$\circ 1\left(\bullet\frac{1}{2}+\bullet\frac{1}{2}\right)=-1$	-1
K_o-θ	$-\frac{1}{2}$	$+\frac{1}{2}$	$-\frac{1}{2}$	0	$\circ\frac{1}{2}$	$\bullet\frac{1}{2}$	0	
K_π-θ	$-\frac{1}{2}$	$+\frac{1}{2}$	$-\frac{1}{2}$	0	$\bullet\frac{1}{2}$	$\circ\frac{1}{2}$	0	
K_o-ϕ	$-\frac{1}{2}$	$+\frac{1}{2}$	$-\frac{1}{2}$	0	$\bullet\frac{1}{2}$	$\circ\frac{1}{2}$	0	
K_π-ϕ	$-\frac{1}{2}$	$+\frac{1}{2}$	$-\frac{1}{2}$	0	$\circ\frac{1}{2}$	$\bullet\frac{1}{2}$	0	
$+V$-ϕ	0	$+\frac{1}{2}$	$-\frac{1}{2}$	$\circ\frac{1}{2}$	$\bullet\frac{1}{2}$	$\bullet\frac{1}{2}$	$\circ 1\left(\bullet\frac{1}{2}+\bullet\frac{1}{2}\right)=-1$	$\left[-1\right]=-i1$
$-V$-ϕ	0	$+\frac{1}{2}$	$-\frac{1}{2}$	$\bullet\frac{1}{2}$	$\circ\frac{1}{2}$	$\circ\frac{1}{2}$	$\bullet 1\left(\circ\frac{1}{2}+\circ\frac{1}{2}\right)=-1$	

Figure 38 – Charge and Spin Table for Ordinary Matter

	1	2	3	4	5	6	7	8
Diagram, Node/Antinode, Rotation	$\mu\cdot\varepsilon$ $\varepsilon,\mu = \frac{1}{\sqrt{2}}$	$\mu\cdot$ Into θ,ϕ	$\varepsilon\cdot$ Into θ,ϕ	$S=\mu\times\varepsilon$ $\mu,\varepsilon=\frac{1}{\sqrt{2}}$	$\mu\times$ Into θ,ϕ	$\varepsilon\times$ Into θ,ϕ	$q=\frac{S}{\lvert S\rvert}\left(\mu\times+\varepsilon\times\right)$	Total Charge q_{W-}, q_{W+} $q_{V\pm}, q_{V\mp}$
Diagram 2 - Neutron W_{+x}-θ	0	$+\frac{1}{2}$	$+\frac{1}{2}$	$\bullet\frac{1}{2}$	$\bullet\frac{1}{2}$	$\circ\frac{1}{2}$	$\bullet 1\left(\bullet\frac{1}{2}+\circ\frac{1}{2}\right)=0$	
W_{-x}-θ	0	$+\frac{1}{2}$	$+\frac{1}{2}$	$\circ\frac{1}{2}$	$\circ\frac{1}{2}$	$\bullet\frac{1}{2}$	$\circ 1\left(\circ\frac{1}{2}+\bullet\frac{1}{2}\right)=0$	0
K_o-θ	$+\frac{1}{2}$	$+\frac{1}{2}$	$+\frac{1}{2}$	0	$\circ\frac{1}{2}$	$\circ\frac{1}{2}$	0	
K_π-θ	$+\frac{1}{2}$	$+\frac{1}{2}$	$+\frac{1}{2}$	0	$\bullet\frac{1}{2}$	$\bullet\frac{1}{2}$	0	
K_o-ϕ	$+\frac{1}{2}$	$+\frac{1}{2}$	$+\frac{1}{2}$	0	$\bullet\frac{1}{2}$	$\bullet\frac{1}{2}$	0	
K_π-ϕ	$+\frac{1}{2}$	$+\frac{1}{2}$	$+\frac{1}{2}$	0	$\circ\frac{1}{2}$	$\circ\frac{1}{2}$	0	
$+V$-ϕ	0	$+\frac{1}{2}$	$+\frac{1}{2}$	$\bullet\frac{1}{2}$	$\bullet\frac{1}{2}$	$\circ\frac{1}{2}$	$\bullet 1\left(\bullet\frac{1}{2}+\circ\frac{1}{2}\right)=0$	
$-V$-ϕ	0	$+\frac{1}{2}$	$+\frac{1}{2}$	$\circ\frac{1}{2}$	$\circ\frac{1}{2}$	$\bullet\frac{1}{2}$	$\circ 1\left(\circ\frac{1}{2}+\bullet\frac{1}{2}\right)=0$	[0]
Diagram 5 – Anti Proton W_{+x}-θ	0	$+\frac{1}{2}$	$-\frac{1}{2}$	$\circ\frac{1}{2}$	$\bullet\frac{1}{2}$	$\bullet\frac{1}{2}$	$\circ 1\left(\bullet\frac{1}{2}+\bullet\frac{1}{2}\right)=-1$	
W_{-x}-θ	0	$+\frac{1}{2}$	$-\frac{1}{2}$	$\bullet\frac{1}{2}$	$\circ\frac{1}{2}$	$\circ\frac{1}{2}$	$\circ 1\left(\bullet\frac{1}{2}+\bullet\frac{1}{2}\right)=-1$	-1
K_o-θ	$-\frac{1}{2}$	$+\frac{1}{2}$	$-\frac{1}{2}$	0	$\circ\frac{1}{2}$	$\bullet\frac{1}{2}$	0	
K_π-θ	$-\frac{1}{2}$	$+\frac{1}{2}$	$-\frac{1}{2}$	0	$\bullet\frac{1}{2}$	$\circ\frac{1}{2}$	0	
K_o-ϕ	$-\frac{1}{2}$	$-\frac{1}{2}$	$+\frac{1}{2}$	0	$\circ\frac{1}{2}$	$\bullet\frac{1}{2}$	0	
K_π-ϕ	$-\frac{1}{2}$	$-\frac{1}{2}$	$+\frac{1}{2}$	0	$\bullet\frac{1}{2}$	$\circ\frac{1}{2}$	0	
$+V$-ϕ	0	$-\frac{1}{2}$	$+\frac{1}{2}$	$\bullet\frac{1}{2}$	$\bullet\frac{1}{2}$	$\bullet\frac{1}{2}$	$\bullet 1\left(\bullet\frac{1}{2}+\bullet\frac{1}{2}\right)=+1$	
$-V$-ϕ	0	$-\frac{1}{2}$	$+\frac{1}{2}$	$\circ\frac{1}{2}$	$\circ\frac{1}{2}$	$\circ\frac{1}{2}$	$\circ 1\left(\circ\frac{1}{2}+\circ\frac{1}{2}\right)=+1$	$\left[+1\right]=+i1$
Diagram 6 - Positron W_{+x}-θ	0	$-\frac{1}{2}$	$+\frac{1}{2}$	$\circ\frac{1}{2}$	$\circ\frac{1}{2}$	$\circ\frac{1}{2}$	$\circ 1\left(\circ\frac{1}{2}+\circ\frac{1}{2}\right)=+1$	
W_{-x}-θ	0	$-\frac{1}{2}$	$+\frac{1}{2}$	$\bullet\frac{1}{2}$	$\bullet\frac{1}{2}$	$\bullet\frac{1}{2}$	$\bullet 1\left(\bullet\frac{1}{2}+\bullet\frac{1}{2}\right)=+1$	+1
K_o-θ	$-\frac{1}{2}$	$-\frac{1}{2}$	$+\frac{1}{2}$	0	$\circ\frac{1}{2}$	$\bullet\frac{1}{2}$	0	
K_π-θ	$-\frac{1}{2}$	$-\frac{1}{2}$	$+\frac{1}{2}$	0	$\bullet\frac{1}{2}$	$\circ\frac{1}{2}$	0	
K_o-ϕ	$-\frac{1}{2}$	$-\frac{1}{2}$	$+\frac{1}{2}$	0	$\bullet\frac{1}{2}$	$\circ\frac{1}{2}$	0	
K_π-ϕ	$-\frac{1}{2}$	$-\frac{1}{2}$	$+\frac{1}{2}$	0	$\circ\frac{1}{2}$	$\bullet\frac{1}{2}$	0	
$+V$-ϕ	0	$-\frac{1}{2}$	$+\frac{1}{2}$	$\bullet\frac{1}{2}$	$\bullet\frac{1}{2}$	$\bullet\frac{1}{2}$	$\bullet 1\left(\bullet\frac{1}{2}+\bullet\frac{1}{2}\right)=+1$	$\left[+1\right]=+i1$
$-V$-ϕ	0	$-\frac{1}{2}$	$+\frac{1}{2}$	$\circ\frac{1}{2}$	$\circ\frac{1}{2}$	$\circ\frac{1}{2}$	$\circ 1\left(\circ\frac{1}{2}+\circ\frac{1}{2}\right)=+1$	

Figure 39 – Charge and Spin Table for Anti Matter

	1	2	3	4	5	6	7	8
Diagram, Node/Antinode, Rotation	$\mu \cdot \varepsilon$ $\mu, \varepsilon = \sqrt{\frac{2}{3}}$	$\mu \cdot$ Into θ, ϕ	$\varepsilon \cdot$ Into θ, ϕ	$S = \mu \times \varepsilon$ $\mu, \varepsilon = \sqrt{\frac{2}{3}}$	$\mu \times$ Into θ, ϕ	$\varepsilon \times$ Into θ, ϕ	$q = \frac{S}{\lvert S \rvert}\left[\mathrm{T}\left(\mu \times + \varepsilon \times\right)\right]$ $\mathrm{T} = \frac{\sqrt{3}}{2}$	Total Charge q_{W-}, q_{W+} $q_{V\pm}, q_{V\mp}$
Diagram 2 - Neutron								
W_{+x}-θ	0	$+\frac{1}{\sqrt{3}}$	$+\frac{1}{\sqrt{3}}$	$\bullet\frac{2}{3}$	$\bullet\frac{1}{\sqrt{3}}$	$\circ\frac{1}{\sqrt{3}}$	$\bullet 1\left(\bullet\frac{1}{2}+\circ\frac{1}{2}\right) = 0$	
W_{-x}-θ	0	$+\frac{1}{\sqrt{3}}$	$+\frac{1}{\sqrt{3}}$	$\circ\frac{2}{3}$	$\circ\frac{1}{\sqrt{3}}$	$\bullet\frac{1}{\sqrt{3}}$	$\circ 1\left(\circ\frac{1}{2}+\bullet\frac{1}{2}\right) = 0$	0
K_o-θ	$+\frac{2}{3}$	$+\frac{1}{\sqrt{3}}$	$+\frac{1}{\sqrt{3}}$	0	$\circ\frac{1}{\sqrt{3}}$	$\circ\frac{1}{\sqrt{3}}$	0	
K_π-θ	$+\frac{2}{3}$	$+\frac{1}{\sqrt{3}}$	$+\frac{1}{\sqrt{3}}$	0	$\bullet\frac{1}{\sqrt{3}}$	$\bullet\frac{1}{\sqrt{3}}$	0	
K_o-ϕ	$+\frac{2}{3}$	$+\frac{1}{\sqrt{3}}$	$+\frac{1}{\sqrt{3}}$	0	$\bullet\frac{1}{\sqrt{3}}$	$\bullet\frac{1}{\sqrt{3}}$	0	
K_π-ϕ	$+\frac{2}{3}$	$+\frac{1}{\sqrt{3}}$	$+\frac{1}{\sqrt{3}}$	0	$\circ\frac{1}{\sqrt{3}}$	$\circ\frac{1}{\sqrt{3}}$	0	
$+V$-ϕ	0	$+\frac{1}{\sqrt{3}}$	$+\frac{1}{\sqrt{3}}$	$\bullet\frac{2}{3}$	$\bullet\frac{1}{\sqrt{3}}$	$\circ\frac{1}{\sqrt{3}}$	$\bullet 1\left(\bullet\frac{1}{2}+\circ\frac{1}{2}\right) = 0$	
$-V$-ϕ	0	$+\frac{1}{\sqrt{3}}$	$+\frac{1}{\sqrt{3}}$	$\circ\frac{2}{3}$	$\circ\frac{1}{\sqrt{3}}$	$\bullet\frac{1}{\sqrt{3}}$	$\circ 1\left(\circ\frac{1}{2}+\bullet\frac{1}{2}\right) = 0$	[0]
Diagram 3 - Proton								
W_{+x}-θ	0	$-\frac{1}{\sqrt{3}}$	$+\frac{1}{\sqrt{3}}$	$\bullet\frac{2}{3}$	$\bullet\frac{1}{\sqrt{3}}$	$\bullet\frac{1}{\sqrt{3}}$	$\bullet 1\left(\bullet\frac{1}{2}+\bullet\frac{1}{2}\right) = +1$	
W_{-x}-θ	0	$-\frac{1}{\sqrt{3}}$	$+\frac{1}{\sqrt{3}}$	$\circ\frac{2}{3}$	$\circ\frac{1}{\sqrt{3}}$	$\circ\frac{1}{\sqrt{3}}$	$\circ 1\left(\circ\frac{1}{2}+\circ\frac{1}{2}\right) = +1$	+1
K_o-θ	$-\frac{2}{3}$	$-\frac{1}{\sqrt{3}}$	$+\frac{1}{\sqrt{3}}$	0	$\circ\frac{1}{\sqrt{3}}$	$\bullet\frac{1}{\sqrt{3}}$	0	
K_π-θ	$-\frac{2}{3}$	$-\frac{1}{\sqrt{3}}$	$+\frac{1}{\sqrt{3}}$	0	$\bullet\frac{1}{\sqrt{3}}$	$\circ\frac{1}{\sqrt{3}}$	0	
K_o-ϕ	$-\frac{2}{3}$	$+\frac{1}{\sqrt{3}}$	$-\frac{1}{\sqrt{3}}$	0	$\circ\frac{1}{\sqrt{3}}$	$\bullet\frac{1}{\sqrt{3}}$	0	
K_π-ϕ	$-\frac{2}{3}$	$+\frac{1}{\sqrt{3}}$	$-\frac{1}{\sqrt{3}}$	0	$\bullet\frac{1}{\sqrt{3}}$	$\circ\frac{1}{\sqrt{3}}$	0	
$+V$-ϕ	0	$+\frac{1}{\sqrt{3}}$	$-\frac{1}{\sqrt{3}}$	$\circ\frac{2}{3}$	$\bullet\frac{1}{\sqrt{3}}$	$\bullet\frac{1}{\sqrt{3}}$	$\circ 1\left(\bullet\frac{1}{2}+\bullet\frac{1}{2}\right) = -1$	
$-V$-ϕ	0	$+\frac{1}{\sqrt{3}}$	$-\frac{1}{\sqrt{3}}$	$\bullet\frac{2}{3}$	$\circ\frac{1}{\sqrt{3}}$	$\circ\frac{1}{\sqrt{3}}$	$\bullet 1\left(\circ\frac{1}{2}+\circ\frac{1}{2}\right) = -1$	$\left[-1\right] = -i1$
Diagram 4 - Electron								
W_{+x}-θ	0	$+\frac{1}{\sqrt{3}}$	$-\frac{1}{\sqrt{3}}$	$\bullet\frac{2}{3}$	$\circ\frac{1}{\sqrt{3}}$	$\circ\frac{1}{\sqrt{3}}$	$\bullet 1\left(\circ\frac{1}{2}+\circ\frac{1}{2}\right) = -1$	
W_{-x}-θ	0	$+\frac{1}{\sqrt{3}}$	$-\frac{1}{\sqrt{3}}$	$\circ\frac{2}{3}$	$\bullet\frac{1}{\sqrt{3}}$	$\bullet\frac{1}{\sqrt{3}}$	$\circ 1\left(\bullet\frac{1}{2}+\bullet\frac{1}{2}\right) = -1$	-1
K_o-θ	$-\frac{2}{3}$	$+\frac{1}{\sqrt{3}}$	$-\frac{1}{\sqrt{3}}$	0	$\circ\frac{1}{\sqrt{3}}$	$\bullet\frac{1}{\sqrt{3}}$	0	
K_π-θ	$-\frac{2}{3}$	$+\frac{1}{\sqrt{3}}$	$-\frac{1}{\sqrt{3}}$	0	$\bullet\frac{1}{\sqrt{3}}$	$\circ\frac{1}{\sqrt{3}}$	0	
K_o-ϕ	$-\frac{2}{3}$	$+\frac{1}{\sqrt{3}}$	$-\frac{1}{\sqrt{3}}$	0	$\bullet\frac{1}{\sqrt{3}}$	$\circ\frac{1}{\sqrt{3}}$	0	
K_π-ϕ	$-\frac{2}{3}$	$+\frac{1}{\sqrt{3}}$	$-\frac{1}{\sqrt{3}}$	0	$\circ\frac{1}{\sqrt{3}}$	$\bullet\frac{1}{\sqrt{3}}$	0	
$+V$-ϕ	0	$+\frac{1}{\sqrt{3}}$	$-\frac{1}{\sqrt{3}}$	$\circ\frac{2}{3}$	$\bullet\frac{1}{\sqrt{3}}$	$\bullet\frac{1}{\sqrt{3}}$	$\circ 1\left(\bullet\frac{1}{2}+\bullet\frac{1}{2}\right) = -1$	$\left[-1\right] = -i1$
$-V$-ϕ	0	$+\frac{1}{\sqrt{3}}$	$-\frac{1}{\sqrt{3}}$	$\bullet\frac{2}{3}$	$\circ\frac{1}{\sqrt{3}}$	$\circ\frac{1}{\sqrt{3}}$	$\bullet 1\left(\circ\frac{1}{2}+\circ\frac{1}{2}\right) = -1$	

Figure 40 – Charge and Spin Table for Ordinary Matter for C & L = 1

	1	2	3	4	5	6	7	8
Diagram, Node/Antinode, Rotation	$\mu \cdot \varepsilon$ $\mu, \varepsilon = \sqrt{\frac{2}{3}}$	$\mu \cdot$ Into θ, ϕ	$\varepsilon \cdot$ Into θ, ϕ	$S = \mu \times \varepsilon$ $\mu, \varepsilon = \sqrt{\frac{2}{3}}$	$\mu \times$ Into θ, ϕ	$\varepsilon \times$ Into θ, ϕ	$q = \frac{S}{\lvert S \rvert}\left(\mu \times + \varepsilon \times\right)$ T= $\frac{\sqrt{3}}{2}$	Total Charge q_{W-}, q_{W+} $q_{V\pm}, q_{V\mp}$
Diagram 2 - Neutron								
W_{+x}-θ	0	$+\frac{1}{\sqrt{3}}$	$+\frac{1}{\sqrt{3}}$	$\bullet\frac{2}{3}$	$\bullet\frac{1}{\sqrt{3}}$	$\circ\frac{1}{\sqrt{3}}$	$\bullet 1\left(\bullet\frac{1}{2}+\circ\frac{1}{2}\right)=0$	
W_{-x}-θ	0	$+\frac{1}{\sqrt{3}}$	$+\frac{1}{\sqrt{3}}$	$\circ\frac{2}{3}$	$\circ\frac{1}{\sqrt{3}}$	$\bullet\frac{1}{\sqrt{3}}$	$\circ 1\left(\circ\frac{1}{2}+\bullet\frac{1}{2}\right)=0$	0
K_o-θ	$+\frac{2}{3}$	$+\frac{1}{\sqrt{3}}$	$+\frac{1}{\sqrt{3}}$	0	$\circ\frac{1}{\sqrt{3}}$	$\circ\frac{1}{\sqrt{3}}$	0	
K_π-θ	$+\frac{2}{3}$	$+\frac{1}{\sqrt{3}}$	$+\frac{1}{\sqrt{3}}$	0	$\bullet\frac{1}{\sqrt{3}}$	$\bullet\frac{1}{\sqrt{3}}$	0	
K_o-ϕ	$+\frac{2}{3}$	$+\frac{1}{\sqrt{3}}$	$+\frac{1}{\sqrt{3}}$	0	$\bullet\frac{1}{\sqrt{3}}$	$\bullet\frac{1}{\sqrt{3}}$	0	
K_π-ϕ	$+\frac{2}{3}$	$+\frac{1}{\sqrt{3}}$	$+\frac{1}{\sqrt{3}}$	0	$\circ\frac{1}{\sqrt{3}}$	$\circ\frac{1}{\sqrt{3}}$	0	
$+V$-ϕ	0	$+\frac{1}{\sqrt{3}}$	$+\frac{1}{\sqrt{3}}$	$\bullet\frac{2}{3}$	$\bullet\frac{1}{\sqrt{3}}$	$\circ\frac{1}{\sqrt{3}}$	$\bullet 1\left(\bullet\frac{1}{2}+\circ\frac{1}{2}\right)=0$	
$-V$-ϕ	0	$+\frac{1}{\sqrt{3}}$	$+\frac{1}{\sqrt{3}}$	$\circ\frac{2}{3}$	$\circ\frac{1}{\sqrt{3}}$	$\bullet\frac{1}{\sqrt{3}}$	$\circ 1\left(\circ\frac{1}{2}+\bullet\frac{1}{2}\right)=0$	[0]
Diagram 5 – Anti Proton								
W_{+x}-θ	0	$+\frac{1}{\sqrt{3}}$	$-\frac{1}{\sqrt{3}}$	$\circ\frac{2}{3}$	$\bullet\frac{1}{\sqrt{3}}$	$\bullet\frac{1}{\sqrt{3}}$	$\circ 1\left(\bullet\frac{1}{2}+\bullet\frac{1}{2}\right)=-1$	
W_{-x}-θ	0	$+\frac{1}{\sqrt{3}}$	$-\frac{1}{\sqrt{3}}$	$\bullet\frac{2}{3}$	$\circ\frac{1}{\sqrt{3}}$	$\circ\frac{1}{\sqrt{3}}$	$\circ 1\left(\bullet\frac{1}{2}+\bullet\frac{1}{2}\right)=-1$	-1
K_o-θ	$-\frac{2}{3}$	$+\frac{1}{\sqrt{3}}$	$-\frac{1}{\sqrt{3}}$	0	$\circ\frac{1}{\sqrt{3}}$	$\bullet\frac{1}{\sqrt{3}}$	0	
K_π-θ	$-\frac{2}{3}$	$+\frac{1}{\sqrt{3}}$	$-\frac{1}{\sqrt{3}}$	0	$\bullet\frac{1}{\sqrt{3}}$	$\circ\frac{1}{\sqrt{3}}$	0	
K_o-ϕ	$-\frac{2}{3}$	$-\frac{1}{\sqrt{3}}$	$+\frac{1}{\sqrt{3}}$	0	$\circ\frac{1}{\sqrt{3}}$	$\bullet\frac{1}{\sqrt{3}}$	0	
K_π-ϕ	$-\frac{2}{3}$	$-\frac{1}{\sqrt{3}}$	$+\frac{1}{\sqrt{3}}$	0	$\bullet\frac{1}{\sqrt{3}}$	$\circ\frac{1}{\sqrt{3}}$	0	
$+V$-ϕ	0	$-\frac{1}{\sqrt{3}}$	$+\frac{1}{\sqrt{3}}$	$\bullet\frac{2}{3}$	$\bullet\frac{1}{\sqrt{3}}$	$\bullet\frac{1}{\sqrt{3}}$	$\bullet 1\left(\bullet\frac{1}{2}+\bullet\frac{1}{2}\right)=+1$	
$-V$-ϕ	0	$-\frac{1}{\sqrt{3}}$	$+\frac{1}{\sqrt{3}}$	$\circ\frac{2}{3}$	$\circ\frac{1}{\sqrt{3}}$	$\circ\frac{1}{\sqrt{3}}$	$\circ 1\left(\circ\frac{1}{2}+\circ\frac{1}{2}\right)=+1$	$\left[+1\right]=+i1$
Diagram 6 - Positron								
W_{+x}-θ	0	$-\frac{1}{\sqrt{3}}$	$+\frac{1}{\sqrt{3}}$	$\circ\frac{2}{3}$	$\circ\frac{1}{\sqrt{3}}$	$\circ\frac{1}{\sqrt{3}}$	$\circ 1\left(\circ\frac{1}{2}+\circ\frac{1}{2}\right)=+1$	
W_{-x}-θ	0	$-\frac{1}{\sqrt{3}}$	$+\frac{1}{\sqrt{3}}$	$\bullet\frac{2}{3}$	$\bullet\frac{1}{\sqrt{3}}$	$\bullet\frac{1}{\sqrt{3}}$	$\bullet 1\left(\bullet\frac{1}{2}+\bullet\frac{1}{2}\right)=+1$	+1
K_o-θ	$-\frac{2}{3}$	$-\frac{1}{\sqrt{3}}$	$+\frac{1}{\sqrt{3}}$	0	$\circ\frac{1}{\sqrt{3}}$	$\bullet\frac{1}{\sqrt{3}}$	0	
K_π-θ	$-\frac{2}{3}$	$-\frac{1}{\sqrt{3}}$	$+\frac{1}{\sqrt{3}}$	0	$\bullet\frac{1}{\sqrt{3}}$	$\circ\frac{1}{\sqrt{3}}$	0	
K_o-ϕ	$-\frac{2}{3}$	$-\frac{1}{\sqrt{3}}$	$+\frac{1}{\sqrt{3}}$	0	$\bullet\frac{1}{\sqrt{3}}$	$\circ\frac{1}{\sqrt{3}}$	0	
K_π-ϕ	$-\frac{2}{3}$	$-\frac{1}{\sqrt{3}}$	$+\frac{1}{\sqrt{3}}$	0	$\circ\frac{1}{\sqrt{3}}$	$\bullet\frac{1}{\sqrt{3}}$	0	
$+V$-ϕ	0	$-\frac{1}{\sqrt{3}}$	$+\frac{1}{\sqrt{3}}$	$\bullet\frac{2}{3}$	$\bullet\frac{1}{\sqrt{3}}$	$\bullet\frac{1}{\sqrt{3}}$	$\bullet 1\left(\bullet\frac{1}{2}+\bullet\frac{1}{2}\right)=+1$	$\left[+1\right]=+i1$
$-V$-ϕ	0	$-\frac{1}{\sqrt{3}}$	$+\frac{1}{\sqrt{3}}$	$\circ\frac{2}{3}$	$\circ\frac{1}{\sqrt{3}}$	$\circ\frac{1}{\sqrt{3}}$	$\circ 1\left(\circ\frac{1}{2}+\circ\frac{1}{2}\right)=+1$	

Figure 41 – Charge and Spin Table for Anti Matter for C & L =1

Figures 40 and 41 give the same information as Figures 38 and 39 for the dot and cross products of μ and ε, however using a value of 1 for the torques C and L instead of $\frac{\sqrt{3}}{2}$. This is done to give an indication of the tie-in of this analysis with the current quark phenomenology of the standard model. I will leave it to others to work out the details. The correct value of C and L is worked back into the analysis in Column 7 of these tables to arrive at the correct charge values as indicated at the Column heading.

Figure 42 gives a comparison of the strain cycle states for each of the states delineated above. It shows the strain sequence over $\theta_{(0,1,2,3)}$ for the position (y, z) as taken from the Figures 28, 31 & 35. For the neutron, proton, and antiproton, the same sequence occurs for the three remaining positions, (y,-z), (-y,-z), and (-y, z) with appropriate transposition of the sequence numbers, rotating clockwise around the axial vector $\boldsymbol{\theta}$ as viewed from the top of the cube. The strain is therefore rotationally symmetric for each of the four strains. In the case of the electron and positron states, the (y, z) and the (-y,-z, not shown) strains are half-rotationally symmetric about $\boldsymbol{\theta}$, as are the (y,-z) and the (-y, z, not shown) strains. This asymmetry is an indication of two properties of these states; a significant elongation from a generally spherical to a pronounced prolate form of the strain along the x or

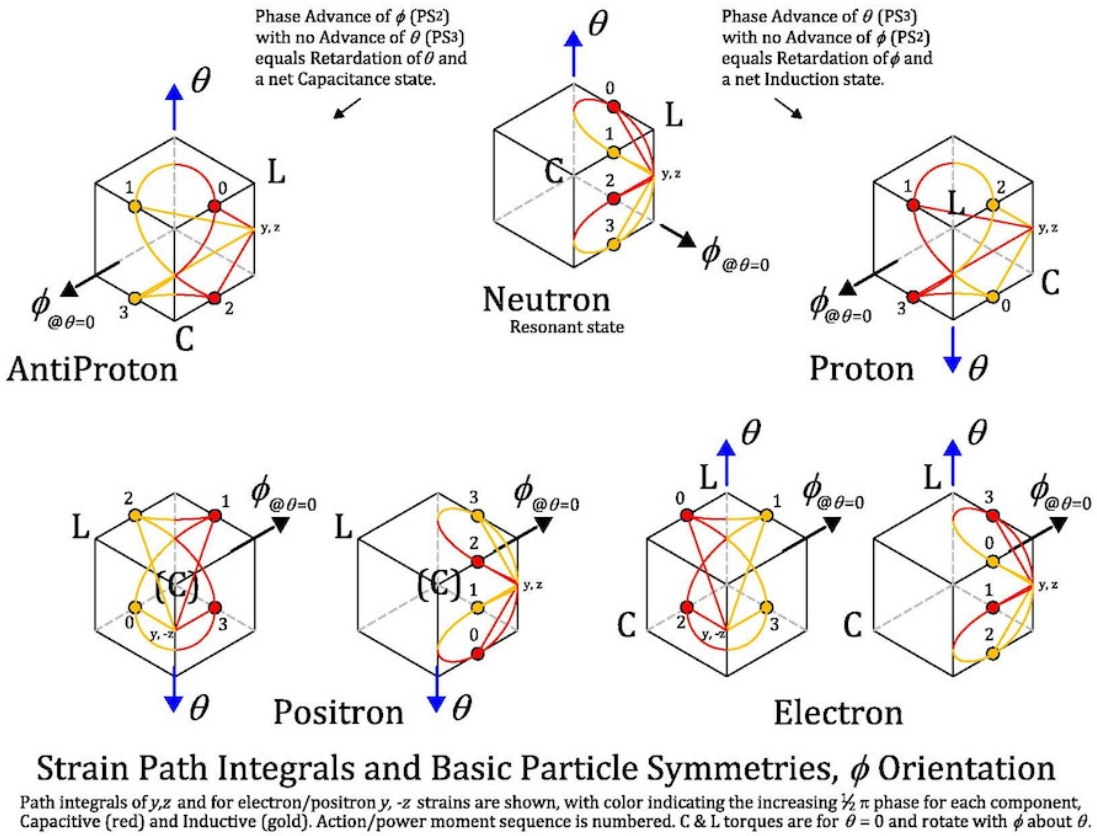

Figure 42 – Comparison of Strain States

generally (y, z)-(-y,-z) axis, and a propensity for $\boldsymbol{\theta}$ to flip about the generally (y, -z)-(-y, z) and X axis plane. Such a flip transmits a traveling torsion wave that is recognized in the standard phenomenology as a photon or boson, a force carrier.

In Figure 43, the same particles are shown so that all the $\boldsymbol{\theta}$ vectors are parallel. This gives a better view of the symmetry between ordinary and anti matter, the first of which is advanced in the rotation of $\boldsymbol{\theta}$ and the second of which is retarded. Notice that the same advanced/retarded symmetry holds for the emitted states, the leptons of the standard phenomenology, electron and positron. For the positron, two $\boldsymbol{\theta}$ flips are shown for the position (y, -z). One is an observational flip, which means a snapshot view of its position shown in Figure 42 taken from the backside and upside down and shows the same strain state as in Figure 42. The physical spin flip shown represents an actual flip of the spin due to a recoil of the strain as shown. Note the difference in the initial position of (y, -z) in the two depictions. A similar condition applies to the electron as well. These physical flips indicate a reduction in stress/strain of the state to that of the basic or ground energy state with the emission of a photon.

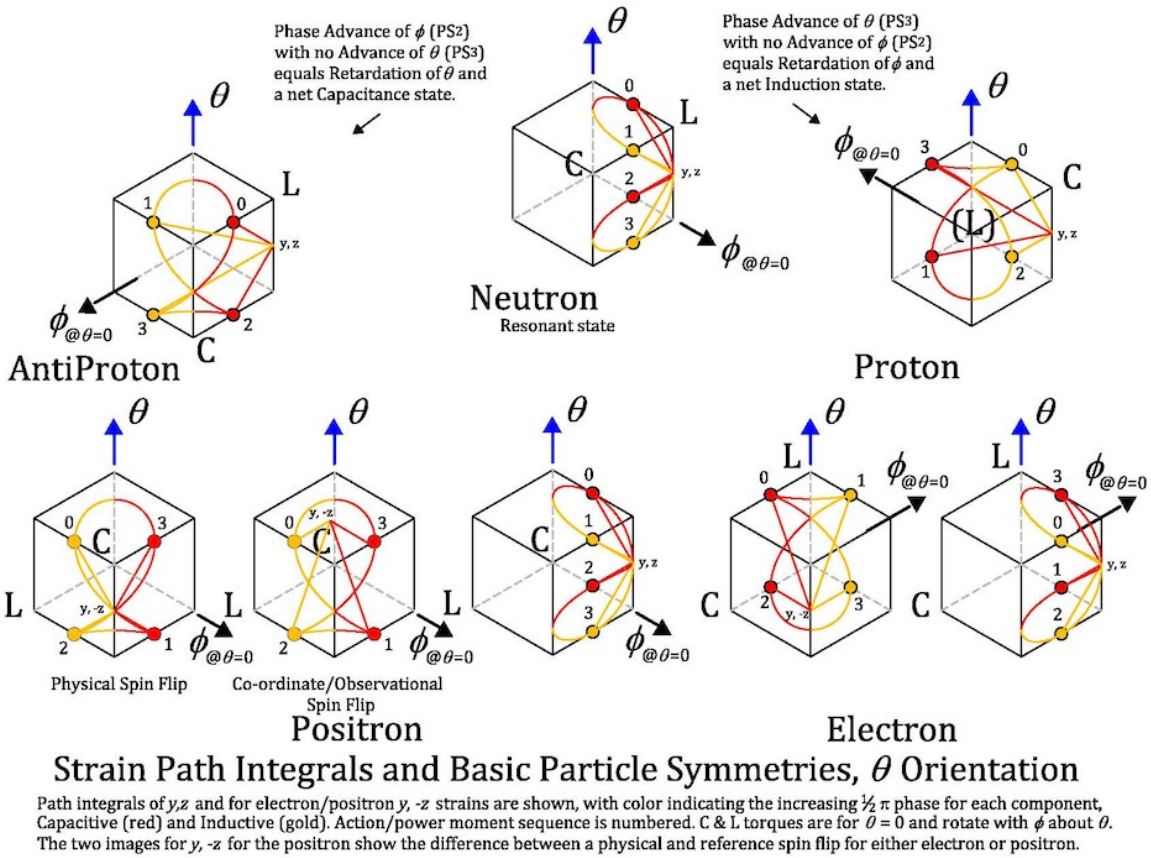

Figure 43 – Comparison of Strain States with Parallel Spin

The following photos are of toy models representing the strain phase and spin states of the neutron, proton and antiproton based on the above analysis and diagrams. The smaller red and gold (or yellow) nubs represent the E and M moments and their relationship to the long brown ϕ axial vector along the rotating *x* axis. The longer red and gold vectors represent the C and L torques all of which circulate about the blue spin angular momentum vectors. The orange vectors parallel or antiparallel to the spin vectors represent the effective magnetic moments of the quantum states.

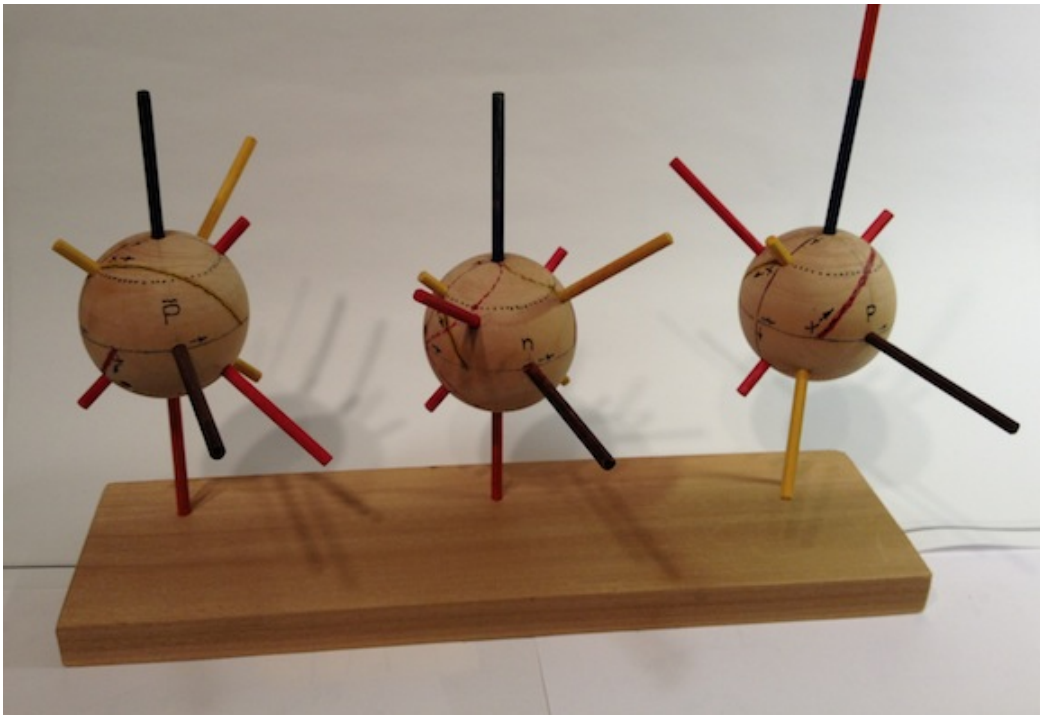

PS_3 Anti-Proton PS_3 Neutron PS_3 Proton

Toy Models of 3-D Phase Space for the neutron, proton and anti-proton. The 2 capacitive moments (small red vectors) and 2 inductive moments (small yellow vectors) are in the plane of the 2-D phase space whose rotation is indicated by the brown axial vector representing the principal restorative force of SHM. These moments in turn generate the capacitive (long red axial vector) and inductive (long yellow axial vector) torques that prevent energy dispersion and generate spin angular momentum (blue axial vectors). The magnetic dipole moments (orange vectors) are determined by the inductive torque and roughly anti-parallel to it. The proton results from an advance of PS_2 about the angular momentum and the resulting flip in the inductive torque. The anti-proton results from a retardation of PS_2 about the angular momentum and the resulting flip of the capacitive torque.

Photo 7

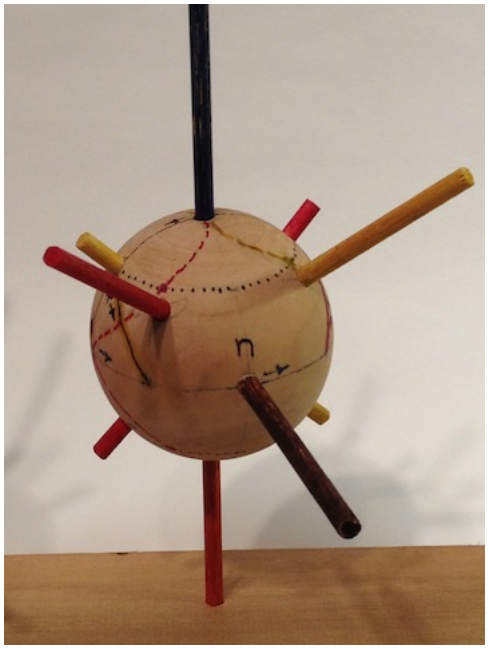

Neutron state at capacitive torque showing displacement of inductive moment behind

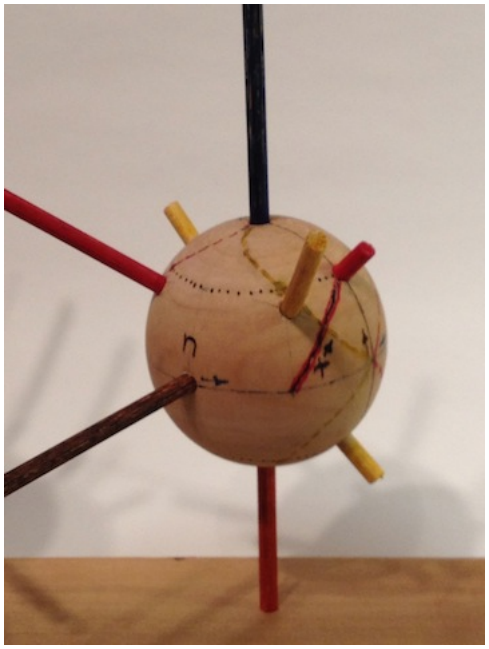

Neutron state at inductive torque showing displacement of capacitive moment behind

The small arrow to the right of the "n" shows direction of the PS_2 disk axis revolution in PS_3. The arrow beneath and pointed toward the red capacitive moment in the right photo shows the direction of rotation of the PS_2 disk about its center. The top portion of the figure 8 path crossing at that point shows the oscillatory path etched by that point of the disk on the PS_3 spherical shell as the disk rotates. The neutron state is a resonant state.

Photo 8 Photo 9

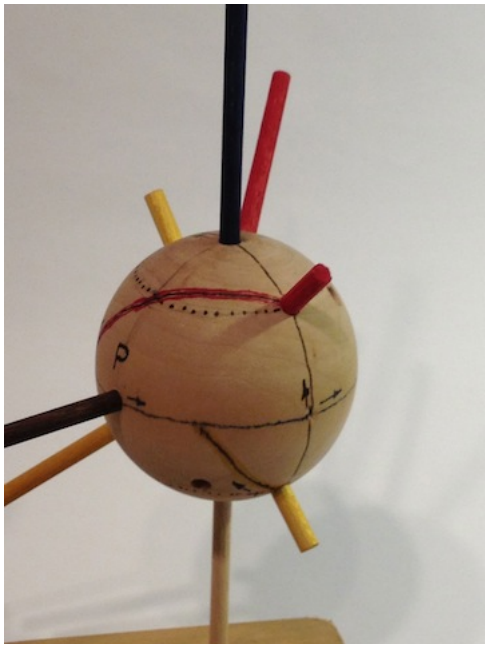

Proton state showing the advance of the capacitive and inductive moments and their displacement paths

Photo 10

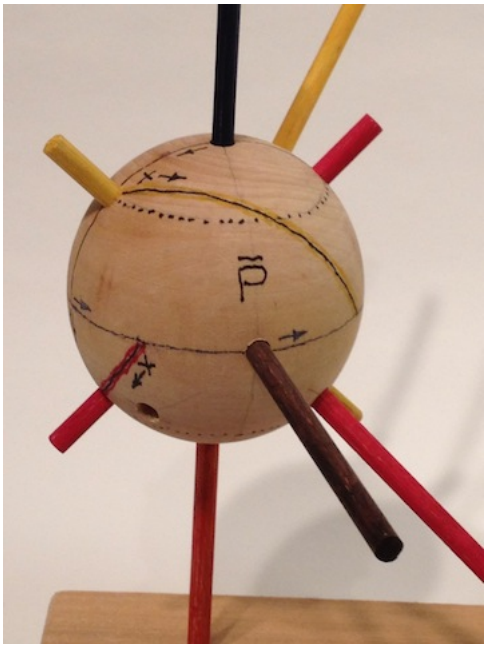

Anti-proton state showing the retardation of the capacitive and inductive moments and their displacement paths

Photo 11

Verification

Our discussion on with Simple Harmonic Motion started with its representations in classical phase space and sinusoidal functions, took an aside into some basic notions of calculus and isotropic differential change, developed an extension of phase space to three dimensions to incorporate potential and kinetic energy, took another aside into the stress-strain analysis of three-dimensional materials and mediums and the difference between body and surface forces, examined some properties of an expanding spacetime fabric (STF), including the inevitable emergence of geometric constraints due to the stress-strain relationship of inertial continuity, to finally arrive at the statement that the basic particles of matter that we observe everywhere about us necessarily arise in such inertially continuous spacetime in the process of expansion as microscopic individual or quantum instances of SHM. This may be reasonable, but if it is true it should be accurate. We should be able to predict some of the readily observed properties of such matter and in a way that current models cannot.

Specifically, as functions of an expanding spacetime we should be able to:

1) derive a gravitational quantum, predict Newton's gravitational constant and his law of gravity, in a manner consistent with general relativity, and
2) derive a model of beta decay tied to the expansion, predict the neutron and electron mass ratios, predict the expansion rate of the cosmos, account for the missing mass of beta decay, and predict the value of elementary charge.

1) Quantum Gravity

Current attempts at a unification of theoretical physics rest in part on the dimensional analysis of Newton's gravitational constant, G_N, by Max Planck and its assumed applicability at a theoretically smallest limiting scale, where we have displacement, r_0, mass, m_0, and time, t_0, and τ_0 is a fundamental unit of a presumed body force, the subscript naught again indicating a fundamental unit, i.e. equal to one in some natural scale:

$$G_N = \frac{r_0^2}{m_0^2}(\tau_0) = \frac{r_0^2}{m_0^2}\left(m_0 \frac{r_0}{t_0^2}\right) = \frac{r_0^3}{m_0 t_0^2} \tag{4.1}$$

It bears emphasizing that if we are to anticipate a quantum theory of gravity, then the function of Newton's constant in the context of Newton's gravitational law is to produce the force between two massive bodies by converting their respective masses and the distance of separation of their centers of mass to some fundamental units of each property and multiplying this by a fundamental unit or quantum of force as in the second term above.

Since *c,* the speed of light, and $\hbar$, Planck's quantum of action, are assumed to be invariant at any scale, their expression in terms of the units of some as yet undefined natural length scale, r_0, commensurate with τ_0 is

$$c = \frac{r_0}{t_0} \quad \therefore t_0 = \frac{r_0}{c}, \text{ and}$$
$$\hbar = \frac{m_0 r_0^2}{t_0} \quad \therefore m_0 = \frac{\hbar}{c r_0} \tag{4.2}$$

Substituting these conclusions for time and mass back into(4.1), and assuming the same natural units for the length scale, we have the following expression for G_N,

$$G_N = \frac{r_0^3}{m_0 t_0^2} = \frac{c^3}{\hbar} r_0^2 = \frac{c^3}{\hbar} \mathrm{A}_0 \tag{4.3}$$

Since G_N, c, and $\hbar$ have reasonably well determined values, we can rearrange and solve to evaluate the Planck scale, here in SI units, via the Planck area, A_P,

$$\mathrm{A}_0 = r_0^{\,2} = \frac{G_N \hbar}{c^3} = 2.6116\ldots x10^{-70} \text{ meter}^2 = \mathrm{A}_P \tag{4.4}$$

and its square root, the Planck length, l_P, where

$$r_0 = 1.616\ldots \mathrm{x}10^{-35} \text{ meter } = l_P \ . \tag{4.5}$$

The remainder of the Planck scale values are easily determined using (4.2).

$$t_0 = 5.3908\ldots x10^{-44} \text{ second}$$
$$m_0 = 2.1766\ldots x10^{-8} \text{ kilograms} \tag{4.6}$$

A_P is generally deemed to be a low end cutoff scale for definable physical phenomena, but this shows that if it had any other value, lesser or greater, the invariance of one or more of the three familiar constants would be challenged. In addition, in the above discussion concerning cosmic expansion and its implications for the nuclear scale, we have already encountered meaningful distance and time intervals far below even the Planck scale values.

In (4.1), τ_0 is presumed to be a body force of mass times acceleration and when evaluated using the Planck scale values, due to that extremely short time scale indicats a truly astronomical acceleration and force of

$$\tau_0 = 1.2104\ldots x10^{44} \text{ newton } . \tag{4.7}$$

Hence the need for a big bang, of whatever unknown cause, to overcome gravity at this scale . . .

Gravitational Quantum

However, in keeping with the analysis of general relativity, τ_0 can, and in this writers opinion should, be considered a surface or stress force, the product of a fundamental cross-sectional area, A_0, and a fundamental unit of tension stress, f_0, as previously discussed and recapitulated here as

$$\tau_0 = \mathrm{A}_0 f_0 \tag{4.8}$$

and a differential stress force at that. Rearranging this to indicate stress as a function of force and cross-section and taking the total derivative gives

$$f_0 = \frac{\tau_0}{\mathrm{A}_0}$$
$$df_0 = \frac{\partial f_0}{\partial \tau_0} d\tau_0 + \frac{\partial f_0}{\partial \mathrm{A}_0} d\mathrm{A}_0 = \frac{1}{\mathrm{A}_0} d\tau_0 - \frac{\tau_0}{\mathrm{A}_0{}^2} d\mathrm{A}_0 \tag{4.9}$$

The unit or fundamental mode subscript designations remain, because we are examining changes in those fundamentals over time. Separating and inverting this function we have two differential equations, the first as a differential change in force as a function of a change in tension stress or

$$d\tau_0 = \mathrm{A}_0 df_0 \tag{4.10}$$

and the second as a differential change in cross-section as a function of that change in stress as

$$d\mathrm{A}_0 = -\frac{\mathrm{A}_0^2}{\tau_0} df_0 = -\frac{\tau_0}{f_0^2} df_0 = -\frac{\mathrm{A}_0}{f_0} df_0 = -\mathrm{A}_0 d\ln f_0 \tag{4.11}$$

From our comments on isotropic stress, T_0, at (6.11) in the asides we know that an isotropic stress resulting in an isotropic dilatation is related to the stress at each face by a factor of 6. In addition, if that isotropic stress is operating along the diagonals of the cube or along the cuboctahedral 4-axis octahedral component, it will be equiangular to all three faces or at a factor of $\sqrt{3}$ for a total factor of $6\sqrt{3}$, denoted γ_3, to give

$$df_0 = \frac{dT_0}{6\sqrt{3}} \tag{4.12}$$

making the differential stress force

$$d\tau_0 = \frac{\mathrm{A}_0}{6\sqrt{3}} dT_0 = \frac{\mathrm{A}_0}{\gamma_3} dT_0 \ . \tag{4.13}$$

Newton's Gravitational Constant

If we now use this differential stress force in Planck's dimensional analysis instead of the body force, we have

$$G_N = \frac{r_0^2}{m_0^2}\left(d\tau_0\right) = \frac{r_0^4}{\hbar^2/c^2}\left(\frac{r_0{}^2}{6\sqrt{3}} dT_0\right) = \frac{c^2}{\gamma_3 \hbar^2} r_0^6 dT_0 = \frac{r_0^6}{\gamma_3 \text{ⶉ}^2} dT_0 \tag{4.14}$$

From Aside #1, since dT_0 equals 1, and we know the values of the other invariants, we can rearrange again and solve for the fundamental length scale, applicable to the current expansion extent of the cosmos and get

$$r_0 = \left(\gamma_3 \frac{G_N \hbar^2}{c^2} \frac{1}{dT_0}\right)^{\frac{1}{6}} = \left(\gamma_3 G_N \text{ⶉ}^2 \frac{1}{dT_0}\right)^{\frac{1}{6}} = 2.1002\ldots x10^{-16} \text{ meter } = \text{ƛ}_{C,n} \tag{4.15}$$

As indicated, this evaluates as the reduced Compton wavelength of the neutron. This indicates that the neutron scale, the resonant state of a quantum PS_3, is the fundamental physical scale. Applying this result to (4.2) we get the neutron mass as the fundamental mass, (fundamental need not mean smallest in regards to mass), and to (4.11) and (4.12), we find that

$$d\mathrm{A}_0 = \mathrm{A}_P \tag{4.16}$$

the Planck area, and a gravitational quantum, G_0, for use in (4.14) and in Newton's Law is

$$G_0 = d\tau_0 = \gamma_3^{-1} r_0^2 dT_0 = \gamma_3^{-1} \lambda\!\!\!^{-2}_{C,n} dT_0 = 4.2443...x10^{-33} \ \ Newton \tag{4.17}$$

Using (4.14) and the current CODATA values for $\lambda\!\!\!^{-}_{C,n}, \hbar$ and c gives a theoretical value for G_N of 6.6731971...x10^{-11} m^3 / kg-s^2, within the standard uncertainty of the current CODATA value of 6.67384(80) x 10^{-11}, in conformance with our PS_3 model. This does not indicate that it is the reduced Compton wavelength that produces gravity, rather it is the change in central force as a result of in a change in the expansion stress that determines both $\lambda\!\!\!^{-}_{C,n}$ and G_0.

Evaluation of the tension stress <u>force</u> at the boundary of a unit PS_3 based on this scale is

$$\tau_n = \tau_0 = \frac{\hbar}{c}\frac{c^2}{\lambda\!\!\!^{-2}_{C,n}} = \frac{\hbar}{c}\omega_n^2 = \frac{m_n c^2}{\lambda\!\!\!^{-}_{C,n}} = 7.1676...x10^5 \ \ Newton \tag{4.18}$$

.

The ratio of tension stress force to differential force or gravitational quantum, which is also the ratio of the tension <u>stress</u> to the differential stress is

$$\frac{\tau_0}{d\tau_0} = \frac{\tau_0}{G_0} = \frac{T_0}{dT_0} = 1.6887...x10^{38}. \tag{4.19}$$

Inverting this gives the differential of the natural log of the expansion stress

$$d\ln T_0 = {dT_0}\Big/{T_0} = 5.9214...x10^{-39} \tag{4.20}$$

This is also the general scale of the ratio of the gravitational force to the strong force, this latter interaction being what τ_0 represents. It will prove of interest that the square root of (4.19) is equal to the ratio of the neutron reduced Compton wavelength and the Planck length as

$$\frac{r_0}{l_P} = \sqrt{\frac{T_0}{dT_0}} = \sqrt{d\ln T_0^{-1}} = 1.29952...x10^{19}. \tag{4.21}$$

With respect to gravity, the rotational oscillation of the PS_3 results in a centripetally directed tension stress force <u>differential</u> in response to expansion tension force that accounts for gravity, as found in (4.17) above. This is found in the above Spin Diagrams and the Figure 40 and 41 Charge and Spin Tables at the centripetally directed cross products for the W_{+x} and $+V$ nodal points for the neutron, the W_{+x} and $-V$ nodal points for the proton and electron, and the W_{-x} and $+V$ nodal points for the antiproton and positron.

Quantum Newtonian Law of Gravity

A quantum version of Newton's law can thus be shown from the above as

$$F_G = \frac{n_{M1} n_{M2}}{n_{r_0}^2}\left(\frac{\mathrm{A}_0}{\gamma_3} dT_0\right) = \frac{n_{M1} n_{M2}}{n_{r_0}^2} G_0 \tag{4.22}$$

where the mass and distance properties are expressed in units of the fundamental neutron scale. Substituting

$$n_{Ma} = \frac{M_a}{m_0} = M_a \frac{r_0}{\frac{\hbar}{c}} \tag{4.23}$$

$$n_{r_0} = \frac{d}{r_0} \tag{4.24}$$

gives Newton's law

$$F_G = \frac{M_1 M_2}{d^2}\left(\frac{r_0^4}{\left(\frac{\hbar}{c}\right)^2}\frac{\mathrm{A}_0}{\gamma_3} dT_0\right) = \frac{M_1 M_2}{d^2} G_N \tag{4.25}$$

Since the interaction depicted here is mediated directly by the spacetime fabric (STF) and not by any messenger particles or gravitons and since it has been operable with expansion since the initial generation of the rest mass particles, it is not a case of "action at a distance".

Since all the forces in this discussion of PS_3 are stress forces of the STF, the individual PS_3 or rest mass quanta, as well as any transmitted photon, naturally couple with the STF in keeping with the field equation of general relativity. In addition, such generation of quanta from a classical phase space and field is straightforward and requires no other constructs such as Minkowski time for interpretation.

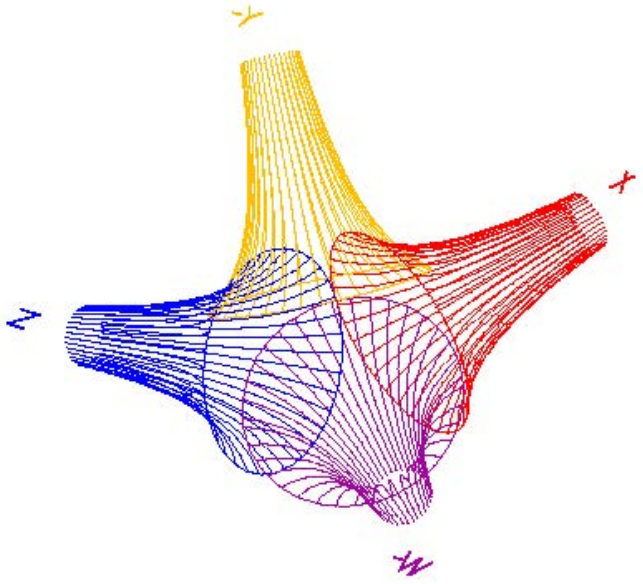

Figure 44 – One Half of an Inversphere

We can, however, offer the following 4 dimensional interpretation of a 2-sphere, the surface of a PS_3, in the context of the above development. Each of the four axes of the cubic diagonals can be defined as the central axis of a pair of pseudo-spheres, one on each side of the central 2-sphere, so that they intersect each other orthogonally at their rims as seen in Figure 44, which shows the top half of such an arrangement. A

pseudo-sphere has constant negative curvature, and the rim intersections will be found to coincide with the intersections of the corresponding three cubic surface axes and the surface of a sphere of curvature related to the positive of the pseudo-spheres; if the pseudo-sphere curvatures are -1, that of the sphere is $+\frac{\sqrt{3}}{2}$. We can call this contraption of eight pseudo-spheres an inversphere. Sequential oscillatory twists of the four axes as in Figure 28 and in the development of the cuboctahedral lattice produces the rotation of PS_2 in PS_3.

2) Quantum PS_3 Oscillation States, Cosmic Expansion and Beta Decay

With expansion, the interstitial areas of the lattice respond primarily to tension, and resulting tension strain leads to a decrease in ambient inertial density. The mechanical impedance of the interstitial area decreases as well, and a portion of the energy of the quantum oscillation is transmitted in the process of beta decay as a lepton and corresponding neutrino. Therefore, we would expect the expansion rate, i.e. the Hubble rate, to be linearly coupled with that decrease in linear density and mechanical impedance and thereby beta decay. Photonic messenger particles, in turn, are generated by the activity of the emitted electron.

Now for a mathematical development of this claim, we review the following:

Classical Wave Mechanics

The mechanisms of harmonic motion of an ideal inertial/elastic, continuous medium give rise to discrete phenomena in the form of wave phasing, θ, expressed as a wave period, semi or quarter period, or here as radian. Such discreteness can be quantized in terms of distance as the angular wave number, κ , and in terms of time as the angular frequency, ω , of the motion. The speed of the motion, *c*, in either standing or traveling form, is then given as the ratio of the frequency to wave number as

$$c = \frac{\omega}{\kappa} = \frac{\frac{\partial\theta}{\partial t}}{\frac{\partial\theta}{\partial r}} = \frac{\partial r}{\partial t}. \tag{4.26}$$

Such ideal wave bearing continuum will typically have a resonant frequency, ω_0, and hence a corresponding resonant wave number, κ_0, and we can thereby designate natural distance and time units based upon these resonance values as

$$r_0 = \kappa_0^{-1} \tag{4.27}$$

and

$$t_0 = \omega_0^{-1} \tag{4.28}$$

and (4.26) can be restated variously as

$$c = \frac{\omega_0}{\kappa_0} = \frac{\frac{\partial\theta}{\partial t_0}}{\frac{\partial\theta}{\partial r_0}} = \frac{\partial r_0}{\partial t_0} = \frac{r_0}{t_0} = r_0\omega_0 \tag{4.29}$$

Note the correspondence of (4.26) with the first line of (4.2) and that as long as the distance and time variables remain coupled by the phase variable, they vary proportionally or are co-variant with respect to any change in θ.

While the relationship given by (4.26) is descriptive of the phenomena of quantization, the dynamics of the wave is explained by the properties of the underlying continuum substrate. According to classical wave mechanics, in this case of an ideal stretched string, the wave speed squared is directly related to the tension force through the string and indirectly related to its inertial or mass density as

$$c^2 = \frac{\tau_0}{\lambda_0}. \tag{4.30}$$

Thus an increase in the tension force or a decrease in inertial density necessarily results in an increase in the wave speed. Coupling (4.29) and (4.30) gives the basic wave equation

$$-\kappa_0^2 = \frac{\partial^2\theta}{\partial r_0^2} = \frac{1}{c^2}\frac{\partial^2\theta}{\partial t_0^2} = \frac{1}{\frac{\tau_0}{\lambda_0}}\frac{\partial^2\theta}{\partial t_0^2} = -\frac{1}{\frac{\tau_0}{\lambda_0}}\omega_0^2 \tag{4.31}$$

In the last term, the dynamic properties of the wave are found in the ratio of force to density, which determines the wave speed and thereby produces the observed quantization found in the displacement and time derivatives. An increase in the wave speed over time will result in a decrease in the wave number, i.e. in a red shift, if the time standard given by t_0 is held fixed. However, if time and displacement standards are co-variant, then the nominal wave speed will remain invariant, even though that speed in absolute terms, i.e. measured against some universal time scale, is increasing.

Note that if the medium, in this case the string, is stretched, it indicates a decrease in inertial density throughout its extent, along with a possible net force increase. We can apply this same reasoning to an arbitrary one dimensional tension component of a three dimensional space under isotropic extension or expansion.

As expressed in the second line of (4.2), if the speed of light is invariant at any scale, then Planck's constant simply points to a more fundamental relationship in which the product of particle mass and length scale, as given by the particle's reduced Compton wavelength, is invariant. Particle mass, m_q then, is an inverse measure of the particle wavelength, and can also be expressed as the particle angular wave number, κ_q. Thus

$$\frac{\hbar}{c} = m_q r_q = m_q \lambda\!\!\!^{-}_{C,q} = \frac{1}{\lambda\!\!\!^{-}_{C,q}}\lambda\!\!\!^{-}_{C,q} = \kappa_q \lambda\!\!\!^{-}_{C,q} = \text{ת} \tag{4.32}$$

where the final term is a constant of inertia, as introduced earlier and designated tav, ת, which is equal to 1 in a natural system as seen in the fourth term, and is simply a proportionality factor relating conventional measures of mass to distance in the second and third term. While there are cases in which the transverse wave speed of a medium may be different from its longitudinal speed, in cases where they

are the same, the greater the wave number, the greater will be the curvature of the wave form. If the wave medium is the spacetime fabric, the greater the curvature, the more particle mass, i.e. inertia, will be incorporated by the wave action. The value in breaking down Planck's constant into the inertial constant and the speed of light, is that it allows us to remove the time dimension from the fundamental invariant, giving us a dynamic component or moment that is invariant in any reference time-frame.

Combining (4.32) with (4.26) and (4.30) gives the quantum wave equation

$$\lambda_q = \hbar\kappa_q^2 = \frac{1}{c^2}\hbar\omega_q^2 = \frac{1}{c^2}\tau_q \tag{4.33}$$

where λ_q is the inertial density of the quantum waveform and τ_q is the wave force of that quantum.

Applying (4.32) to (4.3) with (4.4) gives

$$G_N = \frac{r_0^3}{m_0 t_0^2} = \frac{c^3}{\hbar} r_0^2 = \frac{c^2}{\hbar}\mathrm{A}_P \tag{4.34}$$

and to (4.14) gives

$$G_N = \frac{r_0^2}{m_0^2}\left(d\tau_0\right) = \frac{r_0^4}{\hbar^2}\left(\frac{r_0^2 dT_0}{6\sqrt{3}}\right) = \frac{r_0^4}{\gamma_3\hbar^2}\mathrm{A}_0 dT_0 \tag{4.35}$$

Substituting (4.35) and (4.11) and (4.12) into (4.34) gives

$$\frac{r_0^4}{\gamma_3\hbar^2}\mathrm{A}_0 dT_0 = \frac{c^2}{\hbar}\left(-\frac{\mathrm{A}_0}{\gamma_3} d\ln T_0\right) \tag{4.36}$$

Here the difference in sense between the two terms indicates the centripetal direction of the left term and the counter centripetal of the right. Rearranging so that the space dimensions are on the left and the properties with time dimension, apart from the stress differential, on the right gives

$$\frac{\mathrm{A}_0^2}{\hbar} dT_0 = c^2\left(-d\ln T_0\right) \tag{4.37}$$

while some rearrangement

$$\frac{r_0^4}{\hbar} = c^2\left(\frac{-d\ln T_0}{dT_0}\right) = -c^2\frac{1}{T_0} \tag{4.38}$$

and inversion gives a three dimensional equivalent of the wave speed equation of (4.30)

$$\frac{\hbar}{r_0^4} = -\frac{1}{c^2}T_0\,. \tag{4.39}$$

This is descriptive of the spacetime substrate and not of any particular quantum wave.

Returning to (4.37), assuming that the inertial and space parameters are invariant over time, and that the stress derivative remains at unity, so that the left hand term

of the equation is invariant, if we assume that the log of the tension increases with expansion, that is, over cosmic time, then going back in time indicates an increase in the differential log of the expansion and a corresponding decrease in the square of the wave speed, if the invariance of the left hand term is to be preserved. In other words, expansion results in a decrease in inertial density of the spacetime substrate and a corresponding increase in the wave speed. If the decrease in the differential is not balanced by the increase in wave speed with expansion, then the stress differential on the left must change accordingly, with a corresponding effect on the invariance of the gravitational quantum.

We are assuming that the speed of a traveling wave, i.e. of electromagnetic radiation, is the same as that of a discrete, standing oscillation, a rest mass waveform. Such oscillation is equivalent to an electromagnetic wave circling a center of spin at a distance of the quantum's reduced Compton wavelength. If we think of such wavelength as the arm of a quantum clock whose tip travels always at the speed of light, then extending the length of the arm results in a decrease in its angular velocity. By contrast, if we think of time as a measure of the clocks angular velocity as is customary, then time must slow down as the arm extends if the end speed is to remain invariant.

In general relativity, time is said to dilate, but in a different manner. Increased inertial density, as in a gravitational sink, causes our quantum clock to contract its arm instead of extend it, in keeping with the inertial constant, with a corresponding decrease in angular velocity. The end of the clock arm, then, slows down as measured from some global perspective. Rising out of that sink causes the clock arm to lengthen and the angular velocity to increase.

If the speed of the arm tip is to remain constant with decreasing density and an extension of the arm, either the angular velocity must decrease or the time unit must extend to t_{0e}, to account for an increase in circumferential travel per unit of initial time, t_{0i}. Inverting the usual expression for velocity, the time standard must vary with the length standard if *c* is to remain invariant as

$$c^{-1} = \frac{t_{0e}}{r_{0e}} = \frac{t_{0i}}{r_{0i}}$$
$$\therefore t_{0e} = \frac{r_{0e}}{r_{0i}} t_{0i} \tag{4.40}$$

Similarly in terms of angular frequency

$$c = r_{0e}\omega_{0e} = r_{0i}\omega_{0i}$$
$$\therefore \omega_{0e}^{-1} = \frac{r_{0e}}{r_{0i}\omega_{0i}} \tag{4.41}$$

Beta Decay as a Function of Expansion

We are now ready to tackle our claim concerning the coupling of beta decay to the Hubble rate. Expansion of the STF does not indicate an equal linear decrease in

density either inside, locally outside or remotely outside the fundamental quantum oscillation. The region remotely outside any oscillation is primarily under tension stress and attendant strain, and with extension suffers a decrease in linear density and related mechanical impedance, Z, where impedance, which essentially relates units of time to units of mass of a wave bearing medium, is defined as follows, using the customary theoretical unit values

$$\lambda_0 c = \frac{\tau_0}{c} = Z_0 \tag{4.42}$$

The region about the periphery of the oscillation participates in the oscillation and exhibits a combination of tension and shear stress/strain and corresponding density fluctuations similar to what we might find in the ergosphere of an extreme Kerr quantum black hole, which is what the neutron is. The region between the nodes of the oscillation remains at the same density, unless a change of external impedance allows transmission of a small portion of its energy and therefore a change in inertial density.

Neutron/Electron Mass Ratio

In order for the energy of beta decay, which we will quantify as the mass of the electron, to be transmitted from the neutron waveform, the density and impedance at its boundary must decrease sufficient to permit that mass-energy to pass. The electron mass, m_e, is determined according to geometric constraints of the neutron oscillation and is approximately 0.000543867 . . . of the neutron mass, m_0.

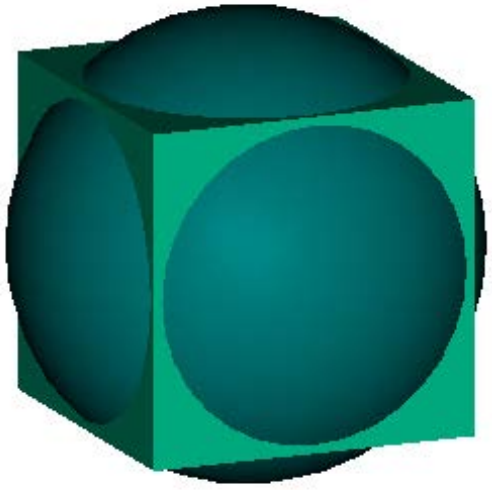

Figure 45

Figure 45 shows a concentric sphere and cube which have equal individual surface areas. Assuming a sphere of radius r_0 and area A_s and a corresponding cube with area A_c and edge length l_c, we have

$$A_s = 4\pi r_0^2 = 4\pi = 6l_c^2 = A_c \tag{4.43}$$

$$l_c = \sqrt{\tfrac{2}{3}\pi} \tag{4.44}$$

Tension stress on the surface of each would be equal, though the sphere represents isotropic stress while the cube represents a breakdown of the orthogonal components of such stress in keeping with the above development. The points mid way along each cubic edge are loci of closest stress/strain equivalence between cube and sphere. They are also the points of optimal shear stress and strain in the PS_3 rotational oscillation, as evidenced by the action/power moments. Such stress force operates in an oscillatory manner toward a leading adjacent vertex, directed by the two resultant torques, C and L, aligned with two of the cubic diagonals, toward one or the other of the two vertices beyond the leading adjacent one.

Over time the length of the moments vary as δr_0, in the context of an expanding STF, generally in an increasing direction. The edge of the cube represents a limit for the increase in the moments, which is reflected by an increase in C and L and their orthogonal vector representations ε and μ of the Spin Diagrams. The result is an increase in the cross-product along the $W_{+x} - W_{-x}$ axis for ϕ, an advance of the moments and a transmission of energy and power at that W_{-x} node as beta decay, where δr_0^2 represents the relative energy and therefore mass of the transmitted oscillation.

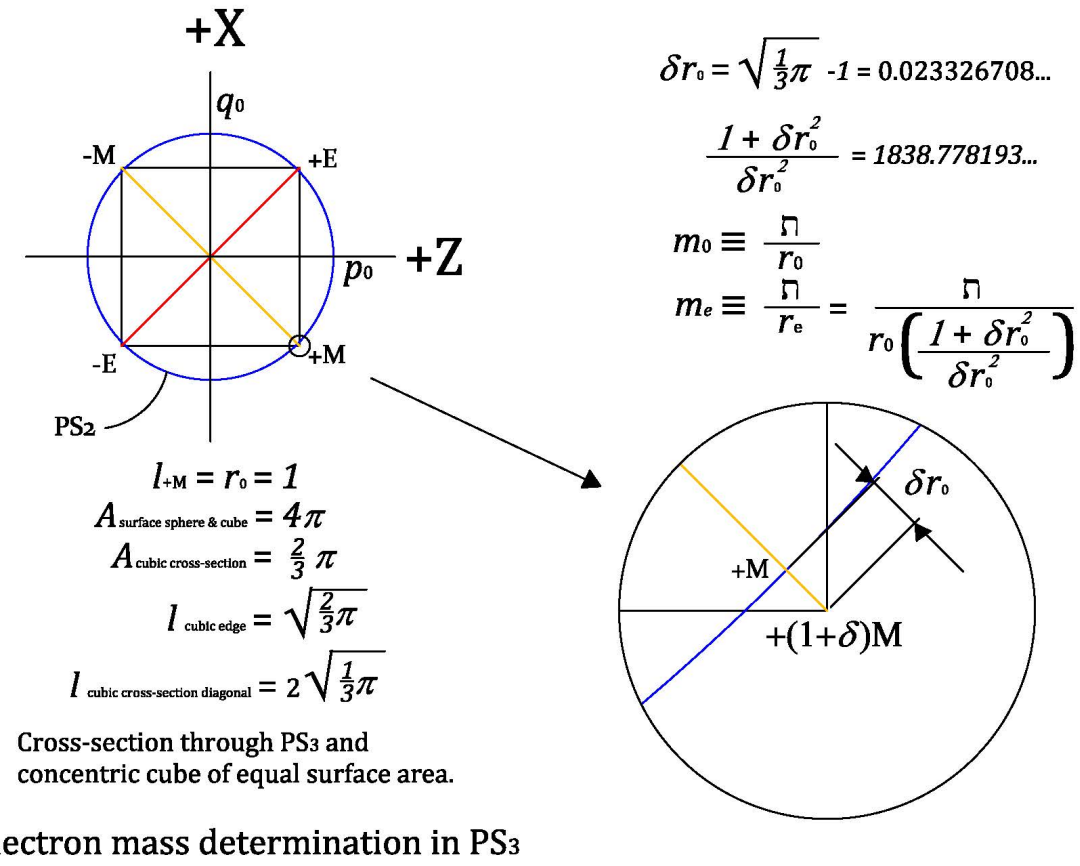

Cross-section through PS_3 and concentric cube of equal surface area.

Electron mass determination in PS_3

Figure 46

Figure 46 shows a cross-section through this structure at the X-Z plane of the developed PS_3 and aligned with PS_2 so that the moments +/-E and +/-M are aligned with the four half diagonals of the cubic cross-section. This indicates the moments rotating in alignment with the mid points of two of the four edges of the upper and lower cubic faces. Each half diagonal length is therefore $\sqrt{\frac{\pi}{3}}$ to the parallel moment length (not strength) of r_0 of 1.

The square of the differential δr_0 is reflected in the cross-product of the differential values of ε and μ as

$$\delta r_0 = \sqrt{\tfrac{\pi}{3}} - 1 = 0.023326708\ldots \tag{4.45}$$

$$\delta r_0^2 = 0.0005441353061\ldots \tag{4.46}$$

The ratio of the differential stress to the augmented total according to the resulting strain is

$$\frac{\delta r_0^2}{1+\delta r_0^2} = 0.0005438393841\ldots \tag{4.47}$$

which when inverted is

$$\frac{1+\delta r_0^2}{\delta r_0^2} = 1838.778193\ldots \tag{4.48}$$

The 2010 CODATA ratio of the electron to neutron mass is 0.00054386734461(32) or inverted 1838.6836605(11). Since mass computation presumably uses Newton's gravitational constant somewhere in the standardization of mass and weight, and given that the relative standard uncertainty of that constant at 1.2 x 10^{-4} is relatively large, it appears that (4.47) and (4.48) are within the relative standard uncertainty of the neutron-electron mass ratio.

Derivation of the Hubble Rate, the Expansion Rate of the Cosmos

Continuing on, the reduced Compton wavelength of the electron is

$$\lambda\!\!\!^{-}_{C,e} = r_e = \frac{\hbar}{m_e} = \frac{m_0 r_0}{m_e} \tag{4.49}$$

According to (4.33) the change in inertial density of the STF required for beta-decay is the loss of mass/energy equal to that of the electron from the region exterior to the neutron oscillation nodes over a distance r_e, to be replaced by beta-decay from the neutron energy or

$$d\lambda_0 = \frac{\hbar}{r_e^2} = \frac{1}{c^2}\hbar\omega_e^2 = \frac{1}{c^2}\tau_e \tag{4.50}$$

where ω_e is the rest mass frequency of the electron given by

$$\omega_e = \frac{c}{r_e} \tag{4.51}$$

and τ_e is the wave force of the electron rest mass. The differential density is the decrease in inertia over the distance of a wavelength required to generate a waveform of such mass.

With separation of one of the wave speed components in (4.50), a change in the linear inertial density over time is equal to a change in the impedance over distance as

$$\frac{d\lambda_0}{dt} = \frac{\tau_e}{c}\frac{1}{dr} = \frac{dZ_0}{dr} \quad . \tag{4.52}$$

Since the values of the inertial constant as Planck's constant over the speed of light and the electron reduced Compton are well determined, we can solve for $d\lambda_0$ and get

$$d\lambda_0 = 2.3589...x10^{-18}\, kg/m \quad . \tag{4.53}$$

Since the change in linear inertial density is a linear change, we might expect this expression to reflect the Hubble rate, which instead of a velocity per megaparsec of recession of galaxies, can be viewed as a dimensionless linear strain of space and therefore of time, and in fact (4.53) is a very close approximation. Converting kilometers per megaparsec to a dimensionless strain over a second, assuming a Hubble, H_0, of 73[1] km per second per mps gives a spacetime strain of $2.3657\ldots x10^{-18}$ per second. This indicates that the Hubble rate is capable of generating the force required for beta-decay. However, we would like something more precise and dimensionally correct.

Returning to (4.50), we can decompose the wave speed invariants

$$\frac{ת}{r_e^2} = \frac{1}{(r_e\omega_e)(r_0\omega_0)}ת\omega_e^2 \tag{4.54}$$

then rearrange and multiply through by r_e to get

$$m_e = \frac{ת}{r_e} = \frac{ת\omega_e}{r_e}\frac{\omega_e}{\omega_0}\frac{r_e}{r_0\omega_e} = dZ_0\left(\frac{\omega_e}{\omega_0}\right)H_0 \tag{4.55}$$

where the change in impedance is stated as the quotient of the change in expansion force and the wave speed and the Hubble rate is shown as the spacetime length and simultaneous time strain for each second, as in (4.40) and (4.41),

$$H_0 = \frac{r_e}{r_0\omega_e} = \frac{r_e}{r_0}\frac{t_0}{\theta_e} = \frac{\omega_0}{\omega_e}\frac{t_0}{\theta_e} = 2.36838922...x10^{-18}\, s\,. \tag{4.56}$$

Transferring the frequency ratios to the mass side of the equation and substituting from (4.41) the resonant mass of the neutron as a function of the product of the expansion rate and the concurrent change in mechanical impedance is

[1] A study by Ron Eastman, Brian Schmidt and Robert Kirshner in 1994 and quoted in Kirshner's book, The Extravagant Universe, found an H_0 of 73 km/s/mps +/- 8 km.

$$m_0 = ħ\kappa_0 = \frac{ħ}{r_0} = \frac{ħ}{r_e}\frac{r_e}{r_0} = dZ_0 H_0 \ . \tag{4.57}$$

Evaluation of (4.56) in conventional astronomical terms is 73.082 kilometers per megaparsec for each second of current time. That is, a unit of space and co-variant time are currently extended/dilated at this rate. The implication is that space and time are currently expanding logarithmically, therefore at an accelerating pace and such expansion drives the resonant frequency as indicated by the conjugate of the frequency, wave number hence mass.

Thus, if the Hubble rate of expansion is roughly 73 kilometers per second per mpc, this indicates that every local section of space is moving away from every other at approximately 2.37 x10^{-18} meters per second per meter of separation. However, we would expect this expansion to show up primarily in the large voids between galactic filaments and clusters and not in these galactic environs or filaments of baryonic matter due to the counter effects of gravity and electromagnetism. It follows conventionally that inversion of this number would give us the approximate time since all the matter was at the same locale and that the universe has been expanding, or 4.22 x10^{17} seconds, which is roughly 13.4 billion years.

However, as this number represents an expansion via a compounded augmentation of the scale of spacetime itself, and not simply an extension of matter within that spacetime, the following equation for the doubling of spacetime applies, giving us the Hubble time, τ_H as

$$\tau_H = \frac{\ln 2}{H_0} = 2.92666...x10^{17}\, s\,, \tag{4.58}$$

This indicates that space is doubling at a current rate of every 9.280 billion years, measured in terms of today's seconds. If we assume that the wavelength of the cosmic background radiation at approximately 5mm embodies that augmentation, while harkening back to a period of primal beta decay as indicated by the Compton wavelength over 2π of an electron, this represents a doubling of some 30 times, or

$$\frac{\ln\left(\frac{\frac{.005}{2\pi}}{r_e}\right)}{\ln 2} = \frac{\ln 2.060...x10^{9}}{\ln 2} = 30.94...doublings \tag{4.59}$$

a lifetime in terms of today's measure of time of roughly 288 billion years. If we extrapolate back on the same basis for the expansion over the scale of r_0 to r_e, prior to beta-decay where it may or may not be applicable, we have an additional doubling of 10.84 times or

$$\frac{\ln(1830.6842...)}{\ln 2} = 10.84.... \tag{4.60}$$

or a total doubling of the Hubble time of 41.78 or 393.47 billion years in current time as

$$\left(2.927...x10^{17}\right)\left(41.78...\right) = 1.2227...x10^{19}\, s \tag{4.61}$$

Finally, if we envision that a current expansion factor can be derived by a comparison of the Planck length and the neutron Compton wavelength, keeping in mind that we can multiply both terms by the speed of light without affecting their ratio and express the quotient as a coefficient of expansion in light seconds, given as

$$\kappa_{\exp} = \frac{r_0}{l_p} = \frac{2.10019...x10^{-16} m}{1.61612...x10^{-35} m} = 1.29952...x10^{19} ls \tag{4.62}$$

We have a close agreement with (4.61) at 412 billion years.

In another vein, we can multiply this figure as with (4.58) to get the extent of doubling, in terms of current time standards over the most recent doubling period, as 285 billion years or

$$C_x = \ln 2\left(\kappa_{\exp}\right) = 9.00758...x10^{18} ls\,. \tag{4.63}$$

Dividing by (4.58) we get the number of doublings since the initial factor established by beta-decay and get

$$\frac{C_x}{\tau_H} = \frac{9.00758...x10^{18} ls}{2.92666...x10^{17} s} = 30.77..doublings \tag{4.64}$$

compared to (4.59).

With respect to the period before beta-decay or the last scattering of the standard model cosmology, it is not clear from this extant modeling that rest mass quanta emerged from an initial big bang. Rather it appears likely that such matter emerges in an ongoing manner from galactic inertial centers, i.e. black holes which can be gravitational field sources as well as sinks, and their connecting filaments in response to the tension stress of expansion of the surrounding, relatively mass free voids, as evidenced by the observance of episodic gamma ray bursts of unknown origin.

The Missing Mass of Beta Decay

We are not quite through with our investigation. While the ratio of neutron-electron mass as developed here is compelling, there is still a matter of the missing mass of beta decay. According to the CODATA ratios, the difference between the neutron-electron mass ratio and proton-electron mass ratio is

$$\frac{m_n}{m_e} - \frac{m_p}{m_e} = 1838.6836... - 1836.1526... = 2.5310... \tag{4.65}$$

Since the relative mass of the electron in this case is 1, there is a relative mass or equivalent energy of 1.530… that is unaccounted for. If it is assumed that mass is a property that is somehow bound up in the confines of a discrete particle, this is a puzzlement. However, if it is understood to be a measure of the resistance of stress to a straight line force, i.e. a measure of redirection of oscillatory energy and therefore of curvature of spacetime strain, the problem vanishes.

Consider the function

$$W(n) = \ln_0 e_n^n \tag{4.66}$$

which is related to the Lambert W function, where n can be any real number, though we will only be considering the integers. The significant feature of this function is that it generates a system of natural logs, $\ln_n$, and corresponding exponential bases, e_n, that can be used as normalizing factors, so that

$$\ln_n e_n = 1,\ \ln_n e_{-n} = -1\ . \tag{4.67}$$

At $n(0)$, this is simply the natural log and exponential base, and

$$W(0) = \ln_0 e_0^0 = 0 \tag{4.68}$$

In the following Figure 47 we have graphed the significant portion of the natural log and exponential functions. Note the functions mirror each other along the line $y = x$, as do their derivatives. We can define the exponential base, e_0, on both x and y axes by the point on each function at which the lines (blue) whose slopes represent the derivatives intersect each other and the origin of the system. The only other instances of such intersection would be when the functions reach negative infinity along both axes, which of course they never do in the context of Euclidean space. They do on the Riemannian complex sphere, however.

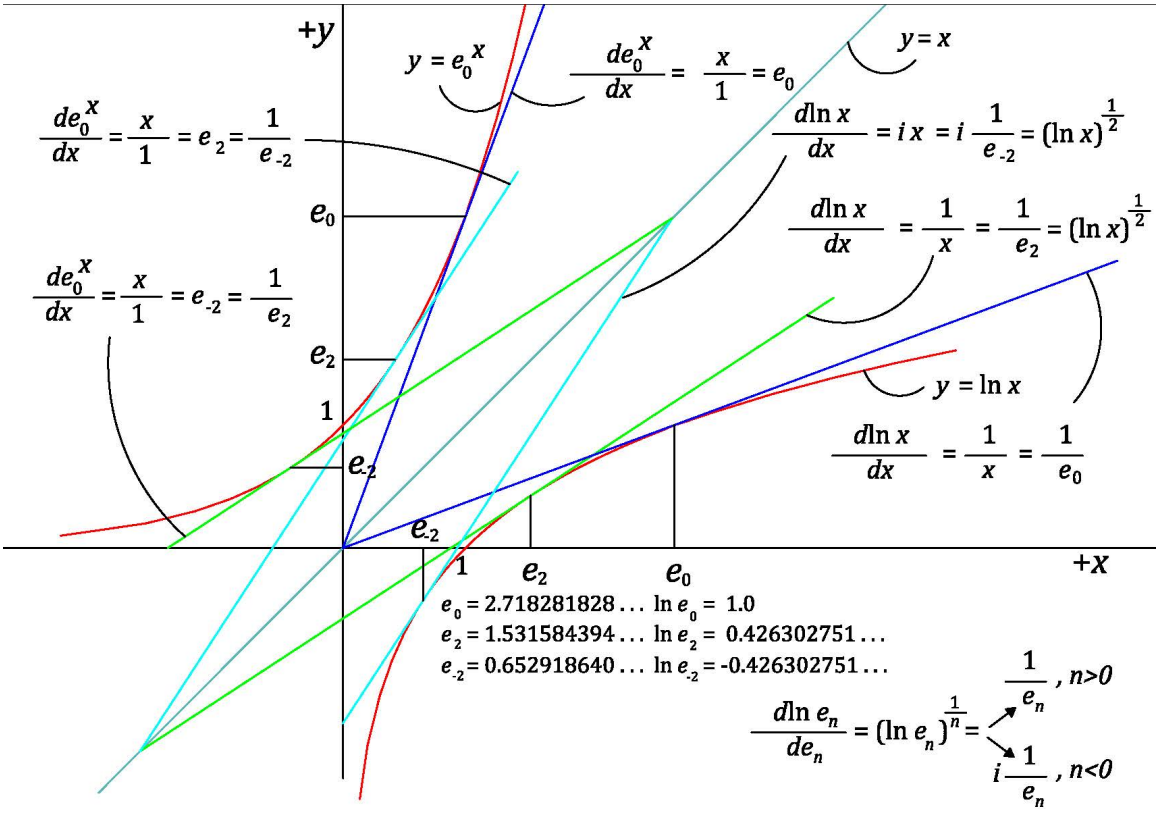

System of exponent bases e_n, shown for e_0 and $e_{\pm 2}$ where $e_{-2} = e_2^{-1}$

Figure 47

The whole system of e_n, for $n>0$, occurs in the range $1 < x < e_0$, and as n increases, the slope values converge while their intersection moves toward the negative infinities of both x and y. At the point $x = 1$, the derivatives of both functions equal 1 and their slopes are parallel. In terms of the Riemannian sphere, the lines actually form to great circles about the spheres equator. From that point, n decreases from negative infinity toward 0 at the y asymptote. Thus $n<0$, occurs in the range $0 < x < 1$. The x and y axes then are the doubles for the slopes e_0 and e_0^{-1}, corresponding to the doubles for the rest of range of n.

For the range $e_0 < x < +\infty$, the slopes of the two derivatives diverge as x increases, and there are no real subscript functions of e_n. Note that for the range n<0, however, according to the derivative of the natural log with respect to a change in x, the slope has imaginary sense, which generally indicates a rotation of some manner or another.

The following Figure 48 table shows the results of this function for the first three integers, and an assumption of results carried to infinity. The second Figure 48 table shows related results with the introduction of imaginary sense to the various function.

$f(n)$ | n	0	1	2	3	…	∞
e_n	2.718281828..	1.763222834..	1.531584394..	1.419024454..		1
$e_{-n}=e_n^{-1}$	0.367879441..	0.567143291..	0.652918640..	0.704709490..		1
e_n^n	1	1.763222834..	2.345750756..	2.857390779..		∞
$e_{-n}^n= e_n^{-n}$	1	0.567143291..	0.426302751..	0.349969632..		0
$\ln_0 e_n$	1	0.567143291..	0.426302751..	0.349969632..		0
$\ln_0 e_{-n}$	-1	-0.567143291..	-0.426302751..	-0.349969632..		0
$\ln_n e_n$	1	1	1	1		1
$\ln_n e_{-n}$	-1	-1	-1	-1		-1
$\ln_0 e_n^n$ $= W(n)$	0	0.567143291..	0.852605502..	1.049908893..		∞
$\ln_0 e_{-n}^n$ $= W(-n)$	0	-0.567143291..	-0.852605502..	-1.049908893..		-∞
$\ln_n e_n^n$	0	1	2	3		∞
$\ln_n e_{-n}^n$	0	-1	-2	-3		-∞

Figure 48

n	$f(n)$	$n \ln_0 e_n$	$in \ln_0 e_n$	$n \ln_0 ie_n$	$in \ln_0 ie_n$
1		0.5671...	i0.5671...	0.5671...+$i\pi/2$ (=+1 $i\pi/2$)	- $\pi/2$ + i0.5671...
2		0.8526...	i0.8526...	0.8526...+$i\,\pi$ (=+2 $i\pi/2$)	- π + i0.8526...
3		1.0499...	i1.0499...	1.0499...+$i3\pi/2$ (=+3 $i\pi/2$)	- $3\pi/2$ + i1.0499...
4		1.2021...	i1.2021...	1.2021...+$i\,2\pi$ (=+4 $i\pi/2$)	-2π + i1.2021...
5		1.3067...	i1.3067...	1.3067...+$i5\pi/2$ (=+5 $i\pi/2$)	- $5\pi/2$ + i1.3067...
6		1.4324...	i1.4324...	1.4324...+$i\,3\pi$ (=+6 $i\pi/2$)	-3π + i1.4324...

Figure 49

The function in (4.66) finds form in the following equation, where the negative sense in the subscript has the same meaning it does in the superscript exponent, that is it represents inversion.

$$\ln_0 e_n = e_n^{-n} = e_{-n}^{n} \tag{4.69}$$

Thus for n = 2, we have the following, where it is understood that e_2 is a normalizing coefficient for any variable *x*, in particular for an instant unit variable property x_0

$$\ln_0 e_2 \left(e_2\right)^2 = \ln_0 e_2 \left(e_{-2}\right)^{-2} = 1 \tag{4.70}$$

and with the variable, x_0, we have

$$\left(\ln_0 e_2 x_0\right)^{\frac{1}{2}} = e_2{}^{-1} = e_{-2} = \frac{d \ln e_2 x_0}{d e_2 x_0} = \frac{1}{1.53158...} \tag{4.71}$$

$$\left(\ln_0 e_{-2} x_0\right)^{\frac{1}{2}} = i e_{-2}{}^{-1} = i e_2 = i \frac{d e_{-2} x_0}{d \ln e_{-2} x_0} = i \frac{1}{1.53158...} \tag{4.72}$$

In the final table, it is clear that the integers, *n*, are the count of the rotations of ½ π and of the powers and hence the number of orders of *i*, both indications of a degree of orthogonal structure.

We are interested here specifically in the factor e_2. As a review of Figure 47 hopefully makes clear, the value in the subscript exponential bases is in determining a coefficient of proportionality between two related differentials, one of which is a function of the *n*th-root of the logarithm to the others linear function. We refer back to the start of our discussion of SHM at (1.2) and the relation between an oscillator's frequency as a function of the square root of the quotient of the pendulum length over the motivating gravitational acceleration. Again in the above development of the neutron scale for quantum gravity at (4.21) we have an expression of the change in the linear scale of r_0 as the square root of the change in the natural log of the expansion stress scale, f_0. We can model quantum mass as a linear function of space by the reduced angular wavelength, r_0, or time by the frequency, ω_0. Using the inertial constant and/or the speed of light we have

$$m_0 = f(r) = ħ r_0{}^{-1} \tag{4.73}$$

$$m_0 = f(\omega) = ħ c \omega_0 = \hbar \omega_0 \tag{4.74}$$

Stress is modeled as a function of the square of both of these

$$f_0 = f\left(\omega^2, r^2\right) = \hbar\omega_0^2 r_0^{-2} \tag{4.75}$$

We will use r_0 for our discussion, since we previously discussed beta decay as a function of its increase. Thus a change in stress with expansion leads to a increase in r_0, where a preliminary decrease in mass of the fundamental oscillation, the neutron, is equal to the mass of the emitted electron or positron as developed above or

$$m_e = \Delta m_0 = m_0\left(\frac{\delta r_0^2}{1+\delta r_0^2}\right) \tag{4.76}$$

The change in stress/energy density of the oscillation is

$$dE_1 = df_0 = f'\left(\mathrm{A}_0{}^{-2}\right) = -\frac{\hbar\omega_0^2}{\mathrm{A}_0^2}d\mathrm{A}_0 = -\frac{\tau_0}{\mathrm{A}_0^2}d\mathrm{A}_0 = -\frac{f_0}{\mathrm{A}_0}d\mathrm{A}_0 \tag{4.77}$$

where it is clear that a change in the log of the stress is inversely equal to a change in the in the log of the cross-section,

$$d\ln f_0 = \frac{df_0}{f_0} = -\frac{d\mathrm{A}_0}{\mathrm{A}_0} = -d\ln \mathrm{A}_0\ . \tag{4.78}$$

Obviously, since both stress and cross-section are unit values,

$$\ln f_0 = \ln \mathrm{A}_0 \tag{4.79}$$

Thus for a logarithmic expansion of the cosmos, in accordance with (4.78) and using (4.72), we substitute f_0 for A_0 which is the square of $r_0 = x$ and get

$$\left(\ln f_0\right)^{\frac{1}{2}} = ie_{-2} = i\frac{df_0}{d\ln f_0} = i\frac{df_0}{d\ln f_0} = i0.65291\ldots = \frac{1.0}{i1.53158\ldots} \tag{4.80}$$

The imaginary sense assigned to the natural log differential is an indication of transverse motion and other energy associated with the change in stress, resulting in the change to that of the reduced Compton wavelength of the proton.

The Hamiltonian or total energy of the system resulting from beta decay is therefore the energy of the neutron, less the rest mass energy of the electron due to the change in stress, less the change in spin energy due to the natural log of the stress, to equal the mass or rest mass energy of the proton.

$$E_0 - E_e\left(df_0\right) - E_0\left(d\,\mathrm{nl}\, f_0\right) - E_p = 0 \tag{4.81}$$

In terms of mass

$$m_0 - 1m_e - 1.53158\ldots\Delta m_0 - m_p = 0 \tag{4.82}$$

This is accurate to a factor of 2.16 x 10^{-7}.

Evaluation of Elementary Charge

An final observation is in order, this about charge. We discussed it as a function of the fundamental oscillation of PS_3, but did not relate it to experimental data and the SI fundamental charge, the coulomb, C. The coulomb, or ampere per second, is equivalent in mechanical dimensions to one kilogram-meter per second, a measure of momentum. A fundamental unit or elementary charge, e_0, is established as

$$e_0 = 1.60217653(14)x10^{-19} \text{ Coulomb} \tag{4.83}$$

As a measure of momentum, in connection with our development of PS_3 and the transmission of momentum with beta decay at W_{-x}, the fundamental unit of conjugate momentum, using angular frequency, is reasonably close to (4.83)

$$p_0 = \hbar\omega_0 = 5.02130...x10^{-19}\, kg \cdot m / s \tag{4.84}$$

Charge is related to each of the two rotational nodes, W_{-x} and W_{+x}, indicating the need to apply semi-periodic frequency, which we can do by dividing (4.84) by π. In addition, the charge generation is conditioned by the product of the momentum and the mechanical impedance of the STF (not to be confused with the electro-magnetically derived characteristic impedance of the vacuum), which is

$$\begin{aligned} Z_0 &= \hbar\omega_0\kappa_0 = 0.002390877...kg / s \\ \zeta &= \left(\frac{1+Z_0}{\pi}\right) = 0.319070926... \\ \zeta^2 &= \left(\frac{1+Z_0}{\pi}\right)^2 = 0.101806256... \end{aligned} \tag{4.85}$$

where we define the total factor, ζ, and its square for later use. Thus we would anticipate an elementary charge of

$$e_0 = p_0\zeta = \hbar\omega_0\zeta = 1.602152647...x10^{-19}\, kg \cdot m / s \tag{4.86}$$

This varies from the established value by a factor of 1.000015…which once again is in the same order of magnitude as the relative uncertainty for the gravitational constant.

Fine Structure Constant

Further development, using the familiar identity for the inverse of the fine structure constant, α, a dimensionless number and therefore the ratio of two like-property magnitudes, as

$$\alpha^{-1} \equiv \hbar c \frac{4\pi\varepsilon_0}{e_0^{\,2}} = 137.0359989... \tag{4.87}$$

and the permeability, μ_0, and permittivity, ε_0, relationship, where μ_0 is in units of inductance per meter or henrys per meter which reduces to units of force per current squared or newton's per ampere squared, and ε_0 is in units of capacitance per meter or farads per meter which reduces to ampere squared per newton over the speed of light in vacuo squared, so that

$$\varepsilon_0 = \frac{1}{c^2\mu_0} \tag{4.88}$$

and with rearrangement in (4.87) gives the following

$$e_0^{\,2} = -\hbar c^2\left(\alpha 4\pi\varepsilon_0\right) = -\hbar\frac{\alpha 4\pi}{\mu_0} = -\hbar\frac{\alpha}{10^{-7}} = -\hbar\left(\hbar\omega_0^{\,2}\right)\zeta^2 \tag{4.89}$$

It is noted that the value of μ_0 is set by convention in relating charge, q, (of which elementary charge, e_0, is an effective quantum) and current, $i = dq / dt$, resulting in

the exactness of the denominator of the next to last term. Since the negative sense of the right terms above can be attributed to the current, therefore charge, squared, it can be incorporated therein, canceling such sense in the charge squared term. This suggests the transparent presence of a current squared argument in (4.89), for which the fine structure constant is a coefficient, since from Ampere's Law for one ampere[2] of current, where the denominator on the right is in newton, we have

$$\mu_0 = 2\pi\left(2x10^{-7}N\right)\frac{d}{L}i_0^{-2} \tag{4.90}$$

2 x 10^{-7} newton is the force generated for each meter length of two conductors of infinite length and negligible cross-section and one meter apart in a vacuum with one ampere of constant current flowing in each conductor. The *d* and *L* obviously cancel and the i_0^2 component and therefore the force is positive or negative depending on whether the currents are parallel and attractive or antiparallel and repulsive.

Inserting this into (4.89) with some rearrangement gives the ratio of elementary charge squared to current squared as the product of the modified fine structure constant, α' as shown, and the inertial constant. If the fine structure constant is dimensionless and its denominator is a force from the above, then α' is an inverse force, which in terms of our PS_3 development is the inertial constant times a frequency squared and *k* is an unknown proportionality factor for the frequency as

$$\frac{e_0^{\,2}}{i_0^{\,2}} = \frac{\alpha}{10^{-7}}ת = \alpha' ת = \frac{k^2}{ת\omega_e^2}ת = \frac{k^2}{\omega_e^2} \tag{4.91}$$

If the force in the last term is the base transverse wave force of the electron as in the above development, then *k* is an angular measure per unit of elementary charge as,

$$k = \omega_e \frac{e_0}{i_0} = \left(\frac{\theta_e}{s}\right)\frac{e_0}{\frac{ne_0}{s}} = 124.3840198...\frac{\theta_e}{e_0} \tag{4.92}$$

Using this value with (4.91) gives

$$\alpha = \frac{k^2\left(10^{-7}\right)}{ת\omega_e^2} = \frac{k^2\left(10^{-7}N\right)}{0.212013671...N} = 0.007297352...\frac{\theta^2}{e_0^2} \tag{4.93}$$

With another look at(4.89), we get the following relationships between the fundamental wave force and α'

$$\alpha' = \tau_0\zeta^2 = ת\omega_0^2\zeta^2 = \zeta\omega_0 e_0 \tag{4.94}$$

Special Relativity and Muon & Tau Families

Concerning the compatibility of this model and special relativity, I have written about this extensively elsewhere. Suffice it to say that the PS_3 model is one of constrained stress/strain in the STF, which acts as discrete units of rest mass with derived properties. Each discrete state, remains a wave form and in response to interaction with other states is free to translate and rotate in space according to the ambient energies. It will therefore contract its characteristic strain radius in

response to acceleration in keeping with the Fitzgerald-Lorentz length contraction, resulting in an increase in spin energy/mass according to the definition of the inertial constant

$$\sqcap \equiv mr \equiv \frac{m}{\kappa} \tag{4.95}$$

As to the two other families of leptons, the muon and tau, and their theoretical related hadrons, based on their short lifetime and granted my limited knowledge of the experimental background for their theoretical introduction, it is my perception that they are simply the basic PS_3 states we have discussed, altered by relativistic dynamics and interaction. We would expect these states to behave in a generally ordered fashion under constraints of high energy collision and those defined by geometry and mathematics. The evolution of a catalogue of such short lived phenomenology, while useful, does not indicate the need or wisdom of elevating that phenomenology to ontology. I would grant the status of "fundamental rest mass particle" only to common, stable, relatively long-lived states, including the neutron, of course.

Conclusions

We can only talk about nature and the physical world because we have a conscious experience of it. That sensory experience is mediated by minds conditioned to look for patterns to help navigate that world. The degree to which such navigation is so facilitated is largely a measure of how well those patterns can be found and understood as interconnected parts of the complete fabric of experience. The process of such discovery is necessarily marked by periods of progress and temporary setback involving mental effort without recompense, but over the long haul it is a satisfactory venture.

It should be no surprise therefore that these minds feel the need to partition what is essentially an experience of a whole into a physical world and a mental world and perhaps some others in an attempt at understanding. Experience is experimental. What works is real, and what doesn't is, well, just in the mind; imaginary or perhaps just more complex.

We observe, we think with the hope of understanding, we create models in our heads of what we think is going on behind the scenes of our observation, we put the models to the test, and we observe again. When the model is accurate, we take notice, and when it is both accurate and precise, we call it true. The model merges with the field of observation and we quickly forget that the model is just a model. Without diminishing in one iota the relevance of such models, it bears remembering that the reality of the model is in our head. But then so is the conscious experience by way of the senses.

The problem with successful models is that they may be successful in their predictive power without sufficient understanding of the fundamentals on which their success is based. Axiomatic amnesia. It is all too easy to confuse logically necessary results of the way the model is framed with the assumptions made about the necessity of what is going on behind the curtain. Then when a dead end is encountered, it is too often deemed to be a problem with the superstructure of the model rather than a problem with its foundation.

No one has ever seen the microscopic world directly. The invention of that apparatus gave us a view of patterns unimaginable before. The microbiological world in particular teemed with living one-celled entities, quantum life so to speak, and it was natural to assume that the division of inert physical stuff continued down to some fundamental level as well. And so it does. It is just that each of those bacteria and other microbial beings don't create the biosphere. The biosphere is a set of ambient conditions that allow such beings to thrive. In a similar manner it is not the quantum particles of physics that create the phenomenal physical world, rather it is the principal of change of inertial continuity in space, which necessarily means over time, that creates the particles. If there is a Higgs field, this is what it is.

It is this writer's position that the center stage quantum world can only be understood against its classical backdrop of an expanding cosmos. I can't see behind the stage anymore than anyone else. What I do know is that if we are to understand what is going on back there, we must be logical. I know that there must be some ontological regime that operates more or less the same across the whole of the cosmos, if we are to make sense of it, and that it is more likely that such regime is to be physically found universally instead of replicated exactly at each microscopic locale across its extents. That is, the mass of a neutron here and 10 billion light years from here (after doing all the de rigueur relativistic computations) must be the same now not because of some initial investment at the big bang, but due to an operative condition at *both locales right now*. This sounds like a function of space itself.

The instant development of PS_3 as a model for understanding, for accounting for momentum and displacement and kinetic and potential energy and action and power and then spin angular momentum and charge within the context of Simple Harmonic Motion is a mental construct. I don't know for a fact if the void that space appears to be among the multitude of stars is a true vacuum or the only thing that really is. What I do know is that if we treat it as such, as an inertial – elastic wave bearing continuum, which appears to be fully consistent with the structure of PS_3, we can correctly account for or predict, without any extraneous factors:

Newton's gravitational constant as a quantum effect
Quantum spin invariance and magnitude
Quantum charge invariance and magnitude
The ratio of neutron/electron mass
The missing mass of beta decay and therefore
The ratios of neutron/proton and proton/electron
The nature of ordinary and anti matter
Relationship to the fine structure constant
All this as a function of an exponential Hubble rate

I don't know about the tauon and muon families, but there is more with respect to the consistency of this model with special and general relativity, including a description of the neutron as an extreme Kerr quantum black hole.

I believe this is a step up the ladder from the existing understanding. If it furthers the discussion, it deserves to be vetted.

You be the judge.

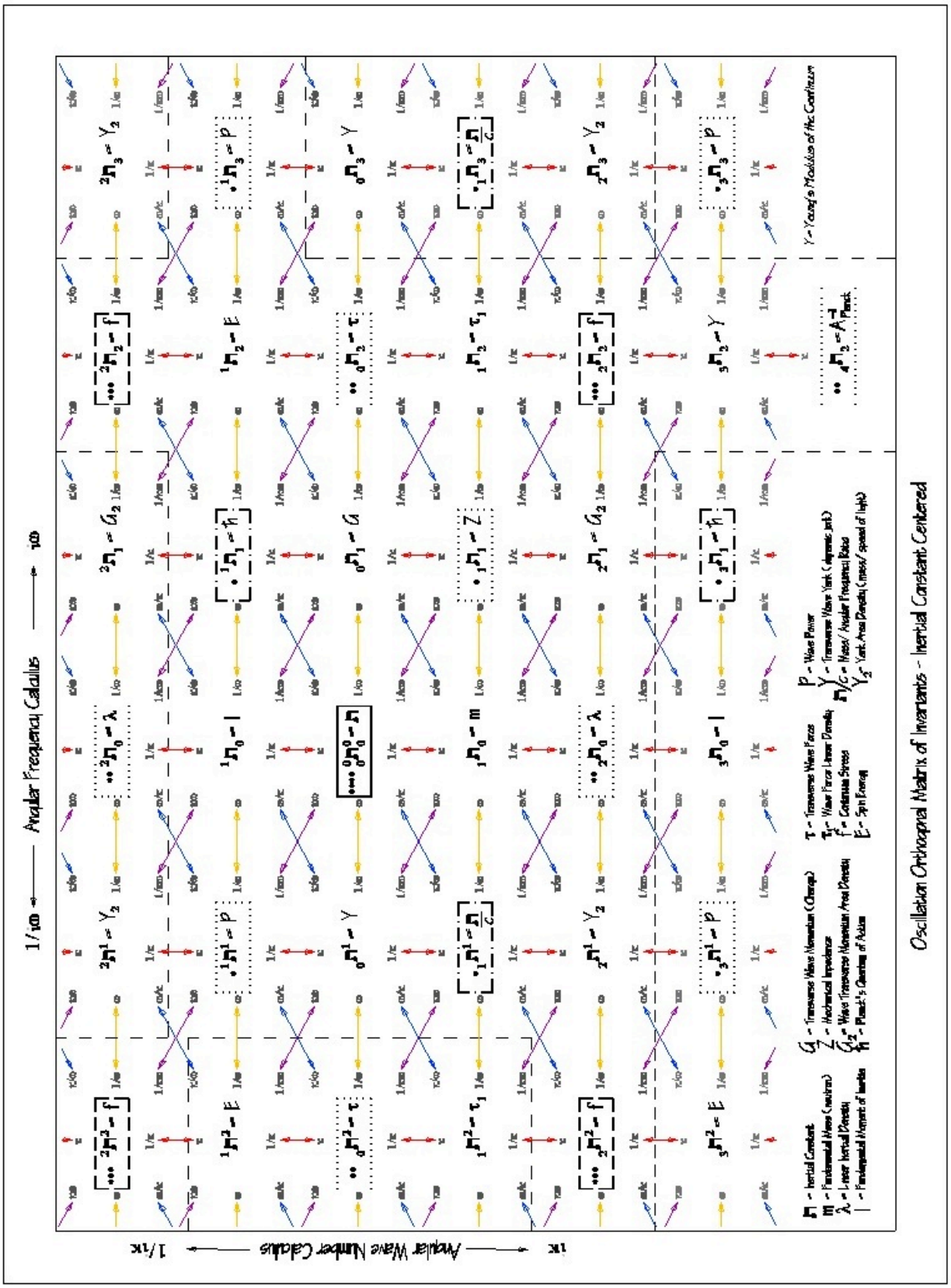

Matrix of PS_3 Functions and Invariants

Aside #1

Before we go further, it may be worthwhile to take a brief detour into the fundamentals of calculus. While this is very basic, it is hoped it will be helpful. A function is a mathematical structure, $F(x$, etc.) that establishes the relationship between an independent variable(s) numerical value, (x, etc.) and a mathematical result of computation, (y), using that value. Thus, y is equal to some function of x or

$$y = F(x) \tag{5.1}$$

The specifics of the function are given by some equation, such as

$$\begin{aligned} y &= 2x + 3, \text{ or} \\ y_n &= x^n \end{aligned} \tag{5.2}$$

where x is generally held to vary continuously over some interval, $a \le x \le b$. In this latter example, y_n might be a line segment length if $n = 1$, an area if $n = 2$, or a volume if $n = 3$. The n is not normally used in this manner for the y, of course, but we will find it useful. Thus

$$F_n(x) = y_n = x^n \tag{5.3}$$

The derivative of the function is the ratio of the rate of change in the function $F(x)$, generally expressed as $F'(x)$, resulting from a change in x, indicated by the letter d and expressed as dx. Thus

$$F_n'(x) = \frac{dy_n}{dx} = ? \tag{5.4}$$

The question is how do we figure the derivative and what does it mean? Let's say n is 1, and we have the following function

$$\begin{aligned} F_1(x) &= 2x^1 \\ y_1 &= 2x^1 \end{aligned} \tag{5.5}$$

x might be the weight of some variable commodity we want to ship, 2 might be the shipping cost in dollars per ounce of commodity, and y is then the cost of shipping. The shipping rate is then the derivative of the shipping cost with respect to a change in shipping weight or

$$F_1'(x) = \frac{dy_1}{dx^1} = 2\,. \tag{5.6}$$

Some folks would say at this point, "Why do you need calculus for this? The value of y per unit of x gives us the same thing." Indeed, provided we know x is in units of ounces. If n had been some number larger than 1, calculus might be more persuasive, however. The way we derive (5.6) is important. Since $F(x)$ is a linear function of x, the function of x plus a little bit more or $F(x + dx)$ is just

$$F_1(x + dx) = y_1 + dy_1 = 2(x + dx)^1 = 2x^1 + 2dx^1 \tag{5.7}$$

The difference or differential amount of $dF(x)$ or y is

$$\begin{aligned} dF_1(x) &= F_1(x + dx) - F_1(x) = y_1 + dy_1 - y_1 = 2x^1 + 2dx^1 - 2x^1 \\ dF_1(x) &= dy_1 = 2dx^1 \end{aligned} \tag{5.8}$$

and the derivative is the rate at which a differential amount of *y* is generated for every differential amount of *x*,

$$\therefore F_1'(x) = \frac{dy_1}{dx^1} = 2\frac{dx^1}{dx^1} = 2 \tag{5.9}$$

Here we get into the ambiguities of language. The derivative asks, "what is the cost of shipping per ounce of commodity equal to?" and the answer generally given by the last term in the equation is "it equals 2 dollars." Everyone knows what is being asked and everyone understands the answer. The problem is that it is not good grammar. As the good math and science student will remember being told, "The dimensional units on each side of the equation have to be the same."

The correct answer to the question is " it equals 2 dollars *per ounce of commodity*." Looking at the next to the last term of (5.9) does not help. Obviously the *dx* terms cancel out, but before that operation, the term reads "it equals 2 dollar*ounce per ounce", or for the purist, ""2 dollar*very small weight per very small weight". What type of unit is a "dollar*weight" anyway?

What is happening is that the nimble human mind understands the implicit context even if it is only subconsciously aware of it and fills in the gaps. Usually. (5.9) really becomes

$$F_1'(x) = \frac{dy_1}{dx^1} = \frac{2y_0}{x_0} \tag{5.10}$$

where y_0 is, of course, a unit of *y*, in this case a dollar, and x_0 is a unit of *x*, in this case an ounce. We are assuming in this discussion that the differential amount, *dx* can be much smaller than 1, as will *dy* as a result, but the derivative is still expressed in units of both *as a limiting rate*. If *dy* is contextually in fact $2y_0$, then *dx* becomes x_0.

If *x* is some function of time, *F*(*t*), then so is *y*, since

$$\begin{aligned} F(t) &= x = ct \\ F'(t) &= \frac{dx_1}{dt^1} = \frac{cx_0}{t_0} \\ \therefore dx_1 &= \frac{cx_0}{t_0}dt^1 \end{aligned} \tag{5.11}$$

then

$$\begin{aligned} F_1'\big(F(t)\big) &= \frac{dy_1}{dt^1}\left(\frac{t_0}{cx_0}\right) = \frac{2y_0}{x_0} \\ &= \frac{dy_1}{dt^1} = \frac{cx_0}{t_0}\left(\frac{2y_0}{x_0}\right) = c\left(\frac{2y_0}{t_0}\right) \end{aligned} \tag{5.12}$$

In the above example, *c* is the number of ounces, say 480, of commodity *x* being produced in a unit of time, say a day, so (5.12) becomes 480 ounces per day times 2

dollars shipping cost per ounce or 960 dollars in shipping costs per day, i.e. the rate of change in *y* per *one unit change* in *t*.

The take away here is that while we are accustomed to thinking of the derivative as expressing the ratios of exceedingly small quantities, at the limit that ratio is between two finite numbers, the consequent or denominator of which is always expressed as one unit.

A second observation about calculus is that it is generally stated with respect to an anisotropic differential. That is, one end of a linear mapping in a Cartesian system representing an independent variable is held fixed with respect to the appropriate axis as is its function on the second axis. This is reflected in the math as in the following, where the subscript after the independent variable indicates the number of differentials per variable,

$$\begin{aligned} F_2(x)_1 &= y_2 = x^2 \\ F_2(x+dx)_1 &= y_2 + dy_2 = (x+1dx)^2 = x^2 + 2xdx + dx^2 \\ F_2(dx)_1 &= dy_2 = 2xdx + dx^2 \\ F_2'(x)_1 &= \frac{dy_2}{dx} = \frac{2xdx + dx^2}{dx} \end{aligned} \tag{5.13}$$

and finally

$$F_2'(x)_1 = \frac{dy_2}{dx} = 2x + dx \tag{5.14}$$

This is all well and good if one is only interested in an interpretation in which the derivative is the slope of the curve given by $F(x)$ in the above. If dx is much less than unity it can be discarded in most cases in the example of (5.14). It can become important in integration of some such functions, however.

$F(x)$ might also represent the area of a physical space in which the relationship of the perimeter, $4x$, to the area, y_2, is of interest. We then might need to think of the differential as isotropic or bilateral, as in the following, where the differential occurs at both ends of the linear variable, thus

$$F_2(x+2dx)_2 = y_2 + dy_2 = (dx + x + dx)^2 = (x+2dx)^2 = x^2 + 4xdx + 4dx^2 \tag{5.15}$$

and

$$F_2'(x)_2 = \frac{dy_2}{dx} = \frac{4xdx^1 + 4dx^2}{dx} = 4x + 4dx^1 \tag{5.16}$$

For a volume function or

$$F_3(x)_2 = y_3 = x^3 \tag{5.17}$$

$$F_3'(x)_2 = \frac{dy_3}{dx} = \frac{6x^2dx^1 + 12xdx^2 + 8dx^3}{dx} = 6x^2 + 12xdx^1 + 8dx^2 \tag{5.18}$$

The magnitude of the resultant of addition of two orthogonal unit vectors, v_{01} and v_{02}, is $\sqrt{2}v_0$, and that of three orthogonal unit vectors is $\sqrt{3}v_0$. Therefore in a

condition in which an isotropic volume change, dy_3, is represented by an orthonormal unit vector on each of six cubic faces, the ratio of the magnitude of a vector equidistant from all six, i.e. along one of the cubic diagonals, to each of the normal unit vectors will be $6\sqrt{3}$. Okay. Returning to Phase Space 3.

Aside #2

In non-technical contexts, the terms "stress" and "force" are often used interchangeably, though the distinction is generally understood even then. In informal settings "force" is generally used to convey the idea of an external agent operating on a separate system to produce some change. "Stress" is used to convey an internal change in some system resulting generally from the operation of an external agent, though there is the possibility of internally generated stress. As discussed earlier, this common understanding finds technical expression in the distinction between a body force, F_b, and a surface or stress force, $\tau_{t,s}$. Both have the properties of mass times displacement over time-squared. Displacement indicates the physical change occurring and time-squared indicates the acceleration with which the change occurs. Mass represents a property of the agent or the system that, at least in a classical, non-relativistic context, is not affected by the change or its rapidity, the property of inertia, a property to stay the same whatever else is happening. A surface or stress force has the additional definition as a stress integrated over the surface or cross-sectional area of its operation.

In a discussion of the interaction of separate agents, i.e. bodies, where the transfer of momentum and energy is conceptually concentrated to a point, we can generally do pretty well without reference to the concept of stress. When we get into a discussion of more diffuse arrangements of energy, such as in the behavior of fluids or the concept of gravitational or electromagnetic fields, we often need to use the concept of stress, that is a force operating over an area and the related concept of an energy/inertial density, the energy, mass or analogous property such as charge contained within a linear, planar, volume or higher dimensional boundary.

In various modeling, such as the ideal gas law and as expressed in Gauss's divergence theorem, the energy content, E, of a defined volume, V, is equal to the tension stress, f_t, general described as a pressure, at the surface or boundary of that volume, the stress being the tension force, τ_t, per unit area, A_0. Here we will confine that volume to a unit cube volume, V_0, so that

$$\frac{E}{V_0} = \frac{\tau_t}{A_0} = f_t \tag{6.1}$$

The energy might be the kinetic energy of an ideal gas or an electric charge and the stress, the corresponding pressure or electric flux at a boundary surface.

In mechanical terms, the energy might be the elastic potential energy of a beam or other structural material, giving a potential energy density, $\mathcal{V}_1$, for the left hand term above, and the stress, in accordance with Hooke's law, is the expression of Young's modulus of elasticity, Y, and the strain, ε_t, i.e. the stretching or extension that occurs in the volume as a linear response to the stress or

$$\mathcal{V}_1 = \frac{\mathcal{V}}{\mathrm{V}_0} = \tfrac{1}{2} f_t \varepsilon_t = \tfrac{1}{2} Y \varepsilon_t^{\,2} = \frac{f_t^2}{2Y} \tag{6.2}$$

where the strain is defined as a relative change in the length of the material, here designated by a unit displacement, and is therefore a dimensionless number,

$$\varepsilon_t \equiv \frac{\Delta q_0}{q_0} \ . \tag{6.3}$$

For convenience, we will state that

$$\mathrm{V}_0 = \mathrm{A}_0 q_0 = q_0^3 \ . \tag{6.4}$$

Young's modulus

$$Y = \frac{f_t}{\varepsilon_t} \tag{6.5}$$

is a stress potential, an inherent property of the material, with the dimensions of stress, as shown here, the linear ratio of stress to strain. This calls for some mathematical clarification, since Y is not a function of ε_t or f_t, and does not become undefined if ε_t is zero. Rather f_t is a function of ε_t and Y or ε_t is a function of f_t and Y. Y is a ratio such that if ε_t equals 1, theoretically f_t equals Y.

From (6.2) it is clear that if there is no strain, Y is equal to the elastic potential energy density, $\mathcal{V}_1$. The one half coefficient of Y is a function of the work, W, done to extend the structural member the distance Δq_0, as

$$W = \tfrac{1}{2} \tau_t \Delta q_0 \tag{6.6}$$

In general, an extension in an isotropic elastic solid material along one dimension, x, results in a decrease or negative lateral extension along the other two dimensions, A, where A can refer to either lateral dimension, y or z. The lateral extension, ε_A, is then

$$\varepsilon_A \equiv \frac{\Delta \mathrm{A}}{\mathrm{A}} \tag{6.7}$$

and is inversely related to the longitudinal extension by a ratio known as Poisson's ratio, σ, which in an ideal isotropic solid will be 1/3, or

$$\sigma = -\frac{\varepsilon_\mathrm{A}}{\varepsilon_t} = \frac{1}{3} \ . \tag{6.8}$$

The discussion will be facilitated if we use the following index convention to designate the arbitrary principal axes, where the first of the indices indicates the direction of a unit vector normal to a unit cross-section and the second indicates the direction of the surface force and therefore stress vector. Thus for a tension force, the indices are the same, and the complete set of elastic tension stress equations for a unit cube are

$$\sum_{t=0}^{6} \varepsilon_t = \begin{bmatrix} +\frac{1}{Y} f_{xx} & -\frac{\sigma}{Y} f_{yy} & -\frac{\sigma}{Y} f_{zz} \\ -\frac{\sigma}{Y} f_{xx} & +\frac{1}{Y} f_{yy} & -\frac{\sigma}{Y} f_{zz} \\ -\frac{\sigma}{Y} f_{xx} & -\frac{\sigma}{Y} f_{yy} & +\frac{1}{Y} f_{zz} \end{bmatrix} + \begin{bmatrix} +\frac{1}{Y} f_{-x-x} & -\frac{\sigma}{Y} f_{-y-y} & -\frac{\sigma}{Y} f_{-z-z} \\ -\frac{\sigma}{Y} f_{-x-x} & +\frac{1}{Y} f_{-y-y} & -\frac{\sigma}{Y} f_{-z-z} \\ -\frac{\sigma}{Y} f_{-x-x} & -\frac{\sigma}{Y} f_{-y-y} & +\frac{1}{Y} f_{-z-z} \end{bmatrix} \tag{6.9}$$

For a condition of isotropic stress in an isotropic material this becomes

$$\sum_{t=0}^{6}\varepsilon_t = \begin{bmatrix} +\frac{1}{3Y}f_{xx} & & \\ & +\frac{1}{3Y}f_{yy} & \\ & & +\frac{1}{3Y}f_{zz} \end{bmatrix} + \begin{bmatrix} +\frac{1}{3Y}f_{-x-x} & & \\ & +\frac{1}{3Y}f_{-y-y} & \\ & & +\frac{1}{3Y}f_{-z-z} \end{bmatrix} \quad (6.10)$$

The scalar value or magnitude of the total isotropic stress, *T*, is then

$$\sum_{t=0}^{6}\varepsilon_t = 6\left|\tfrac{1}{3Y}f_t\right| = 2\frac{f_t}{Y} = \frac{T}{Y}\ . \quad (6.11)$$

As all the stress vectors are directed out from the surface of the unit cube, this results in a net increase in its volume or a volume strain called a dilatation, ε_Δ or

$$\varepsilon_\Delta \equiv \frac{\Delta \mathrm{V}}{\mathrm{V}} \quad (6.12)$$

The dilatation is inversely related to a hydrostatic or mechanically analogous pressure, p_h, a negative tension, at the surface of the volume by a volume or bulk modulus, *B*, itself analogous to Young's modulus,

$$p_h = -B\varepsilon_\Delta\ . \quad (6.13)$$

In fact, in an ideal isotropic material, we find that

$$\begin{aligned} Y &= 3B(1-2\sigma) \\ \therefore Y &= B \end{aligned} \quad (6.14)$$

As a result, the pressure, bulk modulus and dilatation are analogously related to the potential energy density of a material as

$$\mathcal{V}_1 = -\tfrac{1}{2}p_h\varepsilon_\Delta = \tfrac{1}{2}B{\varepsilon_\Delta}^2 = \frac{p_h^2}{2B} \quad (6.15)$$

There are two other related types of stress in an elastic material, shear stress and the related concept of torsion. While tension stress operates normal or perpendicular to the surfaces of the unit cube, shear stress operates parallel to its edges. It should not be too surprising, therefore, if the first tension stress in (6.10) above, f_{xx}, also contributed to the shear stress in the four adjacent cubic faces, in fact, once to each edge of each adjacent face. However, since each edge is shared by two surfaces, in an isotropic condition the net is one fourth of the total shear force in each direction per face. If we think of the normal tension vector, f_{xx}, as equally divided as extension vectors to each of the adjacent surface mutual boundary edges, we have

$$\left|f_{xx}\right| = \left|f_{yx} + f_{zx} + f_{-yx} + f_{-zx}\right|\ . \quad (6.16)$$

Shear is not just the force across the appropriate cross sectional area, however. If this same condition applied to all six faces of the cube, there might be a dilatation or increase in volume, but there would be no shearing distortion, which is a relative flattening of the cross sectional surface by an increase in one of the diagonals vis-à-vis the other. The shear, once again a dimensionless value, is measured as the ratio of the displacement of one cubic edge, *e*, to the length of the adjacent, orthogonal

edges, $e_{\perp}$, in the same plane, in this case the *yz* plane. Therefore the shear strain, ε_s, is

$$\varepsilon_s \equiv \frac{\Delta e}{e_{\perp}} = \tan\alpha \tag{6.17}$$

where α is obviously the arctan of ε_s.

The total shear on a unit cube in the *yz* plane then is

$$\varepsilon_{yz} = \varepsilon_{zy} = \tfrac{1}{2}\left(\frac{\Delta e_y}{e_{0z}} + \frac{\Delta e_z}{e_{0y}}\right) \tag{6.18}$$

The shear strain and stress, f_s, have a shear modulus or modulus of rigidity, μ, given as

$$f_s = 2\mu\varepsilon_s \tag{6.19}$$

and an analogous relationship to Young's modulus as

$$Y = 2\mu(1+\sigma)\ . \tag{6.20}$$

The corresponding potential energy density in terms of shear along any dimension is

$$\mathcal{V}_1 = f_s\varepsilon_s = 2\mu\varepsilon_s^2 = \frac{f_s^{\,2}}{2\mu} \tag{6.21}$$

If the shear stresses along all edges of a given cross-section are not equal, there will be a rotation, ϕ_{yz}, here shown about the *yz* plane, in the direction of the net angular increase given by

$$\phi_{yz} = \tfrac{1}{2}\left(\frac{\Delta e_z}{e_{0y}} - \frac{\Delta e_y}{e_{0z}}\right) \tag{6.22}$$

For a unit cube, assuming no rotational shear strain, the total strain at the surface of the cube is the following symmetric matrix, where the diagonals represent the tension strain as in (6.10)

$$\mathrm{E} \equiv \begin{bmatrix} \varepsilon_{xx} & \varepsilon_{xy} & \varepsilon_{xz} \\ \varepsilon_{yx} & \varepsilon_{yy} & \varepsilon_{yz} \\ \varepsilon_{zx} & \varepsilon_{zy} & \varepsilon_{zz} \end{bmatrix} + \begin{bmatrix} \varepsilon_{-xx} & \varepsilon_{-xy} & \varepsilon_{-xz} \\ \varepsilon_{-yx} & \varepsilon_{-yy} & \varepsilon_{-yz} \\ \varepsilon_{-zx} & \varepsilon_{-zy} & \varepsilon_{-zz} \end{bmatrix} \tag{6.23}$$

The following antisymmetric matrix represents the rotational components of the shear as

$$\Phi = \begin{bmatrix} 0 & \phi_{xy} & \phi_{xz} \\ \phi_{yx} & 0 & \phi_{yz} \\ \phi_{zx} & \phi_{zy} & 0 \end{bmatrix} + \begin{bmatrix} 0 & \phi_{-xy} & \phi_{-xz} \\ \phi_{-yx} & 0 & \phi_{-yz} \\ \phi_{-zx} & \phi_{-zy} & 0 \end{bmatrix} \tag{6.24}$$

Whether a material responds to a shear stress by flattening across its corresponding cross-section or rotating about the cross-sectional axis is a function of the configuration of the shear stress about the axis and the torsional rigidity of the material, its resistance to torque or twisting.

In the event of a shear stress and strain uniformly distributed in one angular direction about the cross-section, we have an instance of torsion or twisting of the elastic medium in response to a torque. This is generally modeled on a rigid tube or rod whose length largely exceeds its cross-section. For a solid rod, the torque, *M*, is given as the product of the radius of the rod, *r*, and the circumferential shearing stress, f_ϕ, and the cross sectional area of the rod, A = $2\pi r^2$ or

$$dM = 2\pi r^2 f_\phi dr \tag{6.25}$$

The shearing strain is in keeping with (6.17) where $\Delta\varepsilon = r\phi$ is the circumferential displacement or rotation of the cross-section about the longitudinal axis and $\varepsilon_\perp = l$ is the length of that axis and the rod exhibiting a reacting torque to the applied torque. In terms of the SHM of a pendulum, the pendulum length and the length of the torsion rod are analogous as are the displacement of the plumb bob and the torsion shear. In fact, the torsion pendulum is common and is responsible for determining Newton's gravitational constant. Thus we have

$$f_\phi = \mu\varepsilon_\phi$$
$$\text{where } \varepsilon_\phi = \frac{r\phi}{l} \ . \tag{6.26}$$

Thus the torque for a solid rod is

$$M = \frac{\pi}{2}\mu\frac{r^4}{l}\phi \ . \tag{6.27}$$

The elastic potential energy density per unit length of the rod is

$$\mathcal{V}_1 = \tfrac{1}{2}\frac{M\phi}{l} = \frac{\pi}{4}\mu\frac{r^4}{l^2}\phi^2 = \frac{M^2}{\pi\mu r^4} \tag{6.28}$$

In summary, stress potential, quantified as a stress modulus, is the property of a three dimensional elastic material or medium that distributes a change in one or more spatial dimensions, and therefore its potential energy density, to all three dimensions in the form of various stress forces and that distributes a change in stress in one or more spatial dimensions, and therefore its potential energy density, to all three dimensions in the form of various physical strains. It is the property by which such a medium stretches, compresses, bends, shears, and rotates in response to a change in configuration within its extent or at its boundary. The elasticity of such a medium is a measure of the degree to which the original physical configuration is restored with a cessation or diminution of the initial stress and strain. The plasticity of such a medium is a measure of the degree to which the original physical configuration fails to be restored with a cessation or diminution of the initial stress and strain. In general an elastic medium will become plastic beyond a certain limit at which the stress to strain ratios, as given by (6.5), cease to be

linear, and the strain or deformation becomes permanent. In addition, physical elastic media generally have the propensity for hysteresis in varying degrees, in which an oscillating medium during its kinetic energy phases exhibits greater kinetic energy as it moves away from its equilibrium condition toward either point of maximum displacement than on the returns back towards the equilibrium position. Thus it results in a loss of energy over time, in contrast to SHM in which the ideal system is defined as being closed.

Stress and strain are perhaps best described mathematically using the stress, **F**, and strain, **E**, tensors, so that the elastic potential energy density of a material is

$$\mathcal{V}_1 = \tfrac{1}{2}\mathrm{F} : \mathrm{E} \tag{6.29}$$

Where in an anisotropic condition or for one half of a unit cube the double dot product expands as

$$\mathcal{V}_1 = \tfrac{1}{2}\left[f_{xx}\varepsilon_{xx} + f_{yy}\varepsilon_{yy} + f_{zz}\varepsilon_{zz} + 2\left(f_{yz}\varepsilon_{yz} + f_{zx}\varepsilon_{zx} + f_{xy}\varepsilon_{xy} \right) \right] \tag{6.30}$$

Aside #3 (taken from an earlier work-in-progress copy of this development)

In a manner that relates to the cuboctahedral lattice, we can examine the effect of an isotropic strain, along with the corresponding stress, on a unit volume of space. In light of previous comments, we can imagine the center of this cube as one center of expansion and the other as extra dimensional, represented by the indefinite extension of the four diagonals through the eight vertices. We will integrate the differential components of the cube to compare the work done on each boundary component to the change in the corresponding core, in this case a volume. We are interested in the relative contributions of each component as an order of differentiation over time to the initial unit volume, *V*, and not to the changing magnitude of the volume itself. That is, from (5.18) in Aside #1, we have $6x^2dx$ differential surfaces, $12xdx^2$ differential edges and $8dx^3$ differential vertices. We substitute the following boundary place-hold identities for Surface, Edge and vertices (Corner), $1^2S \equiv x^2$, $1^1E \equiv x^1$, and $1^0C \equiv x^0$ so as to maintain proper integration. It will be helpful if we assign a "normal" boundary strain vector to each of these components, which in each case will be in the direction in which the boundary is increasing. Thus

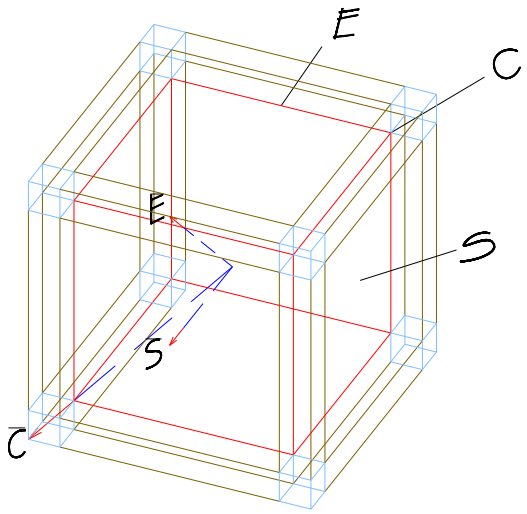

Cubic Expansion

$$|\mathbf{S}| = \left|\sqrt{\tfrac{1}{2}}\,\mathbf{E}\right| = \left|\sqrt{\tfrac{1}{3}}\,\mathbf{C}\right| \tag{7.1}$$

$$|\mathbf{E}| = \left|\sqrt{2}\,\mathbf{S}\right| = \left|\sqrt{\tfrac{2}{3}}\,\mathbf{C}\right| \tag{7.2}$$

$$|\mathbf{C}| = \left|\sqrt{3}\,\mathbf{S}\right| = \left|\sqrt{\tfrac{3}{2}}\,\mathbf{E}\right| \tag{7.3}$$

In the following discussion, no assumption is made about the universal configuration or number of dimensions of the space in which the unit cube is embedded. We are only interested, at least initially, in the local geometry, which is

assumed to be flat and therefore Euclidean. Thus it is background-independent. As to a fourth spatial dimension, we will see that change in or motion of such dimension is interchangeable with a dimension of time in a three spatial dimension context.

In this case the integration will be simultaneous on each order, as indicated by the pre-subscript *n*, in $\int_n dx^n$ so that we have

$$\int_V dV = 6x^2 \int_0^a {}_1dx^1 + 12x^1 \int_0^a {}_2dx^2 + 8x^0 \int_0^a {}_3dx^3 \tag{7.4}$$

$$\int_V dV = 6S\int_0^a dx + 12E\left(\int_0^a dx\right)\left(\int_0^a dx\right) + 8C\left(\int_0^a dx\right)\left(\int_0^a dx\right)\left(\int_0^a dx\right) \tag{7.5}$$

$$\Delta V = 6aS + 12a^2E + 8a^3C \tag{7.6}$$

Solving for the following ratios, all at unity, where the designations S, E and C are unit names, their dimensional quantities being absorbed in the numerical coefficients of a^n, i.e. 6 square units times a, 12 length units times a^2, etc., gives the value of a for each equivalence. The ratios have been stated with the highest order in the consequent or denominator so they are decreasing from infinity as dx increases, until unity is reached as stated. We have (showing the negative for the sake of symmetry)

$$\frac{S}{E+C} = \frac{6a}{12a^2+8a^3} = \frac{1}{2a+\frac{4}{3}a^2} = 1 \therefore a = -\tfrac{3}{4} \pm \tfrac{1}{4}\sqrt{21} = 0.39564\ldots, -1.89564\ldots \tag{7.7}$$

$$\frac{S}{E} = \frac{6a}{12a^2} = \frac{\frac{1}{2}}{a} = 1 \therefore a = \tfrac{1}{2} = 0.5 \tag{7.8}$$

$$\frac{E}{C} = \frac{12a^2}{8a^3} = \frac{\frac{2}{3}}{a} = 1 \therefore a = \tfrac{2}{3} = 0.66666\ldots \tag{7.9}$$

$$\frac{S}{C} = \frac{6a}{8a^3} = \frac{\frac{3}{4}}{a^2} = 1 \therefore a = \pm\tfrac{\sqrt{3}}{2} = \pm 0.86602\ldots \tag{7.10}$$

$$\frac{E}{S+C} = \frac{12a^2}{6a+8a^3} = 1 \therefore a = \tfrac{3}{4} \pm i\tfrac{1}{4}\sqrt{3} = \tfrac{\sqrt{3}}{2}e^{\pm i\frac{\pi}{6}} = 0.86602\ldots e^{\pm i\frac{\pi}{6}} \tag{7.11}$$

$$\frac{S+E}{C} = \frac{6a+12a^2}{8a^3} = 1 \therefore a = \tfrac{3}{4} \pm \tfrac{1}{4}\sqrt{21} = 1.89564\ldots, -0.39564\ldots \tag{7.12}$$

If we think of the cube as embedded in an isotropic elastic continuum, which is of some inertial density and under tension, dx represents the work done in displacing or distorting the medium, and by virtue of Gauss' theorem, the integration of that work represents the energy of the distortion. By way of reference, in an ideal elastic medium, the stress operating on the locale is a function of the strain and the elastic modulus as

$$\mathbf{F} = \frac{Y\,\mathbf{E} - 3\sigma\bar{P}\mathbf{1}}{1+\sigma} \tag{7.13}$$

where **F** is the stress tensor, **E** is the strain tensor, *Y* is Young's modulus of elasticity, σ is Poisson's ratio or the negative ratio of lateral to axial or shear to tension strain, $\bar{P}$ is the mean pressure in the medium, and **1** is the idemfactor or unit tensor. Assuming a value of σ of -1/3 for an ideal isotropic 3 dimensional medium we have

$$\mathbf{F} = \frac{3}{2}\left(Y\,\mathbf{E} + \bar{P}\mathbf{1}\right). \tag{7.14}$$

The vector fundamental tension stress component is

$$\mathbf{f} = Y\,\mathbf{e} \tag{7.15}$$

and is related to the energy distribution by Gauss' theorem for the radial strain

$$E_r = \int_V \nabla \cdot \mathbf{e}_r dv = \oint_S \mathbf{e}_r \cdot d\,\mathbf{S} \tag{7.16}$$

and Stokes' theorem for the angular or tangential strain

$$E_t = \int_S \nabla \times \mathbf{e}_t \cdot d\,\mathbf{S} = \oint_{\mathbf{r}} \mathbf{e}_t \cdot d\,\mathbf{r}_t \tag{7.17}$$

These boundary order ratios, then, are inflection points indicating the energy contributions and potential energy gradient changes over time among the boundary components. In an ideal static, kinematic case the change in the ratios with an increase in *dx* would have no functional effect on the components, if *dx* has the same magnitude for each of them as it increases. This would amount to a simple change of scale. The real solutions above would appear to reflect this static condition. However, in a dynamic condition, we might imagine that as each ratio decreases below unity and past the inflection point, the magnitude of the consequent exceeds and affects the antecedent or numerator, whose magnitude then becomes a partial function of the consequent. This would appear to be the case for the complex solutions in particular, which correspond with an angular gradient potential of the boundary vectors from that of the antecedent to the direction of that of the consequent.

These evaluations were done with Maple. It is significant that if we convert (7.11) to complex polar notation as in the last term, the modulus is equal to the value for *a* in (7.10). It is important that we understand that the ratios represent the point at which the change in volume due to the sum totals of all component orders in the antecedent and consequent are equal. It is not the point at which one single component of a given S, E, or C times its appropriate $\int_n dx^n$ is equal to another, since this happens for all at the point where *a* = 1.

In these evaluations, the S component of the strain and hence of the work predominates until (7.7) is reached. At this point, the stress will begin to shift from a predominance of tension to that of shear, meaning there will be a potential for the surface and edge strains to oscillate. As the edges and vertices ring each of the surfaces, the system remains basically stable, however. At the point of (7.8) the edges assume dominance over the surfaces and a gradient is produced for the bulk strain and the tension stress in the direction of the edges. Once again, the 2:1 symmetry of edges to surface maintains stability. At (7.9) the vertices contribute

more work than the edges and the strain gradient shifts in their direction. Thus there is a vector potential from the surfaces to the edges to the vertices. Once more the symmetry between vertices and edges maintains stability.

Jumping to (7.12), at this point the strain contributed by the vertices dominates both of the other components combined and the related stress is greatest at these locations. This would result in a dissipation of the energy altogether, were it not for the unusual and unique condition created by (7.10) and (7.11). The point at which the strains of the vertices come to equal those of the surfaces is also the point at which their combined strain comes to equal that of the edges, as given by the modulus of the latter's ratio. We can assume that the imaginary component of this ratio indicates a rotational component of $\pi/6$ or 30°, and since the vertices are assuming a predominance over the surfaces at this point, having already exceeded the edge strain, and as there is an imbalance in the number of vertices to surfaces, a necessary break in symmetry ensues.

We can imagine a rotational potential of the surface strain in the direction of the vertices, which by virtue of the asymmetry between S and C, of 3 degrees of rotational freedom and 4 possible rotational axes, results in an eventual rotational strain about one pair of the axes. This is simultaneous with a shift of the Es in the direction of S + C and a dragging of the strains at each of the two axial C poles. This then leads to a rotation of the axial Cs in the direction of one of the three E pairs extending from those two vertices. The equation of (7.11) gives this rotational relationship. The nature of the ambiguous sense in the argument is indicative of the equation of a rotation and its complex conjugate, when viewed from both senses of its axis, i.e. by rotating it about the real axis, where $\pm$ means plus and minus and not plus or minus, if we adjust the Euler identity to

$$e^{\pm i\theta} = \mathbf{sin}\,\theta \pm i\,\mathbf{cos}\,\theta. \tag{7.18}$$

One end of the axis of strain then can be shown as indicated by the "symmetry breaking" in (7.21).

$$12a^2E = \left(6aS + 8a^3C\right) \tag{7.19}$$

$$12\left(\tfrac{\sqrt{3}}{2}e^{\pm i\frac{\pi}{6}}\right)^2 E = 6\left(\tfrac{\sqrt{3}}{2}e^{\pm i\frac{\pi}{6}}\right)S + 8\left(\tfrac{\sqrt{3}}{2}e^{\pm i\frac{\pi}{6}}\right)^3 C \tag{7.20}$$

$$e^{-i\frac{\pi}{3}}E = \tfrac{1}{\sqrt{3}}\left(e^{+i\frac{\pi}{6}}S + e^{+i\frac{\pi}{2}}C\right) \tag{7.21}$$

Thus, the strain vector E, rotated in some direction $\frac{\pi}{3}$, is equal to $\frac{1}{\sqrt{3}}$ of the S and C strains rotated $\frac{2\pi}{3}$ in the opposite direction, presumably in the same plane. In fact, this states that C rotates $\frac{\pi}{2}$ while S rotates $\frac{\pi}{6}$. We can see specifically how these rotations occur in Spin Diagrams 1 and 2. We can also see there how a rotation back in time of $\frac{\pi}{3}$ equals one forward in time by $\frac{2\pi}{3}$ and vice-versa, if their plane of rotation, ϕ, is itself rotating at a constant rate with respect to an orthogonal plane, θ,

that is where the two axes intersect at the centers of rotation. However, it is shown there that this corresponds with a rotation of θ, back $\frac{\pi}{4}$ and forward $\frac{3\pi}{4}$, indicating a variability in the strain velocity.

It should be understood that this cubic structure is simply an expression of the orthogonal tendency for stress equalization and energy conservation. The condition found at (7.10) and (7.11), then becomes a stable dynamic condition of rotational oscillation or spin, within certain parameters of inertial density and mechanical impedance. If the isotropic tension in this situation was sufficient to increase the strain indefinitely, if the medium was to lose its elasticity and become plastic or even rupture, any tendency to oscillate would be overcome by the transfer of energy via strain to the vertices. Local energy would not be conserved, but be drawn away by the strain.

It is essential to extrapolate this scenario to a hypercube, H, to achieve a full understanding. We will skip the integrals but show the results for the corollary of (7.6) as

$$\begin{aligned} \Delta H &= 8aV + 24a^2S + 32a^3E + 16a^4C \\ &= 1aV + 3a^2S + 4a^3E + 2a^4C \end{aligned} \tag{7.22}$$

There are 25 combinations with corresponding non-ordered permutations or sub-combinations, for the 4-cube; 7 involving all 4 parameters, 12 permutations involving all sub-combinations of 3, and 6 one to one relationships. With the 3-cube, there are 2 single real positive solutions at (7.8) and (7.9), one instance of a complex solution at (7.11), one correspondence between a real and a complex solution at (7.10) and (7.11) where the real value of *a* in one is equal to the complex modulus in the other, and one instance of a correspondence of solutions with sense inversion, (7.7) and (7.12), that is their solutions have the same magnitude, but of opposite sense. As might be expected, the 4-cube shows significantly more of these symmetries. It should be noted that while an attempt has been made to analyze the ratios qualitatively so that all are represented as decreasing with respect to an increasing *dx*, they have not all been checked quantitatively, and some may be increasing as shown. In fact, (7.35) and (7.37) are found to be increasing at the point represented by the first positive solution and decreasing at the second. For (7.32) it is worth stating that for every value of the ratio $0.75 < \left(\frac{S}{V+E}\right) < +\infty$, the modulus is ½ and the argument ranges from 0 to ½ π.

It is important to remember that a given component in the 3-cube is identical to the same component in the 4-cube, but the relationships between them are different. An edge still is bounded by 2 vertices, but there are 4 edges intersecting at each vertex of the 4-cube. A line segment in an *x-y* plane is qualitatively no different than one in the *z-x* or for that matter *z-w* plane. In fact a point in 3-space also has a location in n-space, at least in Euclidean n-space. In the following, it is also important to remember that *a* is not the value of the corresponding ratio, but rather

the value found in both antecedent and consequent when the ratio equals 1. The evaluations are based on the following identities in (7.23),

$$V \equiv 1a, S \equiv 3a^2, E \equiv 4a^3, C = 2a^4 \tag{7.23}$$

$$\frac{V}{S}, a = \tfrac{1}{3} \tag{7.24}$$

$$\frac{V}{E}, a = \pm\tfrac{1}{2} \tag{7.25}$$

$$\frac{V}{C}, a = \tfrac{1}{\sqrt[3]{2}}, -\tfrac{1}{2}\left(\tfrac{1}{\sqrt[3]{2}}\right)\ldots \pm i\,\tfrac{\sqrt{3}}{2}\left(\tfrac{1}{\sqrt[3]{2}}\right) = \tfrac{1}{\sqrt[3]{2}} e^{\pm i\frac{2\pi}{3}} = 0.79370\ldots e^{\pm i\frac{2\pi}{3}} \tag{7.26}$$

$$\frac{S}{E}, a = 0, \tfrac{3}{4} \tag{7.27}$$

$$\frac{S}{C}, a = 0, \pm\sqrt{\tfrac{3}{2}} \tag{7.28}$$

$$\frac{E}{C}, a = 0, 0, 2 \tag{7.29}$$

$$\frac{V}{S+E}, a = -1, \tfrac{1}{4} \tag{7.30}$$

$$\frac{V+S}{E}, a = -\tfrac{1}{4}, 1 \tag{7.31}$$

$$\frac{S}{V+E}, a = \tfrac{3}{8} \pm i\,\tfrac{1}{8}\sqrt{7} = \tfrac{1}{2} e^{\pm i 0.722734248\ldots} \tag{7.32}$$

$$\frac{V}{S+C}, a = 0.31290\ldots, -0.15645\ldots + i1.25436\ldots = 1.26408\ldots e^{\pm i 1.694883228\ldots} \tag{7.33}$$

$$\frac{V+S}{C}, a = -1, -0.36602\ldots, 1.36602\ldots \tag{7.34}$$

$$\frac{V+C}{S}, a = -1.36602\ldots, 0.36602\ldots, 1 \tag{7.35}$$

$$\frac{V}{E+C}, -1.85463\ldots, -0.59696\ldots, 0.45160\ldots \tag{7.36}$$

$$\frac{V+C}{E}, a = -0.45160\ldots, 0.59696\ldots, 1.85463\ldots \tag{7.37}$$

$$\frac{V+E}{C}, a = 2.1120\ldots, -0.05604\ldots \pm i0.48331\ldots = 0.48655\ldots e^{\pm i 1.686235431\ldots} \tag{7.38}$$

$$\frac{S}{E+C}, a = -2.58113\ldots, 0, 0.58113\ldots \tag{7.39}$$

$$\frac{S+E}{C}, a = -0.58113\ldots, 0, 2.58113\ldots \tag{7.40}$$

$$\frac{E}{S+C}, a = 0, 1 \pm i\,\tfrac{1}{\sqrt{2}} = \sqrt{\tfrac{3}{2}} e^{\pm i 0.615479709\ldots} \tag{7.41}$$

$$\frac{V}{S+E+C}, a = 0.24415..., -1.12207... \pm i0.88817... = 1.43105...e^{\pm i2.472026458...} \quad (7.42)$$

$$\frac{E}{V+S+C}, a = -0.24415..., 1.12207... \pm i0.88817... = 1.43105...e^{\pm i0.669566197...} \quad (7.43)$$

$$\frac{V+E+C}{S}, a = -2.63993..., 0.31996... \pm i0.29498... = 0.43519...e^{\pm i0.744798022...} \quad (7.44)$$

$$\frac{V+S+E}{C}, a = 2.63993..., -0.31996... \pm i0.29498... = 0.43519...e^{\pm i2.396794631...} \quad (7.45)$$

$$\frac{V+S}{E+C}, a = -2.51702..., -0.25673..., 0.77375... \quad (7.46)$$

$$\frac{E+S}{V+C}, a = -0.77375..., 0.25673..., 2.51702... \quad (7.47)$$

$$\frac{V+E}{S+C}, a = 1, \tfrac{1}{2} \pm i\tfrac{1}{2} = \tfrac{1}{\sqrt{2}} e^{\pm i\frac{\pi}{4}} \quad (7.48)$$

Once again using Maple, there are a total of 10 couplings involving complex solutions, of which one is exclusively complex and one other has only a zero for the third and real solution. Only one single real positive solution is given. There are, however, 7 corresponding pairs of solutions involving sense inversion, 5 real and 2 complex. Note that all cases of sense inversion involve a combination of one or more components in either the antecedent and/or consequent and the sense change is associated with a transposition of one or two components in each pair. These do not appear to have any special relationship to the conditions of the 3-cube, at first glance, and we have not investigated them further.

There are several, however, that appear to have a direct relationship to some of the ratios of the 3-cube. Two conditions of correspondence are found between a real positive solution and the complex modulus of a complex solution with a positive real component. (7.28) $\left(\frac{S}{C}\right)$ and (7.41) $\left(\frac{E}{S+C}\right)$ are directly related to (7.10) and (7.11) respectively, the real solution and the modulus of the complex of the second two being equal to the product of the first and $\sqrt{2}^{-1}$. The argument of (7.41) is the angle at the center of a cube between a radial normal to an edge of the cube and one extended along a diagonal to a vertex. (7.25) $\left(\frac{V}{E}\right)$ and(7.32) $\left(\frac{V}{E+S}\right)$ are related to (7.8) $\left(\frac{S}{E}\right)_3$ with a common value for their real solutions and the modulus of the complex one. The cosine of the argument of (7.32) is equal to the solution of (7.27) $\left(\frac{S}{E}\right)_4$, which is the same ratio coupling as (7.8). This pairing (7.32) in turn has a modulus equal to the real and imaginary components of an additional complex solution in (7.48) $\left(\frac{V+E}{S+C}\right)$. This latter solution has an argument of $\pi/4$ or 45^o which appears to be an extremely stable condition, as found in a sine wave model as the point of maximum power of the wave, where the product of the transverse wave force and transverse wave speed are maximum. It is also the angle of the strain vector E

discussed above for the 3-cube, with respect to the plane normal to the spin angular momentum vector as shown in the spin diagrams. In the model developed here, this condition is found to be invariant and rotates about the oscillation's angular momentum vector.

Finally, (7.41) $\left(\frac{E}{S+C}\right)$, (7.48) $\left(\frac{V+E}{S+C}\right)$, and (7.26) $\left(\frac{V}{C}\right)$ are found to be related in a most profound way in the mechanism of the oscillation herein described. The imaginary component of (7.41) equals the modulus of (7.48). Note that (7.26) represents a $\frac{2\pi}{3}$ rotation due to the interplay between the volume and vertex components of strain and a modulus of that strain of $\frac{1}{\sqrt[3]{2}}$. Using the equation for (7.26) or

$$aV = 2a^4C \tag{7.49}$$

$$\frac{1}{\sqrt[3]{2}}e^{\pm i\frac{2\pi}{3}}V = 2\left(\frac{1}{\sqrt[3]{2}}e^{\pm i\frac{2\pi}{3}}\right)^4 C \tag{7.50}$$

tells us that a rotational oscillation of the 4-volume (boundary) strain V of modulus $\frac{1}{\sqrt[3]{2}}$ by $\frac{2\pi}{3}$ is equal to 4 axial rotations about the vertices of the same modulus and argument, where the 2 in the consequent indicates simultaneous rotations of opposite sense at each end of an axis. The oscillation of V is fourth dimensional, and therefore beyond our direct sensory ken, however, the 4 vertices are not, and we can envision the above consequent, the expression in 3 dimension of this four dimensional rotation, as a sequence of 4, $\frac{2\pi}{3}$ rotations about the 4 diagonals of a 3-cube. This sequence leaves the cube unchanged and avoids the entanglement condition, i.e. the continuity of Euclidean 3-coordinates of the cube are not twisted by the sequence. This condition of limits on the twistability of the continuum strain is a necessary consequence of its inertial/elastic properties. As the rotation of V is continuous, we would imagine that the sequence of 4 rotations is continuous, i.e. the strain rotates from one reference diagonal to another about one of the three surface axes of the 3-cube. We can also envision this as one diagonal axis rotating $\frac{2\pi}{3}$, followed by a 2 π rotation of the same sense about one of the adjacent 3-cube surface axes. We can also treat it as a sequence of 4 orthogonal permutations.

We can show this configuration simply. If we align a hyperbolic surface of revolution about the *y* axis of the curve

$$xy = \tfrac{1}{2}, \text{ for } x \le \tfrac{1}{\sqrt{2}} \tag{7.51}$$

at each of the eight vertices of a cube so that each of them is at the angle of the argument given by (7.41) as just described, and so that the rims or circles of their bases intersect at the centers of each of the six surfaces of the cube, the following will be found concerning this geometry, which we will call an inversphere. We can also, as an alternative, create a similar construct using a pseudosphere in place of the above surface of revolution. Given a constant negative curvature of -1 for each pseudosphere, the resulting inversphere would have a constant negative curvature. With respect to the inversphere:

1. Each surface of revolution, which we might call a hyper-axis or h-axis and which can be represented by a complex plane, with the imaginary dimension parallel to the circumference of the revolution and the real along the diagonal axis, will have a curvature of negative 1 at the rim, remaining negative while decreasing, that is, moving toward zero or flatness, with distance along the asymptote. Here the left four of Figure 4 are shown, their designations corresponding with the axes of Figure 3 below.

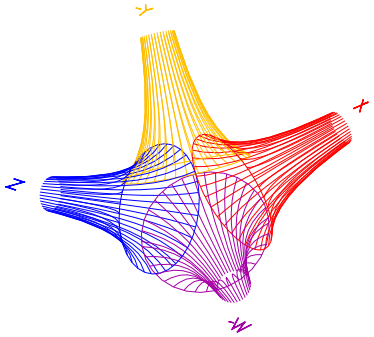

Figure 1

2. The rims will have a radius of $\frac{1}{\sqrt{2}}$. The area of the circle formed by the rim is therefore $\frac{\pi}{2}$, and its complex representation is $\frac{1}{\sqrt{2}}e^{i\theta}$ corresponding with $\left(\frac{V+E}{S+C}\right)$.
3. The rims will intersect orthogonally with each other at the cubic surface centers, so that there are three h-axes adjacent to a given h-axis along the cubic edges which we will refer to as the proximal axes.
4. The rims from h-axes located diagonally across the cubic surface from each other will be parallel or tangential at the same point at which they intersect with their proximal axes. We will call the corresponding parallel axes the distal axes. One set of mutually distal axes can be called the positive h-axes.
5. Each h-axis has a spatial inversion or anti-axis which is proximal to the distal axes of that h-axis. The set of their spatial inversions can be called the negative h-axes.
6. Each rim intersection is a $\frac{2\pi}{3}$ rotation from the others about the cubic diagonal, associating it with $\left(\frac{V}{C}\right)$.
7. The distance between cube surface centers describes an octahedron of edge length $\sqrt{\frac{3}{2}}$. The surface area of the octahedron is therefore $3\sqrt{3}$ and the volume is $\frac{\sqrt{3}}{2}$. The radial normal to the octahedron face is ½.
8. The cube will have an edge measure of $\sqrt{3}$. The surface area of the cube is 18 and the volume is $3\sqrt{3}$.

9. The concentric sphere intersecting at the rim intersections will have a radius of $\frac{\sqrt{3}}{2}$. The surface area is 3π and the volume is $\frac{\sqrt{3}}{2}\pi$.
10. We can think of this arrangement as the expression of a 4-cube in a 3-space, where the orthogonality condition of the 4-D space is met by the rim intersections, the center of each component of sphere, cube, octahedron and h-axis intersections being a common system center.
11. This configuration can be reduced to a 3-space orthogonal system simply by collapsing the cube along the W hyper-axis, as in the figure at left below, resulting in the co-ordinate system at right.

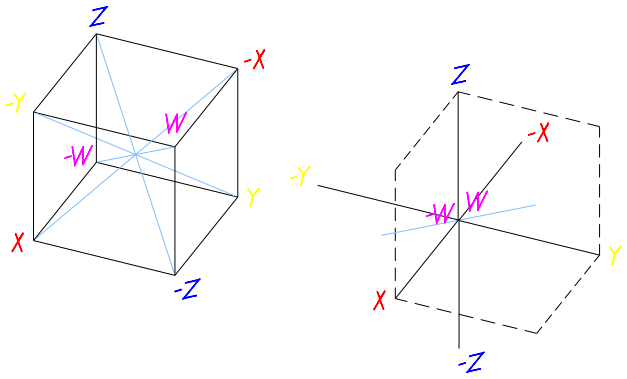

Figure 2

The condition of (7.8) $\left(\frac{S}{E}\right)_3$, (7.25) $\left(\frac{V}{E}\right)$ and (7.32) $\left(\frac{S}{V+E}\right)$ is represented by (7.48) $\left(\frac{V+E}{S+C}\right)$ at each h-axis. Thus the orthogonal projections of the argument of (7.48), described as extending from the system center to each cubic edge midpoint, are equal to the modulus of (7.41) $\left(\frac{E}{S+C}\right)_4$, and the argument of (7.26) $\left(\frac{V}{C}\right)$ is the rotation of that axis between proximal intersections and cubic surface centers.

In terms of $a = \int dx$ we are only interested in positive or increasing real values, although in the context of complex values, some negative real components as in (7.26) are of interest. A deeper analysis would no doubt find significance in all of the couplings, but we are only interested in the general manner in which the 4-cube and the 3-cube couplings might interact. In this regards it is important to remember that in the case of the 4-cube, the volume is a boundary that is increasing while in the case of the 3-cube, it is the base space, held constant, upon which the boundary changes are taking place.

From the perspective of a rotational oscillation, as found in a torsion pendulum or a jump rope oscillation, of interest are those couplings of two boundary parameters, V + E and S+ C, which have an intervening parameter, S and E respectively. More interestingly, in both these cases, V + E for the 4-cube and S + C for both 4-cube and 3-cube, the two-parameter components also have a ratio between themselves whose solution is $(\pm)$ real and equal to the modulus of the companion ratio. (7.48) gives the special case of V + E with S + C. Unlike the other three rotational oscillator

couplings, it has a positive real solution in addition to its complex solution. It also has the two parameter component ratios in common with the other two oscillators of the 4-cube. The remaining couplings with complex solutions all have intervals between their real and complex moduli solutions, for most exceeding 1, which mitigates against oscillation, with one exception. (7.26) $\left(\frac{V}{C}\right)$ has a real solution that equals its modulus, thereby indicating rotational oscillation. In addition, the cosine of its argument is equal to the modulus and real solution for $\left(\frac{S}{V+E}\right)$ and $\left(\frac{V}{E}\right)$ at $\frac{1}{2}$ and its sine, to the 3-cube modulus and real solution for $\left(\frac{E}{S+C}\right)$ and $\left(\frac{S}{C}\right)$ at $\frac{\sqrt{3}}{2}$, and to the 4-cube modulus and real for $\left(\frac{E}{S+C}\right)$ and $\left(\frac{S}{C}\right)$ at $\frac{1}{\sqrt{2}}\frac{\sqrt{3}}{\sqrt{2}}=\frac{\sqrt{3}}{2}$. Thus the rotational parameters of the other rotational oscillation or spin couplings, can be found in the simple ratio of $\left(\frac{V}{C}\right)$.

Within the context of the 4-cube, the first value that arises is (7.42) $\left(\frac{V}{S+E+C}\right)$ followed closely by (7.30) $\left(\frac{V}{S+E}\right)$. This simply shows that the vertex component adds very little at this juncture, although it does have a rotational element, but the negative real component indicates a significant rotation which would seem out of synch with the small real strain. A similar comment could be made about (7.33) $\left(\frac{V}{S+C}\right)$ which is next in the real order, though the potential rotation is much less. This is followed by (7.24) $\left(\frac{V}{S}\right)$ which has no rotational component. It is significant in that it is the value of Poisson's ratio in an ideal isotropic elastic solid, relating the axial to lateral strain and thereby, tension to shear stress.

Next is (7.35) $\left(\frac{V+C}{S}\right)$ with no rotational component, followed by (7.44) $\left(\frac{V+E+C}{S}\right)$, which has a rotational component. The real solution and therefore the strain is negative, however, and is out of scale with the modulus of the complex solution, which would mitigate against rotational oscillation. This modulus and the positive solution of (7.36) $\left(\frac{V}{E+C}\right)$ are the first values to exceed any of the solutions for the 3-cube. The next ratios (7.25) $\left(\frac{V}{E}\right)$ and (7.32) $\left(\frac{S}{V+E}\right)$ involve the first of the oscillatory groups. The real solution of the first and modulus of the second are equal to each other and to that of (7.8) $\left(\frac{S}{E}\right)_3$, while the cosine of the argument of $\left(\frac{S}{V+E}\right)$ coincides with the real solution of (7.27) $\left(\frac{S}{E}\right)_4$. Thus we might associate an actual oscillation of the 4-cube with the potential $\left(\frac{S}{E}\right)_3$ of the 3-cube. This is followed by (7.39) $\left(\frac{S}{E+C}\right)$ which has a real solution and is the 4-cube corollary of the first ratio of the 3-cube. It is of no special interest other than being, along with (7.9) $\left(\frac{E}{C}\right)_3$ a precursor for the next coupling, which is (7.48) $\frac{V+E}{S+C}$, perhaps the most important of the whole assemblage. Together, $\left(\frac{S}{E+C}\right)$ and $\left(\frac{E}{C}\right)_3$ indicate a growing predominance of E and C over S and then C over E, or shear stress over tension, followed eventually by torsion over shear.

The argument of $\left(\frac{V+E}{S+C}\right)$ represents the power of the strain oscillation, first in the oscillatory twisting of the hyper-axes at $\left(\frac{V}{C}\right)$, then subsequently with the rotational oscillation of the 3-cube itself. Given the above description of the inversphere, the modulus of this solution represents the radius of and in the plane of the rim of the h-axis at the point at which its curvature is -1. The argument is the power phase of an oscillation which can be found as a phase constant in the eventual rotational oscillation of the 3-cube. This is followed by (7.46) $\left(\frac{V+S}{E+C}\right)$, which adds no new oscillatory components, but does show the gaining dominance of the higher order boundary components, E and C. This culminates in a new oscillatory condition at (7.26) $\left(\frac{V}{C}\right)$.

Note that the real value and the modulus of $\left(\frac{V}{C}\right)$ is slightly more than the values of $\left(\frac{V+E}{S+C}\right),\left(\frac{V}{E}\right),\left(\frac{S}{E}\right)_4$ and slightly less than the values of $\left(\frac{E}{S+C},\frac{S}{C}\right)_3$ at oscillation. We can interpret the condition at $\left(\frac{V}{C}\right)$ as an oscillation about each of the 8 vertices. Each oscillation involves a twisting or torsion ultimately of $\frac{2\pi}{3}$ in each direction about each h-axis. The proximal axes will twist counter to the instant rotation sense of a given h-axis as will the anti-axis, all as viewed from the exterior of the system. The distal axes will twist with the same sense as the given h-axis, thus the directional sense of these axes corresponds with their rotational sense vis-à-vis the other axes. The strain on the enclosed sphere at maximum twist will be of a simultaneous lengthening along each cubic axis and flattening in the plane of said axis and the cubic axis from which the strain occurred and at which it is at a minimum, ideally zero, as indicated in the figure below. The two pairs of distal axes on each surface create two countervailing torques, which in this oscillatory condition are in equilibrium.

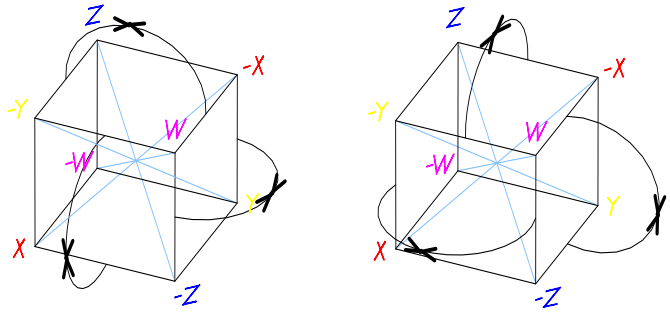

Figure 3

This initial symmetrical condition of $\frac{2\pi}{3}$ rotational oscillation of each of the four diagonals is broken upon *dx* reaching the oscillatory threshold given by $\left(\frac{E}{S+C},\frac{S}{C}\right)_3$ at $\frac{\sqrt{3}}{2}$. This results in a permanent rotation of $\frac{\pi}{3}$ of one pair of the E vectors as indicated by (7.21), thence the whole system strain continues to oscillate, while the stresses rotate and generate an angular momentum vector. (7.26) indicates the

rotation of the stresses in time among and about the four diagonals, which represent the four orthogonal axes of H. The oscillation of the 3-cube is supported and driven by the 4-stress which is concentrated in one transforming axis. (7.48) $\left(\frac{V+E}{S+C}\right)$ represents the power moments or positions of maximum conversion of kinetic to potential energy and vice versa.

Finally, (7.41) $\left(\frac{E}{S+C}\right)_4$ represents, in addition to the diagonals, a capacitive and an inductive torque that is co-linear with two of the diagonals and is the product of crossing into the power moments from their positions of equilibrium strain and rotates with them about the angular momentum vector, all described later. The modulus and the solution to $\left(\frac{S}{C}\right)_4$ at $\sqrt{\frac{3}{2}}$ represents the radial length from the center of the inversphere and 3-cube to the midpoint of the cubic edge. The solution $a=\sqrt{\frac{3}{2}}e^{\pm i0.61547\ldots}$ in this case indicates a rotation of this vector into the diagonal or one of the h-axis or of **E** into **C**. Solving for $\left(\frac{E}{S+C}\right)_4$

$$\begin{gathered} 4a^3E=3a^2S+2a^4C \\ 4\left(\sqrt{\tfrac{3}{2}}e^{\pm i0.61547\ldots}\right)^3E=3\left(\sqrt{\tfrac{3}{2}}e^{\pm i0.61547\ldots}\right)^2S+2\left(\sqrt{\tfrac{3}{2}}e^{\pm i0.61547\ldots}\right)^4C \end{gathered} \tag{7.52}$$

after reduction and some parsing gives

$$2\left(\sqrt{\tfrac{3}{2}}e^{-i0.61547\ldots}\right)E=\left(\sqrt{\tfrac{3}{2}}e^{i\frac{\pi}{2}}\right)^2S+\tfrac{3}{2}e^{+i1.23095\ldots}C\,. \tag{7.53}$$

Here as with the companion relationship for the 3-cube, we have "broken symmetry" with the rotational senses, and see that rotation of two edge strains into an adjacent corner is equal to two orthogonal rotations of a surface strain and a flip of a vertex strain from one h-axis to a proximal axis. The moduli in this case correspond to the metrics of the inversphere, where $\frac{3}{2}$ is the distance from the cubic center to the cubic vertex. We will see that this represents an instance of beta decay, where the surface and vertex rotations indicate the flip of the electrical phase torques from one pair of vertices to one of three proximal pairs. In the case of the inductive torque, we have an electron emission along with a flip of the magnetic moment, and in the case of the capacitive torque, we find a positron emission, without the magnetic moment flip.

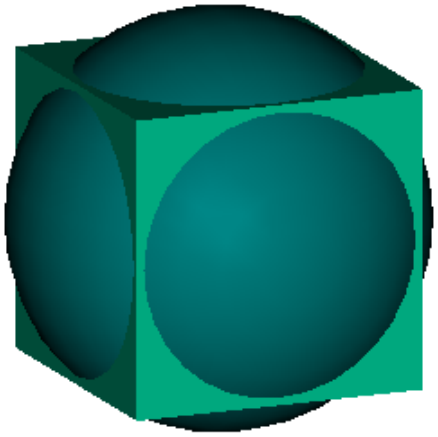

Equal Area Cube and Sphere

The position indicated as the midpoint on the cubic edge is of special interest. If we analyze a concentric cube and a sphere of equal surface area, and presumably of equal total surface stress, we will find that the radial to the midpoint as represented by $\left(\frac{S}{C}\right)_4$ exceeds the spherical radius (and the path of the rotational oscillation strain) at that point by a factor of

$$\delta r = \frac{\sqrt{2\pi}}{3}\left(\sqrt{\frac{3}{2}} - \frac{3}{\sqrt{2\pi}}\right) = \sqrt{\frac{\pi}{3}} - 1 = 0.023326708\ldots. \tag{7.54}$$

This indicates that the rotational path of the strain constricts the diagonals and restricts the operation given by $\left(\frac{E}{S+C}\right)_4$. Thus this differential must be overcome by the increase in stress of that operation. If we assume that the differential given by (7.54) is one component of the cross sectional area on which an orthogonal stress is operating, then the square of that value gives a differential stress required for the diagonal to flip of

$$\delta r^2 = 0.0005441353061\ldots. \tag{7.55}$$

The ratio of differential stress to the augmented total is then

$$\frac{\delta r^2}{1+\delta r^2} = \frac{0.0005441353061}{1.0005441353061} = 0.0005438393841\ldots \tag{7.56}$$

which when inverted is

$$\frac{1+\delta r^2}{\delta r^2} = 1838.778193 \tag{7.57}$$

It bears noting that the 2002 CODATA ratio of the electron to neutron mass is 0.00054386734481(38), or within 2.796…x10^{-8} of the value of (7.56). Thus the ratio of the differential stress needed to produce beta decay and the stress of fundamental oscillation correlates significantly with the ratio of the mass-energy of the product of that decay, the electron, and that of the fundamental oscillation, the neutron.

With reference to beta decay, one additional observation concerns the weak mixing angle yielded by the final measured asymmetry stated in the September, 2005 issue of Physics Today by Bertram Schwarzschild in “Tiny Mirror Asymmetry in Electron

Scattering Confirms the Inconstancy of the Weak Coupling Constant" as $\mathbf{sin}^2\,\theta_W = 0.2397 \pm 0.0013$. If we consider the surface area of a sphere in steradians as 4π, the portion spanned by each cubic edge in conjuction with the above development is one twelfth that or an area of $\pi/3$. A linear component of that measure would therefore be $\sqrt{\frac{\pi}{3}}$ and would correspond generally and perhaps in some statistical manner with the distance from a cubic surface vector to a vertex vector as in the interplay between S and C at $\left(\frac{E}{S+C}, \frac{S}{C}\right)_{3,4}$. The arc distance between the mid-point of that arc and each of the three parameters E, S, and C is then ½ $\sqrt{\frac{\pi}{3}}$. We then have the following, which is stated phenomenologically and without causal analysis

$$\mathbf{sin}^2\left(\tfrac{1}{2}\sqrt{\tfrac{\pi}{3}}\right) = 0.239735827. \qquad (7.58)$$

Bibliography and Other Resources

Astronomy and Astrophysics 338, 856-862 (1998), “Magnetically supported tori in active galactic nuclei”, Lovelace, Romanova, and Biermann.

Exploring Black Holes, Taylor and Wheeler, Addison Wesley Longman, Inc, New York, 2000.

The Extravagant Universe, Kirshner, Princeton University Press, Princeton, NJ, 2002.

The Feynman Lectures on Physics :Commemorative Issue, Feynman, Leighton, Sands, Volume I, Addison-Wesley Publishing Company, Inc., Reading, Massachusetts 1963.

Fundamentals of Physics, Fifth Edition, Halliday, Resnick, Walker, John Wiley & Sons, Inc. New York, 1997.

Gravitation, Misner, Thorne, and Wheeler, W.H. Freeman and Company, New York, 1973.

Mathematical Methods for Physicists, Fifth Edition, Arfken and Weber, Harcourt Academic Press, New York, 2001.

Physics of Waves, Elmore and Heald, Dover Publications, Inc., New York, 1985. This was the primary source for wave, elasticity and tensor equations.

The Six Core Theories of Modern Physics, Stevens, The MIT Press, Cambridge, Massachusetts, 1995.

Three Roads to Quantum Gravity, Smolin, Basic Books, New York, 2001.

Visual Complex Analysis, Needham, Oxford University Press, Oxford, England, 1997

The Theoretical Minimum: What You Need to Know to Start Doing Physics, Susskind and Hrabovsky, Basic Books, New York, 2013

National Institute of Standards and Technology, These are the **2002 CODATA recommended values** of the fundamental physical constants, the latest CODATA values available. For additional information, including the bibliographic citation of the source article for the 1998 CODATA values, see P. J. Mohr and B. N. Taylor, "The 2002 CODATA Recommended Values of the Fundamental Physical Constants, Web Version 4.0," available at physics.nist.gov/constants. This database was developed by J. Baker, M. Douma, and S. Kotochigova. (National Institute of Standards and Technology, Gaithersburg, MD 20899, 9 December 2003).

Table of Nuclides, Nuclear Data Evaluation Lab., Korea Atomic Energy Research Institute (c) 2000-2002, http://yoyo.cc.monash.edu.au/~simcam/ton/index.html

R.R.Kinsey, et al.,*The NUDAT/PCNUDAT Program for Nuclear Data*, paper submitted to the 9 th International Symposium of Capture-Gamma ray Spectroscopy and Related Topics, Budapest, Hungary, Octover 1996.Data extracted from NUDAT database (Jan. 14/1999)

Schwarzschild, Bertram, "Tiny Mirror Asymmetry in Electron Scattering Confirms the Inconstancy of the Weak Coupling Constant", Physics Today, September, 2005

Wapstra, A. H. and Bos, K., "The 1983 atomic-mass evaluation. I. Atomic mass table," Nucl. Phys. A 432, 1-54, 1985, quoted at http://hyperphysics.phy-astr.gsu.edu/hbase/nucene/nucbin2.html